DEVELOPMENT SCOUR HOLE MAASVLAKTE 1 & 2

A. VAN DEN BERG C1062891

SEPTEMBER 2007

Port of Rotterdam

TU Delft

Development scour hole Maasvlakte 1 & 2

Final report (draft)

September 2007

MSc student:

A. van den Berg
Stdnr. C1062891
Westerstraat 90
2613 RJ Delft
a.vandenberg@yahoo.com
06-15512844

Graduation committee

Prof. dr. ir. M.J.F. Stive	Delft University of Technology (Chairman)
Prof. dr. ir. J.A. Roelvink	Unesco-IHE/ WL|Delft Hydraulics
Ir. D.J.R. Walstra	Delft University of Technology/ WL|Delft Hydraulics
Ir. T. Vellinga	Port of Rotterdam/ Delft University of Technology
Ir. S. Boer	Infram International BV
Ir. A.P. Luijendijk	WL|Delft Hydraulics
Ir. G.J. de Boer	Delft University of Technology

Preface

The present M.Sc. thesis study forms the final step of my education at Delft University of technology, Faculty of Civil Engineering and Geosciences, section Hydraulic Engineering.

The study was initiated by the Project Organisation Maasvlakte 2, Port of Rotterdam. The thesis is part of the 'Port Research Centre' which is a cooperation between the Port of Rotterdam and Delft University of technology.

In this thesis the development of the scour hole in front of the Maasvlakte 1 and 2 with different bed compositions are investigated by applying numerical modelling.

The graduation committee consists of the following persons:

Prof. dr. ir. M.J.F. Stive	Delft University of Technology (Chairman)
Prof. dr. ir. J.A. Roelvink	Delft University of Technology
Ir. D.J.R. Walstra	Delft University of Technology
Ir. T. Vellinga	Port of Rotterdam/ Delft University of Technology
Ir. S. Boer	Infram International BV
Ir. A.P. Luijendijk	WL|Delft Hydraulics
Ir. G.J. de Boer	Delft University of Technology

I wish to thank the committee for sharing their knowledge and their support during my thesis. Finally I want to thank my friends, family and especially Bregtje for their support and friendship during the thesis.

Bert van den Berg

Delft, September, 2007

Abstract

Model simulations on the basis of uniform (non-graded) sediment reveal a strong overestimation of the scour hole in the area directly to west of Maasvlakte I when compared to the measured scour hole.

Data analysis shows that the scour hole developed in a former complex estuarine system. The analysis strongly suggests that erosion occurred through a number of different old (clay) layers.

The presence of cohesive layers can reduce the development of the scour hole considerably. Implementation of cohesive layers in the Delft3d model showed that the erosion rate as observed in reality can be simulated with cohesive sediment.

Armouring of the bed, erosion of fine sediments and the harder to erode coarser sediment remains, also result in a reduction of the scour hole. The armouring effect can be simulated in a schematized way by distinguishing a number of fractions and bed layers. Simulations show that armouring indeed reduces the development of the depth of the scour hole. However, the computed erosion is still considerably higher compared to the observed erosion rate.

Computations for the Maasvlakte 2 indicate that the main flow characteristics are similar. It is expected that the development of the scour shows much resemblance. Therefore similar parameters can be used for the Maasvlakte 2 situation. The above mentioned mechanisms result in a lower erosion rate for the Maasvlakte 2 situation. The cohesive layers are positioned deeper and therefore the armouring effect is also of importance.

The development of the scour hole strongly depends on the bed composition while this composition is vaguely known because of inhomogeneity of the bed. Therefore the predictions of the Maasvlakte 2 are expected to be less accurate.

Executive summary

Introduction

This report discusses the scour around the Maasvlakte 1 & 2. Model results on the basis of uniform (non-graded) sediment in previous studies reveals a large scour hole in the area directly to west of Maasvlakte 1 and 2. Validation of the modelled Maasvlakte 1 scour hole against 20 years of field data shows strong overestimation of the scour hole. Computations for the Maasvlakte 2 indicate that the main flow characteristics are similar. Therefore, it is expected that the development of the scour of Maasvlakte 2 will show much resemblance to the Maasvlakte 1 situation. To gain a useful forecast of the Maasvlakte 2 it is important to explain the occurring mechanisms in the Maasvlakte 1 situation. Sorting of graded bed material and natural armouring may result in a strong reduction of the scour process. The presence of cohesive material can also explain the overestimation, since old overconsolidated clay can be considerably difficult to erode.

Study objectives

- Two separate hindcasts of the Maasvlakte 1: The first with implementation of a number of sediment fractions to simulate the armouring effect; the second with the implementation of cohesive layers. Mutual comparison and comparison with reality showed the importance of the two improved bed schematizations.
- Two separate forecasts of the Maasvlakte 2 with the two afore mentioned improved bed schematizations.

Model and method

For the simulations use has been made of the integrated modelling system Delft3D. In this modelling system the armouring effect was simulated in a schematized way by distinguishing a number of fractions and bed layers. There is no hiding and exposure, simply bookkeeping of deposited and eroded material. In Delft3D there is also the possibility to implement cohesive sediment. Combined with a multiple layered bed this gives the possibility to simulate clay layers.

Simulations with non-graded (uniform) sediment and simulations without waves served as reference. Simulations with graded (non-uniform) and cohesive sediment are compared to the reference cases and to reality. The development of the depth and the pattern of the scour hole and also accretion in the Maas trench are used as validation criteria.

Data analysis

The improved bed schematizations require additional data analysis concerning the soil condition. Below the main findings are listed:

Bathymetric data

- In contrast to what has been suggested in former studies the scour hole did not reach equilibrium yet. The scour hole is still developing.
- The erosion rate in the scour hole fluctuates. Three periods can be distinguished:

  1986-1989: High erosion in the whole area which is comparable with the computations done with non-cohesive material (chapter 4)

  1989-2000: Low erosion with more spatial variance

  2000-2006: Higher erosion rate with a low spatial variance

Sieve curves

Analysis of sieve curves in the area of interest showed a wide range of the particle size distribution. There was no clear difference between the upper samples and the samples below. However for two reasons this does not directly imply there is no armouring: 1) An armour layer can be smaller than the range where the sediment samples are taken in; 2) The armouring does not have to occur all the time, but only during certain flow conditions.

Analysis of soil composition and cohesive layers for the MV1-case

For the hindcast of MV1 it is difficult to determine what kind of sediment was scoured in the period 1986-2006. There are four indicators, which suggest that part of the eroded material was cohesive material:

- Strong alternating erosion rate suggest differences in bed material
- An irregular bed level is observed which suggest a spatial variation of the bed material
- Clay is exposed at two locations closest to the centre of the scour hole
- The geotechnical setting shows that the area of interest is a former complex estuarine system, composed of highly mobile tidal channels and tidal flats with a number of layers with different composition in time and space. Analysis suggests the presence of clay layers in the eroded part of the scour hole.

Analysis soil composition and cohesive layers for the MV2-case

Soil samples close to the expected scour hole in front of the Maasvlakte 2 suggests the presence of a cohesive layer which starts between 19 and 22 meters below NAP.

MV1 hindcast; armouring non-cohesive fractions

Computations with a graded sediment model showed a reduction of the depth of the scour compared to the uniform sediment model for two reasons:

1. Armouring: the transport layer coarsens because the relatively fine material erodes faster. This relatively courser layer causes a decrease of the erosion.
2. The finest sediments (100 µm) cause a decrease of the maximum erosion.

Uniform sediment (200 µm) already showed an overestimation of the accretion of the Maas trench. All the simulations with graded sediment show an even larger accretion. However the volume eroded out of the scour hole is smaller compared to the case with uniform sediment. The larger accretion is due to the small fractions which cause a relatively high accretion in the Maas trench. When the five simulations performed with graded sediment are mutually compared a larger accretion is found when a larger volume is eroded out of the scour hole. The total increase of accretion can not be clarified by the larger eroded volume out of the scour hole.

Armouring

The armouring effect is observed well. In and around the scour hole an increase of the content of the larger sediment fractions is found and a decrease for the smaller sediment fractions (except for the smallest particles, 100 µm). The armouring effect depends on the ratio D90/D10. A high value for this rate gives more armouring.

MV1 hindcast with cohesive layers

Computations in a model where cohesive layers were implemented have shown that clay layers can strongly reduce the depth and the extent of the scour hole. Varying erosion rate as observed in reality is explained with the highly stratified bed.

Erosion of cohesive sediment is implemented in Delft3D with the well known Partheniades-Krone formulation. The parameter values in this formulation mainly depend on the clay condition. Appropriate values for these parameters have to be determined by calibration or field observations. It is difficult to simulate the highly stratified soil system and therefore it is difficult to find appropriate values for the erosion parameters by calibration. The extent and the position of the scour hole are not yet simulated satisfactory in the Delft3D environment.

Cohesive layers versus armouring non-cohesive fractions

The computed erosion rate with a non-cohesive graded sediment model is still considerably higher compared to the erosion rate observed in reality. Furthermore this model does not explain the large differences in the observed erosion rate between 1986 and 2006 in the scour hole.

By implementing cohesive material the erosion rates observed in reality can be simulated. The change in erosion rate is due to the highly stratified bottom. The different layers differ in composition and therefore a different erosion rate is observed.

Computations maasvlakte 2

Computations are made with the non-cohesive graded sediment model for the Maasvlakte 2 situation. The same scour reducing mechanisms occurred. The reduction of the scour depth compared to the computations with uniform sediment is 30%. This reduction is comparable to the Maasvlakte 1 situation (30% versus 25%).

Implementation of cohesive layers, according to the data analysis, displayed analogous to the Maasvlakte 1 situation reduction of erosion when compared to the uniform sediment simulations. In the data analysis difference is found in the vertical position of the cohesive layer. Because the lower vertical position of the cohesive layer the cover of non-cohesive material has a larger influence.

The development of the scour hole strongly depends on the bed composition while this composition is vaguely known because of inhomogeneity of the bed. Therefore the predictions of the Maasvlakte 2 are expected to be less accurate.

Recommendations

To obtain better hindcasts of the Maasvlakte 1 and therefore better forecasts of the Maasvlakte 2 a number of recommendations are given for further investigation. The main recommendations are listed below:

- A number of parameters concerning cohesive material are not well known yet. Box cores on location should give more accurate values for these parameters.
- The simulations for cohesive material with the Partheniades formulations that are implemented in Delft3D did not show satisfactory results. Other formulations or even other computer models should be investigated.
- Fine sediment (0.100mm) results in a scour hole with a smaller depth and a larger extent. In this study only relatively fine sediment with a diameter of 0.100mm was investigated. Fine sediments should be further investigated.
- In this study no hiding and exposure correction was adopted which means that finer particles could not hide behind coarser sediments and coarser sediments are not extra exposed to the flow. The effects of hiding and exposure should be further investigated.

Table of contents

Chapter 1 Introduction

1.1 Background information

The port of Rotterdam is the most important port of Europe and one of the largest in the world. The port and industrial area stretches from the city to the North Sea and covers approximately 5000 hectares of industrial sites. In the present port area there is no more space available for new enterprises and expansion of the current companies. If the port wants to carry on developing in a good manner expansion of the port zone is unavoidable. In time, starting in the 15th century, the port developed in the direction of the sea. In the seventies of the twentieth century the last extension has been taken place with the present Maasvlakte as can be seen in figure 1.1. In this figure also the 'Slufter' is shown which is constructed in 1986 for storing of contaminated dredge material.

Figure 1.1 Maasvlakte 1 & the Slufter (source: Google earth,2004)

In response to signals that the present port area became full the Project Mainport development Rotterdam (PMR) was started in 1997. [PMR, 2003]

The project comprises three components:

- Construction of Maasvlakte 2, including compensation for its impact on the natural world.
- Existing Rotterdam Area, execution of projects in the current port and industrial area for better and efficient use of the space and to improve the environment for those living in the area.
- Creation of a 750-hectare new recreation and nature area to the north and south of Rotterdam.

In the next step the Rotterdam Mainport Development Project (PMR) went through the procedure for a Key Physical Planning Decision-plus (PKB-plus). This government decision stipulates, among other things, which goals the project should achieve (the three components) and how this should be achieved. In this study only the first component of the PMR, namely Maasvlakte 2, is important. In part 4 of the PKB-plus, the basic decision for the construction of Maasvlakte 2 was set down. In October 2006 the Dutch Parliament agreed in favour of the reinstated Key Planning Decision. With this agreement Maasvlakte 2 project is in fact no longer on the political agenda. It is now up to the Port Authority and local, regional and national authorities to continue preparations for the land reclamation.

Maasvlakte 2, new land, which will be reclaimed from the sea, is located at the west side of the present Maasvlakte and is linked directly to the current port and industrial zone as can be seen in figure 1.2 and 1.3. The reclamation area will consist of 1000 hectares of commercial sites. Mainly used for deep sea container handling but also for chemical industry and distribution. Another 1000 hectares will consist of infrastructure, such as sea defences, fairways, railways and port basins. Thus the total reclaimed area will be about 2000 hectares.

Figure 1.2 Maasvlakte 2

The reclaimed land will emerge after the construction of a combination of hard and soft sea defences in the North Sea. Beach and dunes form the soft part of the sea defence, rubble or concrete blocks the hard sea wall. Inside these defences, the sites will subsequently be sprayed on. The sand for this will come from carefully selected locations at sea, but will also become available when the port itself is deepened.

The tender phase of Maasvlakte 2 has been started late 2005 which shall result in a contract with one of the tendering consortia during the course of 2007. Construction of Maasvlakte 2 will commence in the spring of 2008 so that the first ship can dock at the quayside in 2013.

The construction of Maasvlakte 2 will have impact on nature. All the lost nature must be compensated. This shall be done according to the Dutch and European regulations. The compensation for the impact of the land reclamation on nature in the Voordelta of the North Sea, the Voorne dunes and the dunes of Goeree consists of:

- Creation of a marine reserve in the Voordelta to the south of the future Maasvlakte 2 (max 31.250 hectares)
- Creation of a new area of dunes on the coast of Delfland (max 100 hectares)

- Creation of foredunes (outer line of dunes) at the Brouwersdam and/or on the land reclamation itself (max 23 hectares).

The actually chosen design for Maasvlakte 2 has less impact on nature than the reference designs. Hence the needed compensation is less and therefore the compensation areas shall be adjusted downward.

Figure 1.3 Artist impression of the Maasvlakte 2

Maasvlakte 2 will influence the hydraulics and therefore the morphological processes. Because of the more seaward position the coastline will be exposed to heavier wave action than the Maasvlakte 1 and the larger bulge in the Dutch coastline causes more contraction of the tide. As can be seen in figure 1.3 Maasvlakte 2 will have a predominantly soft seawall. Only on the north side a hard sea defence will protect Maasvlakte 2 against waves from northern directions. The soft defence consists of dunes behind a beach. Waves and currents erode the beach. Where this happens, the sand on the beach needs to be replenished from time to time.

Contraction of the tide will increase the tidal flow. This will cause erosion along the west side of Maasvlakte 2. A scour hole will develop in time. In theory this scour hole can become dozens of meters deep. The current depth is between fifteen and twenty meters.

1.2 Problem analysis

1.2.1 Problem description

Within the framework of the Maasvlakte 2 project extensive study has been done to determine the impact of the construction on the existing hydraulics, morphological processes and the resulting morphological changes. This study focuses on the determination of the large scale scour in front of the soft defence of Maasvlakte 2. The depth and the extent of this scour are important for the following reasons. [S. Boer et al, 2006]

- Erosion of the seafloor below NAP -20m needs to be compensated because of loss of habitat and loss of potential feeding area for protected birds that tend to feed not deeper than 20 meters below sea level. Necessary compensation for the scour means extension of the marine reserve.
- The large scale scour may cause additional erosion of the soft defence of Maasvlakte 2. This demand for more replenishment of the beach.
- Extensive erosion may cause additional accretion of the existing access channel to the port of Rotterdam. This will require more dredging.

Performed studies and model

From the first design exercises for Maasvlakte 2 an extensive set of computer models are developed to forecast the impact of the construction on the morphology. By using the process-based modelling program DELFT3D this impact on the morphology can be simulated. At WL|Delft Hydraulics the numerical model Delft3D is under continuous development. For Maasvlakte 2 calculations always the latest developed modules are used. As a result, it is now possible to make realistic forecasts of the morphological developments for a relatively long period. The latest refinement of Delft3D, Delft3D-online, is a module within Delft3D which couples hydrodynamic computations simultaneously (online) with calculation of the transport of salinity and heat and also the online computation of sediment transport and morphological changes [Lesser, 2004].

By using this module the morphological development near by the Maasvlakte 2 has been calculated [Roelvink and Aarninkhof, 2005]. It appears that a scour hole will develop along the north-westerly coastline of Maasvlakte 2. According to the used model a scour hole with an area below NAP-20m of 760 hectares and a maximum depth about NAP -27m developed in 20 years. After 20 years the equilibrium is not reached yet, the process of scour still continues.

Maasvlakte 1

After construction of the Maasvlakte 1 in the seventies regular bathymetrical surveys have been carried out. The surveys show the development of a scour hole on the west of Maasvlakte 1. The erosion process is still going on and equilibrium is not reached yet. The maximum bottom depth is approximately NAP -18m and the whole scour hole covers an area of 160 hectares in 2006. A calculation for the present situation showed a persistent scour for the next 20

years. The calculated size and depth of the scour hole are considerably larger compared to the observed data.

The design of Maasvlakte 2 shows resemblance with the present situation. The main flow characteristics show only little difference according to computations. Therefore it is expected that the development of the scour hole in both situations are quite similar.

For the set-up of a model for Maasvlakte 1 at least 20 years of data is available. From 1986, when the Slufter was created, until present.

Armouring by non-cohesive sediments

The computations for Maasvlakte 1 and 2 show a large scour hole on the west side of these reclaimed areas. The computed scour hole for the Maasvlakte 1 is overestimated when compared to reality. In both computations the seabed is schematized by means of uniform non-graded non-cohesive sediment. This could indicate an overestimation of the scour hole because the effect of armouring is neglected.

The natural seabed sediments are non-uniform and therefore natural sorting of bed sediments by the flow velocity occurs. The finer sediment will erode and the coarser material will stay behind forming an armour layer on the surface of the seabed. For erosion of this coarser material higher flow velocity is required and therefore the morphological changes will be smaller which may result in a strong reduction of the scour hole.

In the present version of Delft3D the effect of armouring can be schematized by implementing several sand fractions and a number of bottom layers. The modelling of graded sediment is mainly used for rivers and rarely for coastal areas. Recently the effect of armouring for the Maasvlakte 2 case was investigated by means of a number of sensitivity computations [Elias et al., 2006]. The computations have a comparative nature and do not intend to give an accurate estimate of the dimensions of the scour hole. The sensitivity tests in this study confirm that the incorporation of armouring processes strongly reduces the development of the scour hole. The modelled sediment characteristics show that this reduction is due to eroding of the finer sediment and staying behind of the coarser sediment.

The set up of the model was, where ever possible, conform the former Maasvlakte 2 (MV2) model study, though there are four essential model configurations where the new model differs from the former models:

- In the original MV2 computations the Bijker transport formula is used. The Bijker formula appears to be inconsistently implemented in the used Delft3D framework. Therefore the Van Rijn transport formula is used.
- No wave induced sediment transport in the new model.
- Several sediment fractions and a number of bottom layers are implemented in the new model where formerly uniform non-graded sediment was used.
- In the new model no sand nourishment mode is applied to maintain the cross profile of MV2.

Because of these differences extensive calibration and validation of the new model configurations is needed to give accurate predictions of the scour hole.

Cohesive sediment

All the computations in the previous studies concerning the scour hole are performed with non-cohesive sediment. In the area of interest certain clay layers have been found. Because of the cohesiveness of clay a lower erosion rate is expected. Therefore a scour hole with a smaller depth is expected. Because cohesive sediment is not taken along in the previous studies this can also be an explanation of the overestimation of the scour hole.

1.2.2 Problem definition

The problem definition is threefold:

- The present hindcast of the scour hole in front of Maasvlakte 1 shows an unrealistic strong development of this scour hole compared with field observations. The difference may be explained by the occurrence of natural armouring processes by graded non-cohesive sediments and/or the resistance against erosion by layers with stiff cohesive sediments which were not included in the original hindcast computations.

- Sensitivity computations in Delft3D have shown that armouring effects by non-cohesive sediment reduce the extent and depth of the scour hole in front of the Maasvlakte 2. An accurate prediction is not given by these computations because the model is not calibrated and validated. Furthermore the effect of both wave-induced and flow-induced sediment transport and also a sand nourishment mode are not incorporated in this model. These aspects should be incorporated in the model to give accurate predictions.

- The extent and the depth of the scour hole in front of the Maasvlakte 2 is not yet predicted with a model where cohesive layers are incorporated.

1.2.3 Study objectives

The study objectives of this study are also threefold:

- Two new hindcasts of the scour hole in front of Maasvlakte 1: The first hindcast with a model where the effect of armouring by non-cohesive sediment is schematized by implementing several sand fractions and a number of bottom layers. The second hindcast with a model where also cohesive sediment is implemented. Both models calibrated and validated against 20 years of field observations. The hindcasts should result in parameters for the Maasvlakte 2 model and should show which mechanism is dominant.
- Determining the development of the location and the extent of the scour hole in front of the Maasvlakte 2 using a model where the effects of armouring by non-cohesive sediment, wave- and flow-induced sediment transport and also a sand nourishment mode are incorporated. This model has to be calibrated and validated against known properties of the system following from the Maasvlakte 1 model. This is possible because of the great resemblance between the Maasvlakte 1 and 2.
- Determining the development of the location and the extent of the scour hole in front of the Maasvlakte 2 using a model where cohesive sediment layers are implemented. This model has also to be calibrated and validated against known properties of the system following from the Maasvlakte 1 model.

1.3 Outline of report and modelling approach

The study objectives are worked out as follows:

First a model of the area of interest will be set up in the process based modelling environment of Delft3D (Chapter 2). Because of the importance of the composition and the position of the bed level hereafter an analysis will be made of the available bathymetric data and the sediment samples (chapter 3).

Modelling approach

This study focuses on the modelling of the development of the scour hole in front of the Maasvlakte. The modelling can be divided in two cases.

Case A: Maasvlakte 1

Case B: Maasvlakte 2

Every case can be divided in several phases. Case A will be used to calibrate the model. In such way the optimal parameter settings will be obtained for case B.

Case A, hindcast of Maasvlakte 1

For general insight of the flow around the Maasvlakte 1 this case is first modelled without waves and wind (chapter 4). In chapter 5 the influence of the waves on the scour hole is investigated. In this chapter also the flow and the waves are combined. Armouring of the seabed by non-cohesive material, the process where the finer particles are eroded away and the coarser particles form an armour layer on the remaining sediment, is investigated in chapter 6 by means of implementing more than one non-cohesive fraction and several layers. Chapter 7 contains the investigating of the influence of cohesive sediment layers at the location of the scour hole. Chapter 7 will be concluded with a comparison between the influence of implementing more than one non-cohesive fraction and the implementing of cohesive sediment.

Case B, Maasvlakte 2

The optimal parameters for Maasvlakte 2 are determined in chapter 6 and 7. This case will be started with the investigation of the hydrodynamics (Chapter 8): The flow around the Maasvlakte 2 and the occurring waves will be investigated and compared with the flow and waves occurring in the Maasvlakte 1 case. This chapter will be ended with the reference simulation where uniform non-cohesive sediment has been applied.

In chapter 9 the MV2 case will be modelled with more than one non-cohesive sediment fraction using the best fit parameters of chapter 6. In chapter 10 cohesive sediment layers will be implemented in the MV2-case.

Conclusions and recommendations

The report will be finished with conclusions and recommendations (Chapter 11). The outline of this report is visualized in table 1.1.

Table 1.1 the outline of the report

Chapter 1	Introduction
Chapter 2	Model set up
Chapter 3	Data analysis
Chapter 4	MV1, tide only
Chapter 5	MV1, waves included
Chapter 6	MV1, armouring by non-cohesive fractions
Chapter 7	MV1, cohesive sediment layers
Chapter 8	MV2, hydrodynamics
Chapter 9	MV2, armouring by non-cohesive fractions
Chapter 10	MV2, cohesive sediment layers
Chapter 11	Conclusions and recommendations

Chapter 2 Model set up

In this chapter the set up of the model which will be used in this study will be shown. First the model which will be used for the computations is treated (2.1). The grid which will be used in the model is obtained in paragraph 2.2. Hereafter respectively the bathymetric data and the boundary conditions are given. (2.3 and 2.4) In paragraph 2.5 the general parameter settings which will be used in the model are given. Paragraph 2.6 contains the validation criteria on which the Maasvlakte 1 model will be calibrated and validated. The last paragraph highlights the uncertainties of the current model.

2.1 The Delft3D model

All modelling will be executed with the process based modelling program Delft3D which is a model system that consists of a number of integrated modules which together allow the simulation of hydrodynamic flow, computation of the transport of water-borne constituents, short wave generation and propagation, sediment transport and morphological changes, and the modelling of ecological processes and water quality parameters.

Delft3D-FLOW

In this study at the heart of the modelling framework the FLOW module that performs the hydrodynamic computations and simultaneous (online) calculates the bathymetry has been used. All modelling in this study has been executed with a 2DH, depth averaged area model. Delft3D-FLOW solves the unsteady shallow water equations. The system of equations consists of the horizontal momentum equations, the continuity equation, transport equation and a turbulence closure model.

Delft3D-WAVE

Wave effects can be included in a Delft3D-FLOW simulation by running the separate Delft3D-WAVE module. For the computations of waves the third-generation SWAN (Simulating WAves Nearshore) model can be used. SWAN computes random, short-crested wind-generated waves. The model predicts a 2D wave field on beforehand specified grid points. During a simulation with the flow module the wave module will be called several times. The computed wave field can thereby be updated accounting for the changing water depths, velocities and bathymetry computed in the flow-module. The calculated wave forces will be taken into account in the flow-module.

Sediment transport

For sediment transport in Delft3D the Online Morphology module is used. The transport is calculated at the same time as the flow by the advection diffusion solver in the flow module. Besides this the bottom transport is computed locally. Delft3D computes total change in sediment by summation of the change of the suspended load the change due to the suspended load correction vector and the change due to bed load. Suspended sediment exchange with the bed is implemented by means of computing sediment sources and sinks near the bottom of the flow by using a reference height and a reference concentration.

Bed load transport is computed in vectors at the water level points and uses a different numerical scheme [Lesser et al., 2004].

Bed level changes are calculated each time step in the flow model. The used time steps are equal but there is a significant difference in time scale between the flow and the morphology. Therefore a so called morphological factor can be used. This morphological factor simply increases the depth changes by multiplying with a constant factor n. This means that after a simulation over one time step the morphological changes has been modelled over n time steps. For formulae and further explanation is referred to the Delft3D flow manual and [Lesser et al., 2004].

2.2 Computational grids

2.2.1 Flow grid

In former studies a rather fine grid has been used. This fine grid results in a large computation time. In appendix A a number of grids are investigated with the aim to find a grid that constrains the computation time and still is sufficient for the purpose of the model. In table 2.1 the investigated grids are listed with the according number of grid cells. The number of grid cells is an indicator for the computation time. Figure 2.1 shows the grid that will be used in this study.

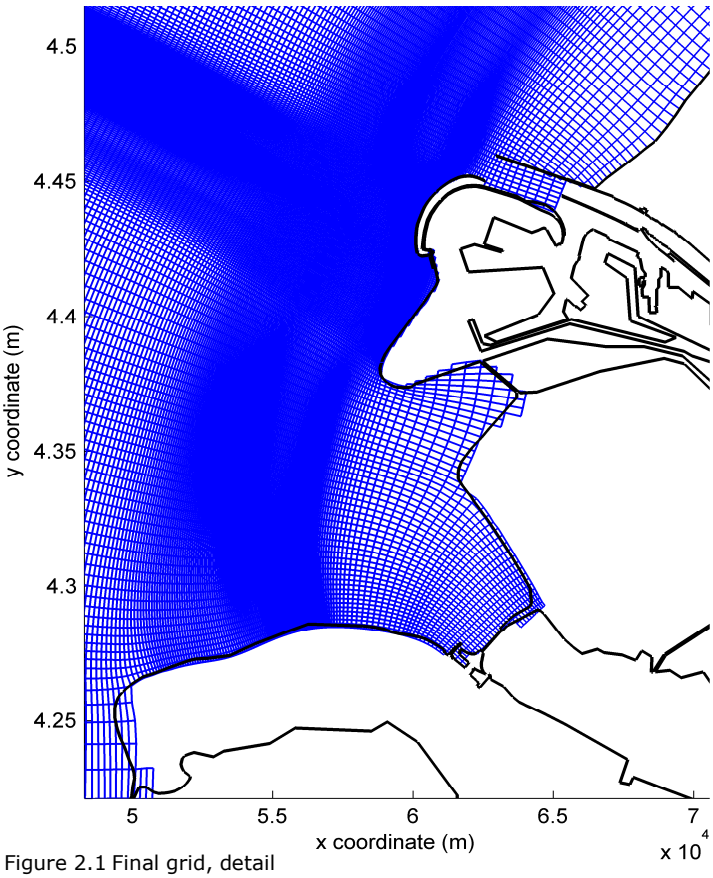

Figure 2.1 Final grid, detail

2.2.2 Wave grids

A coarse grid is used to cover the whole flow grid; this grid is extended a few grid cells in the north and the south direction to avoid boundary phenomena. In the area of interest a grid with the same resolution as the flow grid is used. The grids can be seen in figure 2.2.

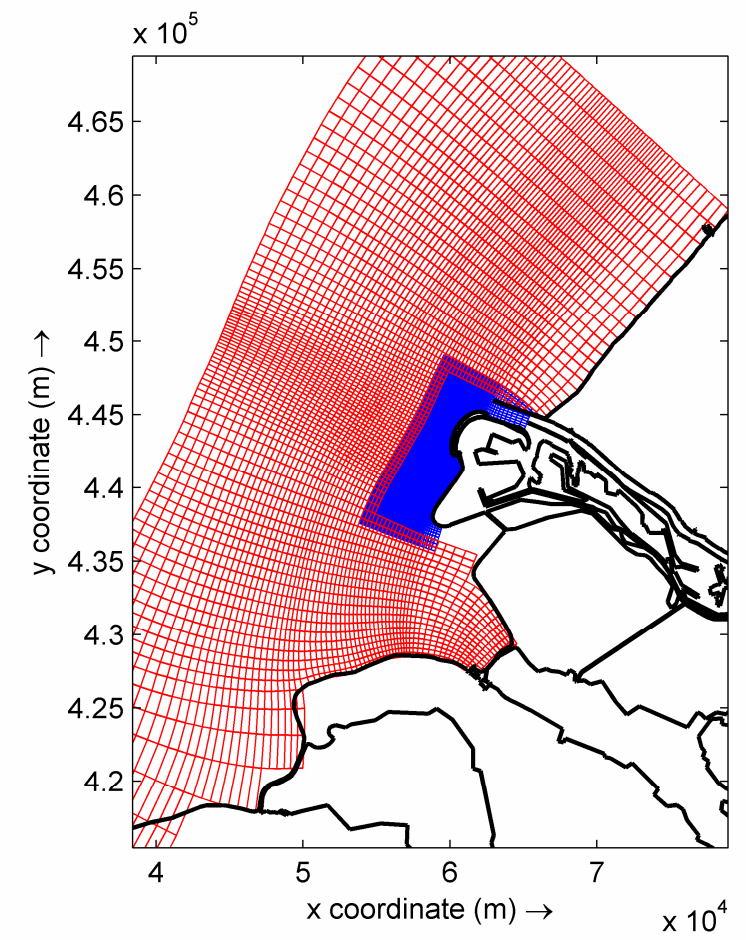

Figure 2.2 wavegrids

Table 2.1 Number of grid cells

		Number of gridcells
Flow	Original grid	50652
	DD-grids	1237+2232+11808=15277
	Circular grid	17607
	Optimal grid	23000
	final grid	32629
Wave	final grid	8016+4186=12202

2.3 Bathymetric data

Full bathymetric data was available for the years 1986, 1993, 2000 and 2006. There most be noted that in the bathymetric dataset of 1986 a triangle of data is incorrect in the area of interest. This triangle covers about half of the scour hole. The bathymetric data of 1986 is depicted in figure 2.3. The area within the dotted area contains the incorrect data. From other years between 1989 and 2000 smaller parts of the area of interest were available. These will be used later on.

Data from the years 1970-1986, so the situation without the Slufter, has been used in former studies. But these datasets are lost or untraceable.

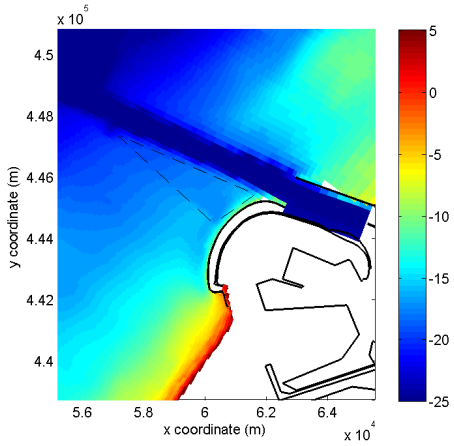

Figure 2.3 Bathymetric data 1986, with incorrect data within the triangle

2.4 Boundary conditions

2.4.1 Water levels and discharges

The boundary conditions for the original grid were deduced in *The small morphological study* [Roelvink, 1998]. These conditions are implemented in the current grid. These boundary conditions consists of water levels at all the sea-boundaries and discharges at the boundaries of the Maas and the Haringvlietsluices.

2.4.2 Wave boundary conditions

The wave boundary conditions were also deduced in [Roelvink, 1998] and are depicted in table 2.2. Here also the according wind velocities and directions are shown.

Table 2.2 Overview of the 11 applied wave conditions

Condition	Hs (m)	Tp (s)	direction (°N)	Windvelocity (m/s)	direction (°N)	Weight (days/yr)	Morphological scale factor	Number tidal cycles 1 mor-year
W00	0.10	5.0	310	0.0	310	136.5	90	3
Z01	1.05	5.0	255	6.7	282	46.0	89	1
N10	2.35	7.1	355	9.7	360	19.7	38	1
Z02	2.75	7.2	245	13.3	252	15.7	30	1
W06	2.35	6.8	295	11.1	283	5.1	10	1
N08	2.35	7.2	345	9.1	347	8.8	17	1
W05	1.05	5.0	295	5.9	255	10.6	21	1
Z04	2.15	6.5	275	11.0	263	6.9	13	1
N09	1.05	6.0	5	4.3	12	65.7	64	2
Z03	1.25	5.3	285	7.5	276	15.0	29	1
N07	1.25	6.3	345	3.1	336	35.0	68	1

2.5 Parameter-settings

All the parameter settings are, where possible, equal to the parameters used in the previous studies. In this paragraph some general parameters are mentioned. Some other parameters which are changing during this study are mentioned in the concerning chapter.

2.5.1 Flow model

The most important used parameters are shown in table 2.3.

Table 2.3 Important parameter settings flow model

Parameter	**Value**	**Unit**
Computational time step	1	minute
Roughnessheight	0,05	m
Horizontal viscosity coefficient	1	m^2/s
Horizontal diffusivity coefficient	1	m^2/s

Though another grid has been used the same time step has to be used as in the former model. This is because the smallest grid cells have the same size as in the original grid. The courant number approaches the value of 30 when a computational step of 1 minute has been used. A value of 10 is normal, but in this study still accurate results are obtained when the computational time step is set to 1.

2.5.2 Wave model

Besides some default settings the following non-default settings are equal to the settings used in the "founding Research EIA MV2" [Roelvink and Aarninkhof, 2005] Breaker parameter gamma: 0.78

- JONSWAP bottom friction type with default settings
- Inactivated triad interactions

In contrast to the EIA-study the wave forces are on the basis of the gradient of the radiation stress tensor. In the EIA-study this was on the basis of the wave energy dissipation.
For the interaction between waves and flow the model of Fredsoe has been used.

2.5.3 Sediment transport

In the original model computations for non-cohesive material have been made with the Bijker transport formula. The Bijker formula is not yet consistently implemented for graded sediment. Therefore the Van Rijn (1993) formula is applied for the sediment transport computations.

For the transport of cohesive material the formulation of Partheniades [Delft3D-flow manual, 2006] has been used, since this is the only formula which is implemented in Delft3D for cohesive sediment transport.

Especially the composition of the sediment varies in this study and will therefore be mentioned for each simulation separately. First a detailed analysis of the available data of these compositions has to be made. This will be done in the next chapter.

2.5.4 Morphological model

Because the difference in time scales between flow and morphology a morphological factor can be used. The morphological factor is shown for each wave condition in table 2.2. This is further elaborated in chapter 5.4.

The effect of armouring by non-cohesive material for the Maasvlakte 2 was already investigated by means of a number of sensitivity computations [Elias 2006]. A drawback of these computations is that the nourishment mode is not included in the system. Therefore, the computations are only of a quantitative nature and can not be used to make a quantitative forecast of the real situation. It is not yet possible to include a nourishment mode in the simulations with the Delft3D model when a stratified system is combined with multiple fractions. Accordingly there will be no nourishment mode in the simulations performed in this study.

Regular dredging maintenance in the Euro Maas trench is accounted for. Accretion above a certain imposed level is immediately removed.

2.6 Validation Maasvlakte 1 model

The Maasvlakte 1 model will be calibrated and validated against several criteria. The following criteria are tested and analyzed for the Maasvlakte 1 case:

- Comparison of measured and calculated erosion and sedimentation pattern. In this way the development of the extent and the depth of the scour hole can be analyzed.
- Comparison of measured and calculated cross-sections on three places through the scour hole (see figure 4.5). In this way a good overview can be seen of the development of the depth of the scour hole in these cross-sections.
- Comparison of measured and calculated eroded volume
- Comparison of computed cumulative dredging demand in the trench of the Euro-Maas with the amount of dredged material in reality.

2.7 Model uncertainties

[Roelvink and Aarninkhof, 2005] highlights the uncertainties which occur in a model. Six causes of uncertainties are mentioned:

1. Level of accuracy of implemented physical processes
2. Level of input reduction (f.e.: morphological tide and wave climate)
3. Level of calibration
4. Forecast period of the simulation
5. Availability and quality of input data
6. Inherent natural variance in the hydraulic boundary conditions

The first two are coupled. The applied boundary conditions in the current study are carefully deduced in [Roelvink 1998]. These boundaries showed very good results in the extensively calibrated study of [Roelvink and Aarninkhof, 2005].

The level of calibration is limited in the current study. The number of calibration criteria is low. The results in the calibrations (as will be seen in chapter 6 and 7) are not satisfactory: An overestimated scour hole and an overestimated accretion in the Maas trench.

The investigated simulation period is smaller than in the previous studies but still rather large.

Because of the data analysis in this study better input data is generated concerning the bed material.

The largest shortcoming in this model however is the absence of a nourishment mode as will be discussed in chapter 5.

Because of the above mentioned shortcomings the simulations in this study are not intended to give an accurate prediction but to show some concepts. Because of the large range in the analysed sieve curves also more simulations should be done for the Maasvlakte 2 case to determine a certain bandwidth.

Chapter 3 Data analysis

This study focuses on the scour hole in front of the Maasvlakte 1 and 2. To get a good insight in the development of the scour hole first all the available bathymetric data will be analysed (3.1).

Former studies ([Roelvink and Aarninkhof, 2005], [Steijn, 2000] etc.) also used the Delft3D model to simulate the scour around the Maasvlakte. The present study differs from former studies because the composition of the bed is considered. In the former studies always uniform (non-graded) and non-cohesive bed material has been used. In reality the composition of the bed material is non-uniform, graded and occasionally cohesive. To obtain the optimal sediment parameters the available sediment data will be analysed.

First the available sieve curves will be analysed in paragraph 3.2. The analysis contains two aspects. 1) A representative curve has to be determined which can be implemented in the model. 2) To determine if there is armouring in the scour hole there will be investigated if the top-layer in the scour hole consists of coarser material than the material below.

There are cohesive layers observed in the area of interest. The exact position and composition is not clear yet. An analysis will be made of the available soil samples to determine this position and composition. Also an indication from a geotechnical setting is given in this paragraph. For the Maasvlakte 1 case this will be done in paragraph 3.3. Because of the spatial difference of the occurrence of the cohesive layer this will be separately elaborated for the Maasvlakte 2 case (3.4).

In paragraph 3.5 the measured accretion in the Maas trench will be treated. This will be used later on for calibration and validation.

Even after this chapter the composition of the sediment in the scour hole is not completely clear. In the first part of the conclusions two hypotheses about the soil composition in the area of interest of the Maasvlakte 1 will be given (3.6.1). These two hypotheses will be further investigated in the rest of this study.

In the second part of the conclusions the main findings of the analysis for the Maasvlakte 2 situation are given (3.6.2).

3.1 Bathymetric data

In figure 3.1 the measured bed-levels for 2000 and 2006 are shown for cross section A. Also the computed bed level for 2006 as computed in chapter 4 (tide only) is shown in this figure. The location of cross section A is shown in figure 4.5. As can be seen in this figure the measured bed level for 2000 shows a smooth course of the cross-section. But as depicted clearly within the green circle the measured bed level for 2006 shows a very irregular course. The computed cross-section for 2006 conversely shows again a smooth course.

All the computed cross-sections in chapter 4,5 and 6 show a very smooth course. The measured bed levels on the other hand alternately shows smooth and irregular courses as can be seen in the green circle in figure 3.1. The smooth course demands an equally distributed soil as actually was implemented in the model. The irregular bed levels are indications for a spatially variation of the composition of the soil. Some parts will erode more easily than other. For example clay will not erode easily.

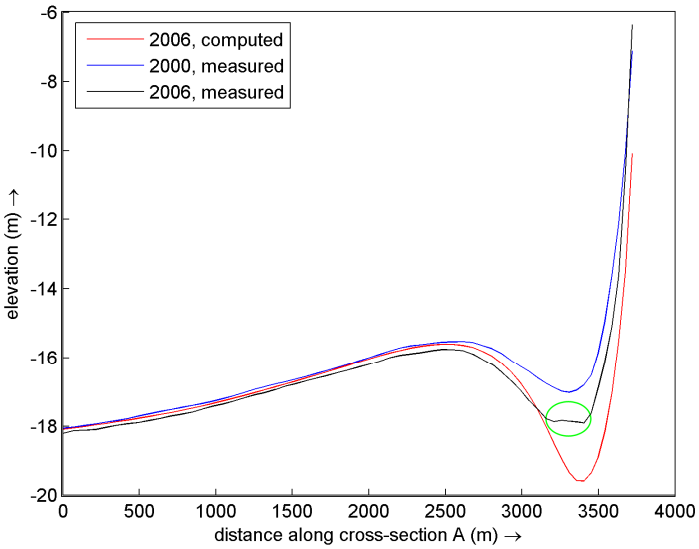

Figure 3.1 Bed levels cross section A, irregular course of the measured bed level inside the green circle

Rate of change

For a number of years bathymetric data is available. But only for a few years there is enough data available to cover the whole area of interest. In this section all the available bathymetric data will be used. Bathymetric data which is covering the area of interest completely are available for the years 1986 (see note paragraph 2.3), 1989, 1993, 2000 and 2006. There is also bathymetric data available for the years 1990 till 1998. This is only partly covering the area of interest. These data extend from the Zuiderdam till 400 meters seaward. Using this data a rate of change can be given for a few points and a cross-section. A lower range of change will indicate a soil layer which is harder to erode. In figure 3.2 an overview of the locations of the investigated points and cross section are shown.

Figure 3.3 shows the bed levels of the cross sections from 1986 till 2006. Also the data which does not cover the whole cross section are included. A relatively large distance between the bed level of 1986 and 1989 and between 2000 and 2006 is found. The bed levels of 1989 and 2000 on the other hand are relatively close to each other.

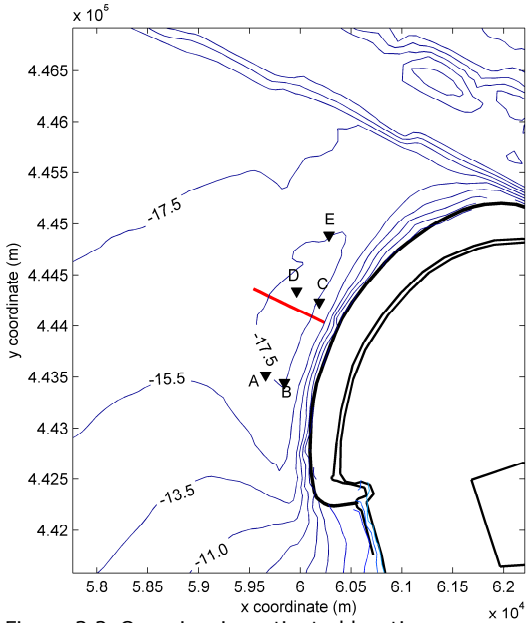

Figure 3.2 Overview investigated locations cross section

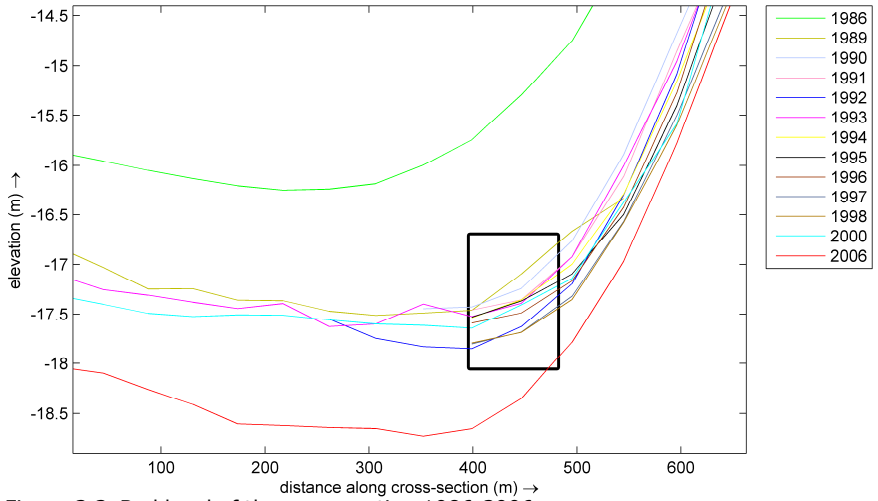

Figure 3.3 Bed level of the cross section 1986-2006

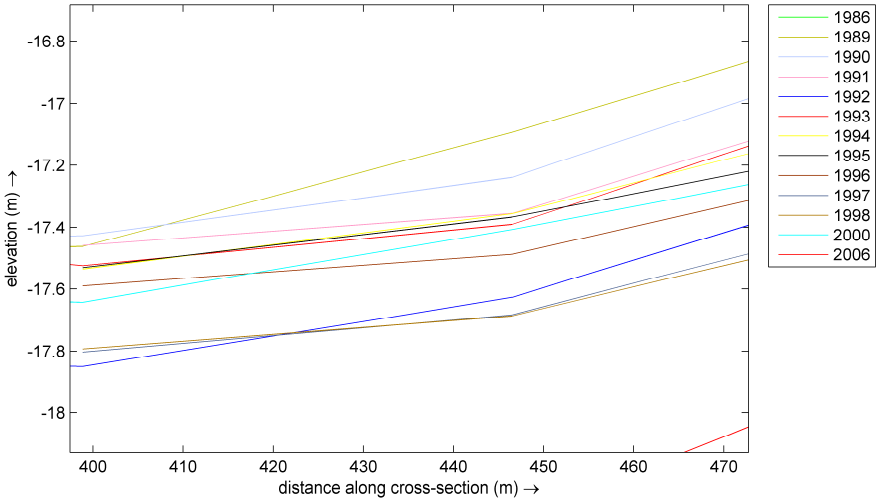

Figure 3.4 Bed level of the cross section 1989-2000, zoom in

The bed level in 1993 shows a very sharp edged profile which also crosses a few other cross sections. The bed level of 1992 is considerably deeper than the next years. It can be assumed that these irregularities are due to wrong measurements or wrong interpretation of the measurements. Figure 3.4 zooms in on this period 1989-2000. As can be seen there is hardly any erosion for the period 1991-1996. Also here there are some crossings of the lines, but the differences are small and can be due to daily fluctuations.

To study the rate of change in more detail five points are highlighted. The development of the bed levels of these points are shown in figure 3.5. Point E starts with a decreasing depth. This is because this point lies within an area which is assumed to contain wrong bathymetric data (See paragraph 2.3). In figure 3.6 the rate of change is depicted for these points. The periods 1986-1989 and 2000-2006 give very clear results. For the period 1986-1989 an erosion rate between 0.35 and 0.58 m/year is found and for the period 2000-2006 a rate between 0.14 and 0.17 m/year. The erosion rates for the period 1986-1989 are comparable with the results given by the computer model.

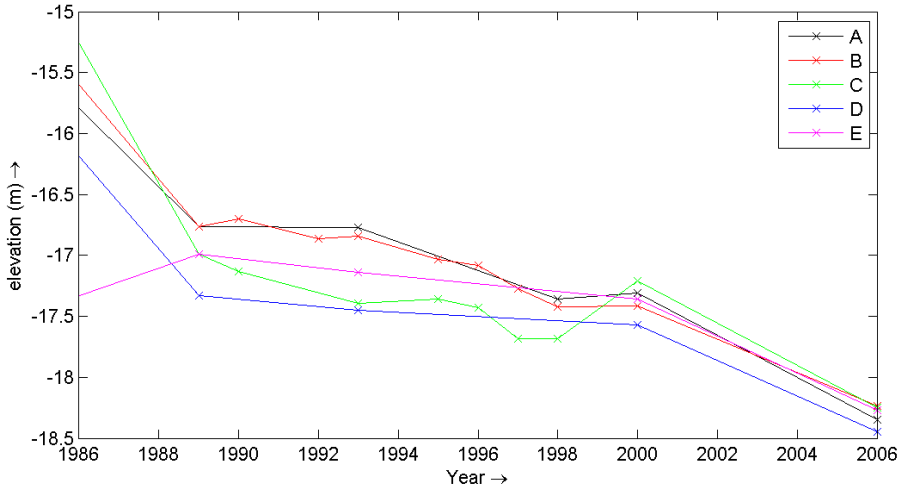

Figure 3.5 Bed levels of five selected points 1986-2006

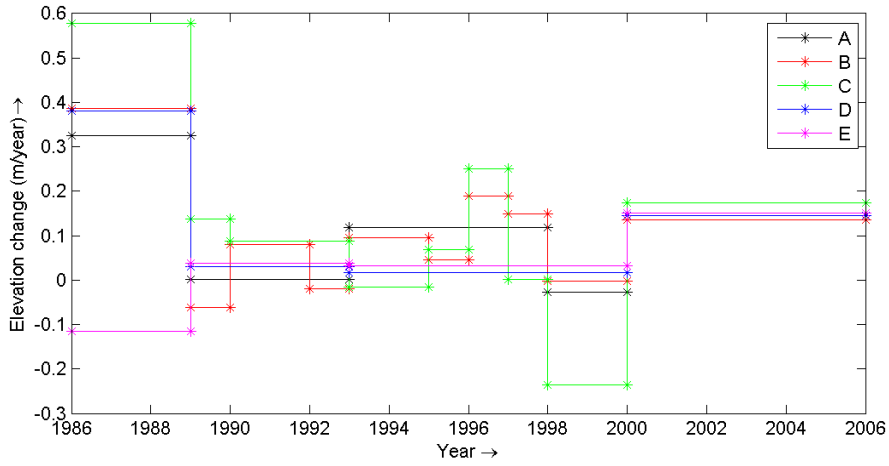

Figure 3.6 Rate of change of the five selected points 1986-2006

For the period 2000-2006 the model gives larger erosion rates. The period between, 1989-2000, is not that straightforward. The average erosion rate is clearly lower than for the other periods. The average is about 3 cm/year. But there is not always erosion in this period. The figure shows occasional accretion. Of course that isn't expected in this area.

From the analysis of the bathymetric data the following conclusions are drawn:

- In the period 1986-1989 there is a high erosion rate in the whole area which is comparable with the computations done with non-cohesive material.
- For the period 1989-2000 a lower erosion rate is observed. There is also more spatial variance.
- The period 2000-2006 shows again a higher erosion rate with a low spatial variance.

The following can be concluded concerning the soil composition:

The soil which is eroded in the period 1986-1989 eroded relatively easily.

In the period 1989-2000 only a few decimetres eroded in the centre of the scour hole. For some periods hardly any erosion is found. A possible explanation for the small erosion rate in this period may be the existence of an erosion resistant layer around a depth of NAP -16.5 and 17.5 m. This will be investigated further in section 3.3.

In the period 2000-2006 no intermediate bathymetric data is available. The average erosion rate is higher than in the period before but lower than expected with merely non-cohesive material.

3.2 Analysis sieve curves

In the former studies a D50 of 0.160mm and a D50 of 0.285mm for the MV2 extension were used. In this study several fractions will be implemented in one case. To determine a good schematization a number of sieve curves are analyzed. Several sieve curves in the area of interest are available. In October 2005 sand samples were taken [Brassinga, Veld-en Laboratorium Gww, Ingenieursbureau Gemeentewerken Rotterdam] and in March 2006 [De Vries, Fugro Ingenieursbureau B.V.] The sample locations are depicted in figure 3.7.

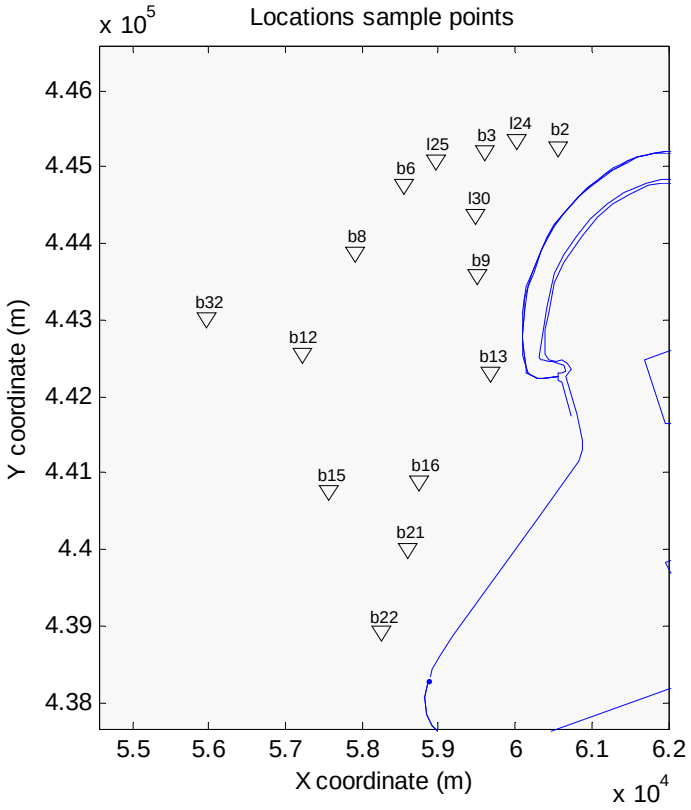

Figure 3.7 Sample locations

At each location a number of samples at varying depths were taken. The fractions in the model have to be vertically uniformly distributed in each defined layer and in this study it will be spatially uniform in the model area. Therefore a representative sieve curve has to be determined from the available curves. In figure 3.7 the locations are depicted and in table 3.1 the depth of sample-position in relation to the bottom are shown for each sample. Also the compositions of the samples are shown here. This composition can explain certain irregularities in the sieve curves.

The locations b2, b3, b6, b8, b9, b13, l24, l25 and l30 are in or around the scour hole. Because of the focus on this area these samples will be rewarded as the most important in the analysis. Sieve curves from other locations will serve only as reference. The samples are taken between 0 and 7.45 meters under the bed-level of the sea (table 3.1).

Table 3.1 Sample depth and composition

Sample nr.	Depth from bed-level (m)	Sand composition	D90/D10
b2_1	0.83-1.15	Sand, clay, soft humus, claylayers, wood-remains	7,4
b2_2	3.68-4.25	Sand, moderate silty, soft humus, claylayers	4,3
b2_3	5.25-6.25	Sand, moderate silty, soft humus	2,4
b3_1	0-0.2	Sand, moderate silty, soft humus, shells	6,4
b3_2	6.0-7.0	Sand, moderate silty, soft humus, shells	3,8
b6_1	0.45-1.45	Sand, moderate silty, soft humus, shells	3,1
b6_2	5.61-6.45	Sand, soft silty, soft humus	3,8
b6_3	6.45-7.45	Sand, soft silty, soft humus, shells	5,2
b9_1	1.4-2.2	Sand, soft silty, soft humus, shells	2,5
b9_2	5.4-6.4	Sand, moderate silty, soft humus, claypieces	5,4
b9_3	6.5-7.4	Sand, soft silty, soft humus	4,6
b8_1	0.75-1.75	Sand, soft silty, soft humus, shells, gravel	2,0
b8_2	2.75-3.49	Sand, moderate silty, soft humus, claypieces, claylayers	3,7
b8_3	4.75-5.75	Sand, moderate silty, soft humus, shells	2,5
b13_1	0-1.0	Sand, soft silty, soft humus, shells, claypieces	3,7
b13_2	2.0-3.0	Sand, soft silty, soft humus, shells, claypieces	3,8
b13_3	4.0-5.0	Sand, moderate silty, soft humus, shells	3,2
b22_1	1.35-2,35	Sand, moderate silty, soft humus, shells	8,4
b22_2	4.35-5.35	Sand, moderate silty, soft humus, shells	3,1
b22_3	7.1-7.45	Sand, soft silty, soft humus, shells	1,9
l24_1	0-0.5	Sand, extreme fine, strong silty, grey, claylayers, shell-remains	3,2
l24_2	1.5-1.9	Clay, grey, moderate fixed, shell remains	4,1
l24_3	2-2.4	Clay, grey, moderate fixed, shell remains	4,4
l25_1	0-0.5	Sand, moderate fine, soft silty, moderate shellcontaining, grey	1,9
l25_2	2-2.5	Sand, very fine, strong silty, moderate clay, soft shellcontaining, grey	9,2
l25_3	2.5-2.6	Clay, grey, moderate fixed	2,5
l30_1	0-0.3	Sand, very fine, moderate silty, moderate clay, clay layers, grey	3,0
l30_2	1.5-1.9	Clay, moderate silty, moderate sandy, shells, grey	5,3
l30_3	2.3-2.4	Clay, moderate silty, strong sandy, grey	3,8

Also deeper sand-samples were available but were considered as irrelevant for this study. All the sieve curves, including the reference sieve curves that are slightly further away from the scour hole, are depicted in figure 3.8. As can be seen in this figure a very wide range of sieve curves is found. For example the D50 has a minimum value of 0.038 mm. and a maximum value of 0.3 mm., which are respectively at location l24 and b6 (figure 3.7) and at comparable depths.

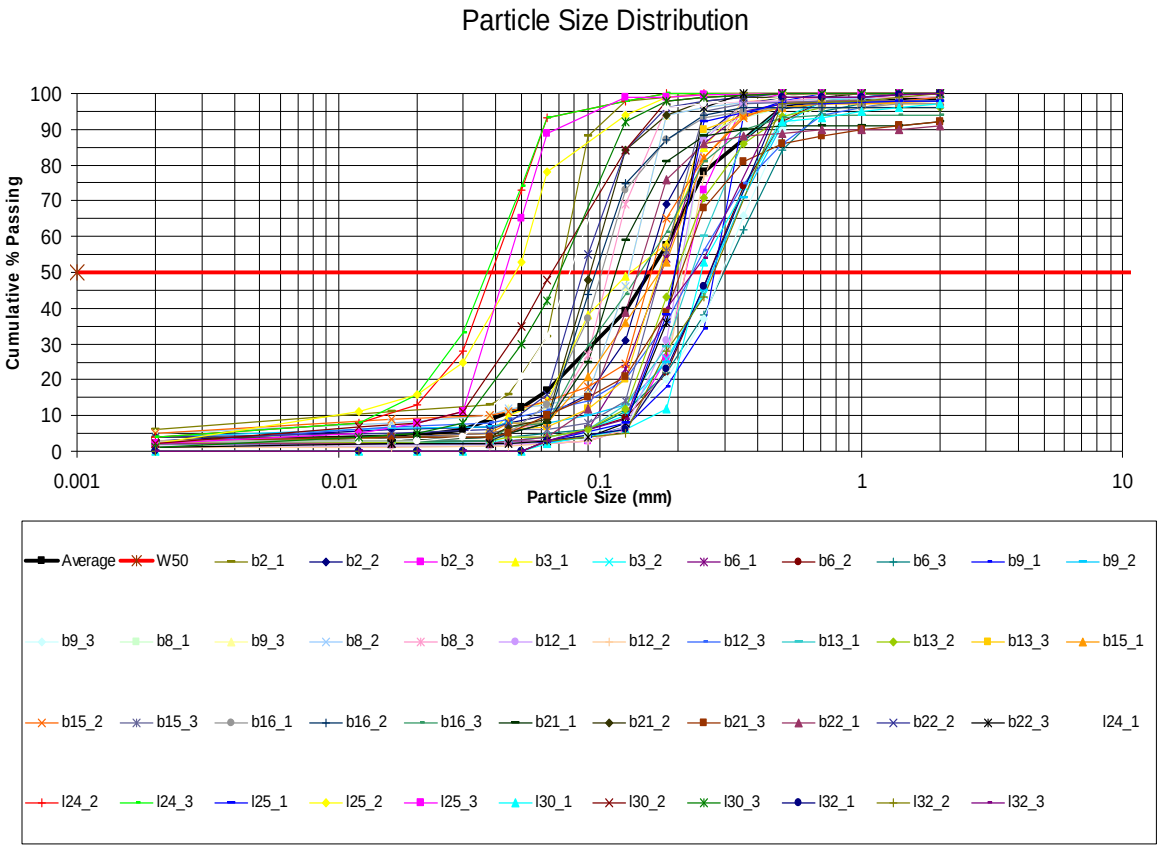

Figure 3.8 sieve curves at all points

3.2.2 Fine material

A remarkable difference can be found between the samples taken in 2005 and the samples in 2006. The samples taken in 2005 were taken in October and the samples in 2006 were taken in March. This can indicate a seasonal difference of the bed composition. The six finest samples were taken in the year 2006. A closer look at these six finest samples (l24_1, l24_2, l25_2, l25_3, l30_3, l32-2) shows that five of these samples are close to the centre of the scour hole. From the remaining 5 samples only sample l24-1 is taken at the surface, the other samples are at least taken 1.5 meter below the sea level. Because of this large depth it is not likely that the fine samples are because of seasonal fluctuations. The particle sizes of the fine samples are classified as mainly silty according to the Wentworth classification where sand is defined as grains with a size between 0.063 mm (very fine sand) and 2 mm (very coarse sand). Material with a grain

size smaller than 0.063 mm can be defined as clay and silt. Also in table 3.1 the samples with the fine gradation are identified as clay or mainly silty. The composition in this table is not derived from the sieve curves but from a direct analysis of the material in the sample.

The fine samples can be defined as mud. (A mixture of water, silt, clay and organic materials) Due to the difference in grain size and cohesiveness, the sediment transport characteristics of sand and mud are different. Because in the model first only non-cohesive material will be modelled the finest samples will not be considered for determining a representative sieve curve.

3.2.3 Armouring by non-cohesive sediment

When armouring occurs the smaller grains are removed from the top layer while the coarser grains remain in place. The top layer of the bed eventually will be transformed into a layer of mainly coarser grains with few sheltered smaller grains. In this sub-paragraph is investigated if the top-layer consists of coarser material than the layers below. If this is not true this will not directly be the evidence for the absence of armouring for two reasons. First, the height of the layer that has been armoured is limited to a few times the particle size. Most of the samples on the other hand are not taken directly at the sea bed but a few decimetres below and is taken in a range of about a meter, which is larger than the height of the armour layer. Secondly, the armouring does not have to occur all of the time, but only during certain flow. In that way it is possible that the curves do not show the armouring effect. This should be recognized in the model.

In figure 3.9 and figure 3.10 the curves of the samples closest to the seabed are compared to the curves of the samples taken directly below. The sieve curves b2_1, b3_1, b6_1 etc. are from samples closest to the seabed and are compared with b2_2, b3_2, etc. which are from samples directly under the upper sample.

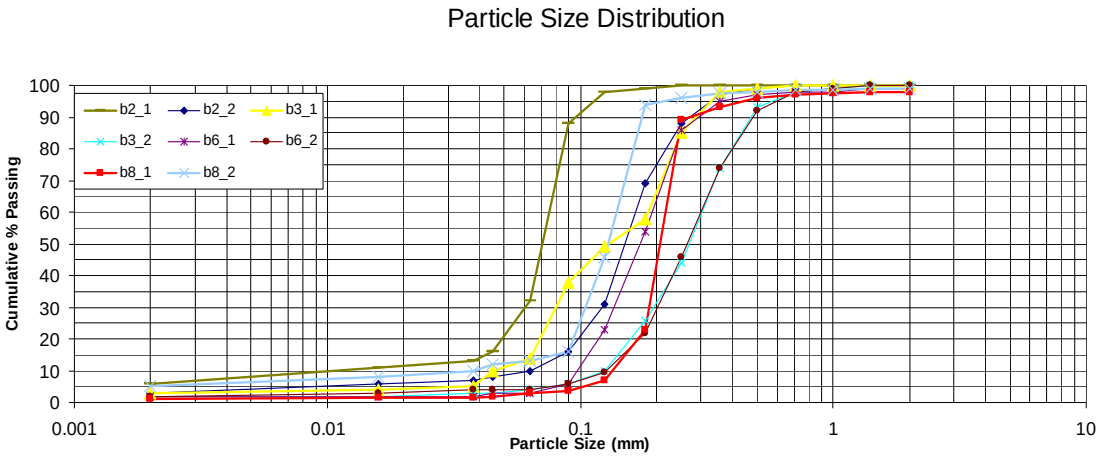

Figure 3.9 Comparison sieve curves

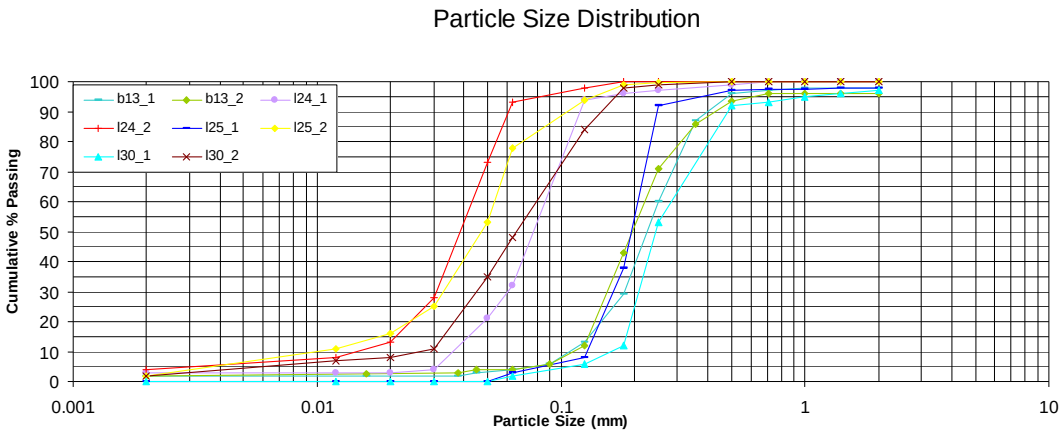

Figure 3.10 Comparison sieve curves

The height between the sea bed and the samples is shown in table 3.1. The table shows that the upper sample of b3, b13, l24, l25 and l30 were taken from the seabed level to several decimetres below. The other samples were taken slightly deeper.

Comparison shows that four of the five locations (b13, l24, l25 and l30) gives a coarser curve for the upper sample compared with the sample directly beneath. The other location shows finer samples at the upper layer. From the three samples taken slightly deeper (b2, b6 and b8 taken at a depth at about a meter under the bed-level) two samples show finer samples at the upper layer. Most of these five sample locations are on the edge of the scour hole and therefore they could show the coarser gradation in the top layer. Because four of the five locations shows coarsening at the top layer these sieve curves can point out the armouring effect.

In table 3.1 also the grading D90/D10 is depicted. Sediment is called well-sorted if the ratio D90/D10 is small (<1.5, although there is no formal classification) and is called well graded for large values of D90/D10 (>3). As can be seen in the table, practically all the samples can be classified as well graded. In well-graded sediment the armouring will happen easier than in well sorted sediment. So this is another indication suggesting armouring in this situation.

3.2.4 Representative curve

Figure 3.11 contains all the remaining sieve curves after removing the curves that are classified as 'clay' or 'mainly silty'. Spatial differences only occur in a few places. Therefore the representative particle size distribution is obtained by averaging all the remaining curves. This representative curve is shown in figure 3.12.

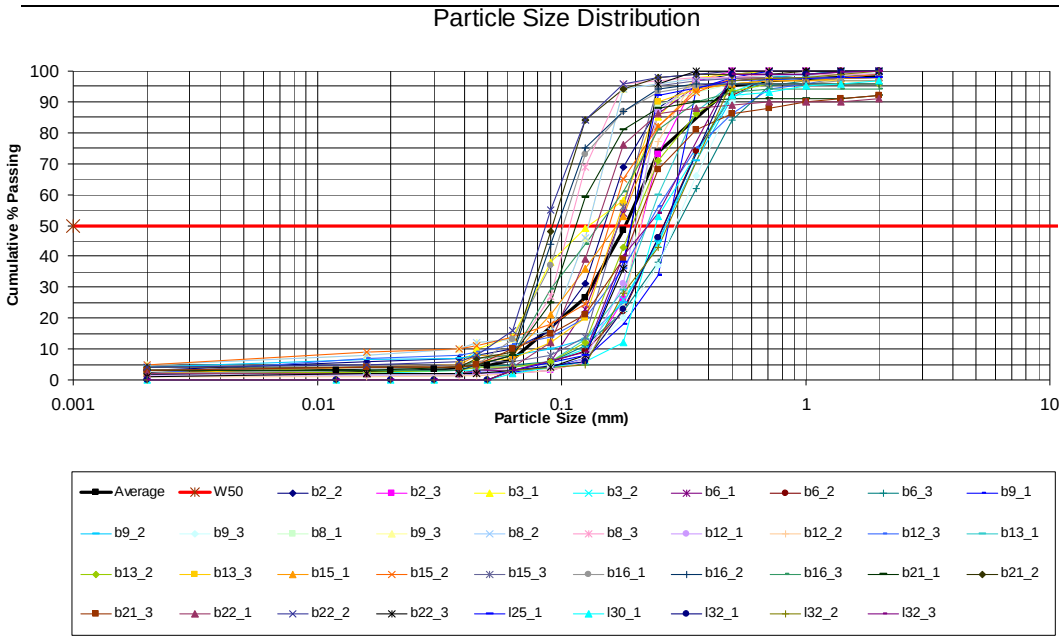

Figure 3.11 Remaining sieve curves

The representative curve as obtained here has a D50 of 0.185 mm and a D90/D10 of 5. The D90/D10 of the representative curve (5.0) is rather high compared to the average value of investigated sieve curves (4.1)

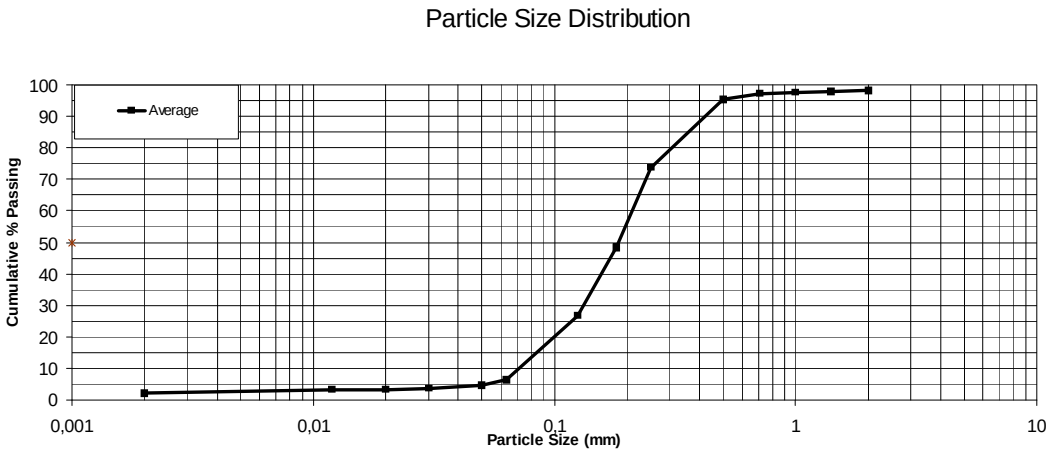

Figure 3.12 Representative curve

3.3 Analysis soil composition MV 1

In the area of interest certain clay layers have been found. Because of the cohesiveness of clay a lower erosion rate is therefore expected and therefore the development of the scour hole will be limited. The area around the scour hole is a former complex estuarine system, composed of highly mobile tidal channels and tidal flats which have resulted in a highly stratified bottom.

In such a stratified system the erosion rate can fluctuate extremely. Sand erodes relatively fast, but when a clay layer has been reached the erosion rate can reduce strongly and in some cases become zero. When a thin layer of clay is eroded away an erosion hole can develop relatively easy again, until a next clay layer will be reached.

To hindcast the scour hole of the Maasvlakte 1 and to forecast the scour hole of the Maasvlakte 2 it is very important to know the position and the location of the cohesive layers. Therefore an analysis will be made of the available sediment samples.

At the sample locations as shown in figure 3.7 a description of the composition of the material is given. One of these descriptions is shown in appendix C. In this appendix the material descriptions are represented from the bed level downwards. In this appendix and also in the material descriptions of the other sample points a very stratified bottom is observed. At every sample point a number of clay layers can be found with different thicknesses and vertical locations. In this paragraph the extension, the height and the number of layers will be analyzed. As can be seen in appendix C there is never just one clay layer but always a number of layers with varying clay content. In this paragraph first the position of the clay layers relatively to the water level and the thickness of the layers will be dealt with. After this the expected soil composition in and around the scour hole is elaborated.

3.3.1 Thickness clay layers and vertical location

In figure 3.13 for each sample location an overview is given of the vertical position of the clay layers. Obviously this is a schematization; there is made a distinction between sand, clay layers and sand with 10 % clay. In paragraph XX the meaning of these layers will be further clarified. There can be made a distinction between the samples found in front of the Slufterbeach (b15, b16, b21 and b22) and the other sample locations (figure 3.7). The samples in front of the Slufterbeach display a thin clay layer around 15 meters below NAP and a very thick layer that begins between 16 and 23 meter below NAP and in three of these four locations this clay layer extends underneath the measurements and therefore the exact height is unknown.
The other locations are of more importance because their location in and around the scour hole. Very clearly the Pleistocene sand underlayer is found. One of the samples (b9) extents until 45 meters below NAP and the sand layer which starts in all the samples around 24 meters below NAP still continues. As can be seen in Figure 3.13 the thickness of the clay layers varies. Most of the clay layers have a thickness around 3 meters. Exceptions are b8, b12 and l32 which have thicknesses around 1 meter and sample location l30 with a thickness around 7 meters. The three locations with the lower clay thickness are located further seaward and can indicate a reduction of the clay layer thickness in the seaward direction. This will be explained in paragraph 3.4.3.

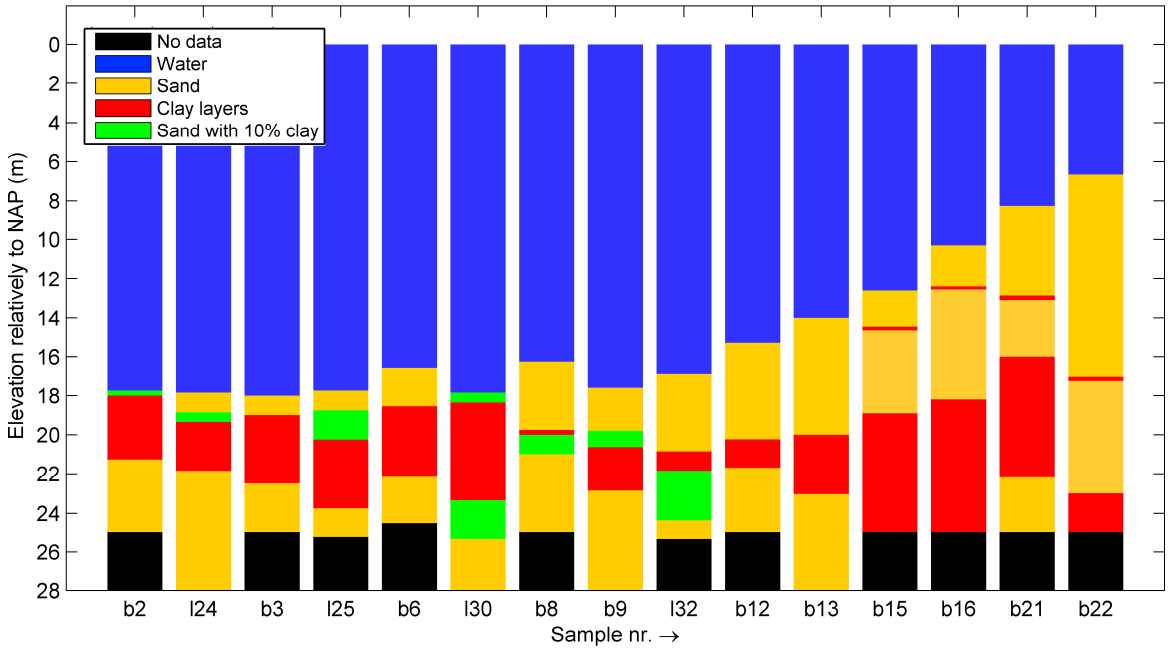

Figure 3.13 Stratification sample points

Vertical location clay layers

The depth on which the clay layers occur also varies from place to place as clearly can be seen in figure 3.13. The clay layers starts between 18 meters and 20 meters below NAP. For the most part of the locations the clay layers are still covered with a layer of sand. There are actually two locations where the clay occurs at the surface of the sea bed. Namely location b2 and l30.

For the Maasvlakte 1 case the clay layers are expected to have a reducing effect on the depth of the scour hole. This will only happen when the clay layer is actually at the surface of the sea bed.

Sample location b9, which is relatively close to the centre of the scour hole, shows that the clay layer is not reached yet. At this location there is still a sand cover of 3 meters. The question whether in the rest of the scour hole the clay layer occurs at the bed surface is difficult to answer. Sample location b9 suggests that there is no effect of the clay-layer and the samples b2 and l30 on the other hand do show a clay layer at the bed surface.

3.3.2 Soil composition in the scour hole

In figure 3.14 the measured bottoms in 1986 and 2006 are shown with the sample locations. The extent of the scour hole is difficult to define because the extent is large but strongly decreasing with the distance to the Zuiderdam. Therefore it is not possible to specify if a location is located in or outside the scour hole. In the figures can be seen that the maximum water depth in the scour hole is around 16 meters in 1986 and 19 meters in 2006. Actually in none of the examples directly around the scour hole a clay layer is observed at 16 meters below NAP. Except the samples in front of the Slufterbeach, which show a very thin clay layer around 15 meters below NAP. According to the former paragraph clay is expected around 17 meters below NAP. Most of the samples show clay at a deeper point.

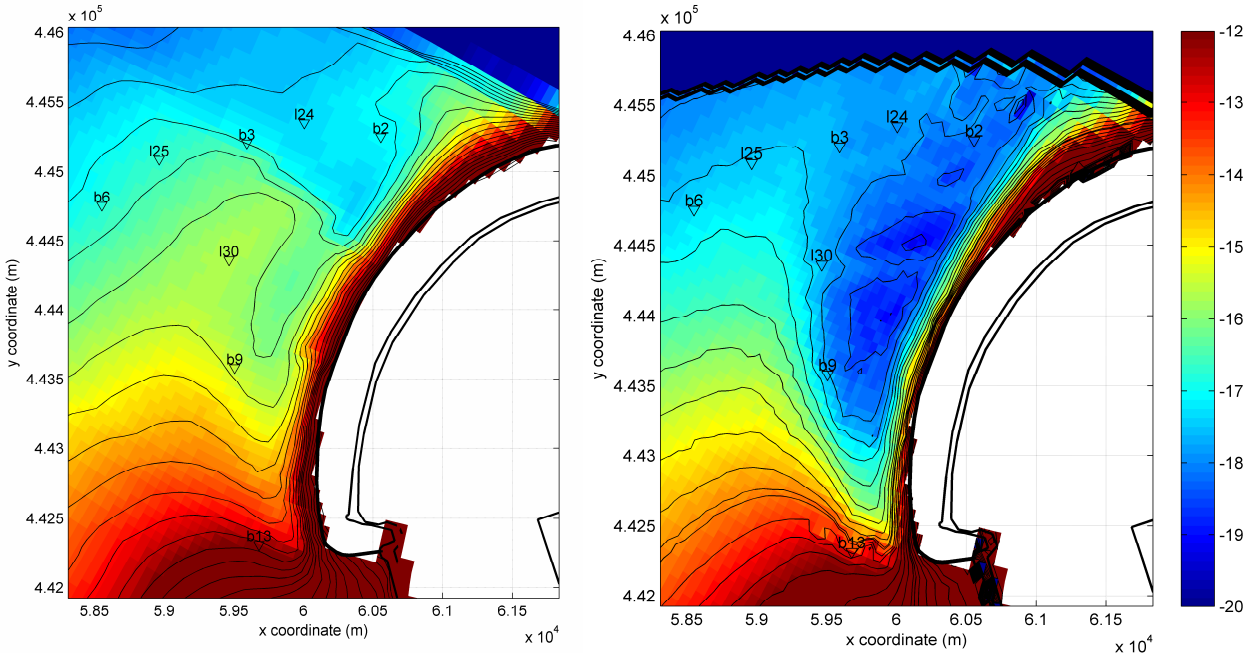

Figure 3.14 Measured bed 1986(left) and measured bed 2006 (right) with sample locations

Three sample points are close to the centre of the scour hole and need a further investigation. Lines are drawn perpendicular to the Zuiderdam and through these sample points as shown in figure 3.15. Cross sections of these lines give a good view of the positions of these samples in the scour hole. In figure 3.16, figure 3.17 and figure 3.18 these cross sections are shown for respectively b2, b9 and l30. In these figures the cross section of the measured bed level in the year 2000, 2006 and the computed bed level in 2006 are depicted. This bed level is computed in chapter 4 and is computed with tide only and uniform sediment with a diameter of 0.200mm. As can be seen none of these samples is in the centre of the scour hole.

In the computations with the Delft3D model as performed in the chapters 4 and 5 the scour hole was overestimated. But as stated in chapter 4 the *extent* of the scour hole is similar for the computations and the measurements. Only the depth of the centre of the scour hole is overestimated. For the points b9 and l30 the scour depth outside the centre becomes larger for the measurements as for the computations for a certain distance to the centre as can be seen in Figure 3.17 and Figure 3.18. Sample point b9 lies in the area where the model underestimates the scour hole.

As stated in the former paragraph sample point b9 suggests that there is no effect of clay because this sample point is still covered with a sand layer of three meters. Because b9 lies within an area where the depth with the model is underestimated is seems to be logical that on that place no clay occurs at the surface.

The underestimated area can be well explained with the fact that the places were clay occurs results in a lack of erodable material and therefore there will be extra erosion on the places were the soil is easier to erode.

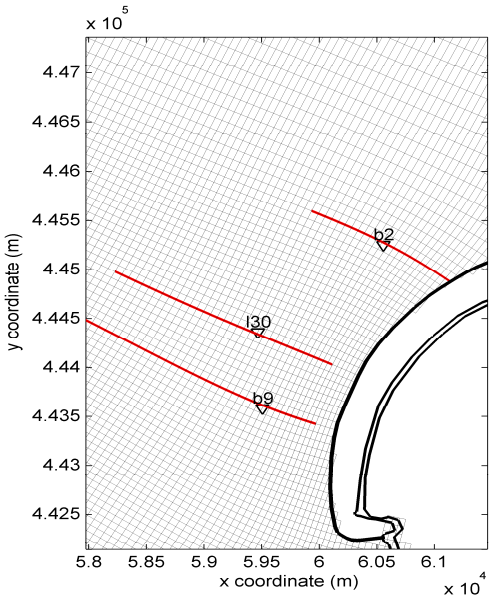

Figure 3.15 Locations cross sections through sample points

The locations b2 and b9 lie on positions in the scour hole which actually are overestimated in the computer model. As can be seen in figure 3.13 these points also expose clay which can be part of the explanation for the overestimation.

3.3.3 Indication from a geological setting

The geological setting is highlighted in appendix B. As concluded in this appendix the area of interest i.e. the stratified part is a former complex estuarine system, composed of highly mobile tidal channels and tidal flats with a number of layers with different composition in time and space. Also is stated that the stratified system is located lower when directed seaward due to the original slope of the bed.

3.3.4 Composition different layers

In figure 3.13 a schematization was made of the clay layers. Distinction between clay layers, sand with 10% clay content and normal sand was made. Sand: as can be seen in appendix C the majority of the soil consists of at least 90% sand.
Clay layers: In every sample point on a certain distance a number of layers with different content is found. The composition of these layers consists of clay, silt, sand, peat and shells in different proportions. Observed proportions are 90% clay mixed with sand, 100% peat, 40% clay with 40% peat silt and 20 % sand and so on. Most of the top of the layers consists of at least 70 % clay with a thickness of one meter.
Sand with 10% clay: recurrently a layer with a content of 10% clay is found near the bed surface, even with this low clay content influence on the erosion process is expected but this influence shall not be as large as with the clay contents observed in the other layers. Therefore these layers are separately mentioned in the figure.

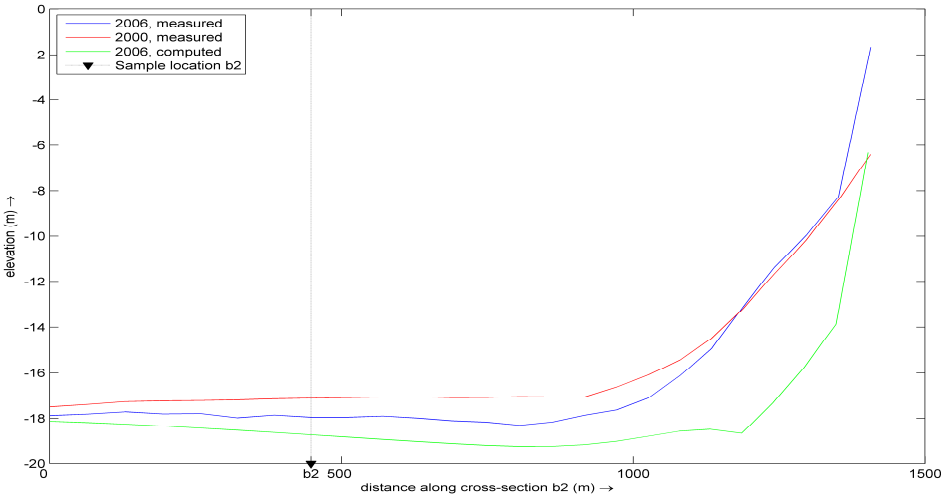

Figure 3.16 Cross section through sample point b2

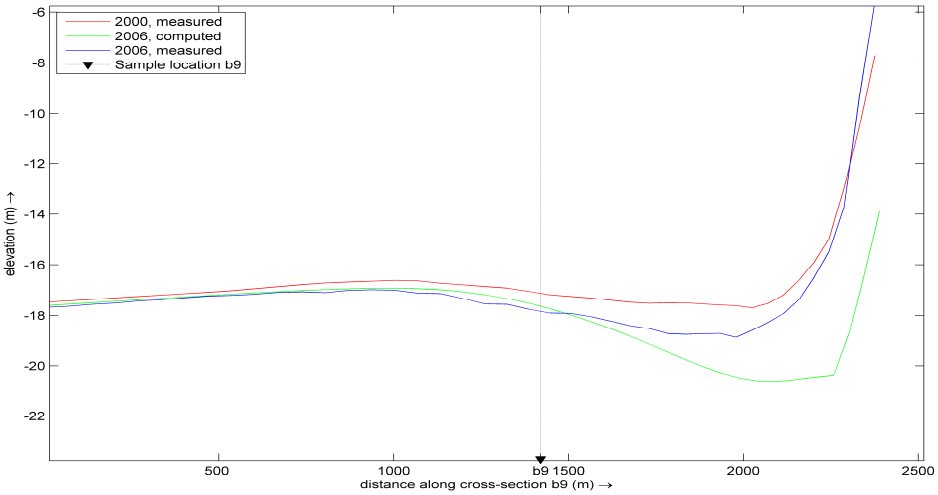

Figure 3.17 Cross section through sample point b9

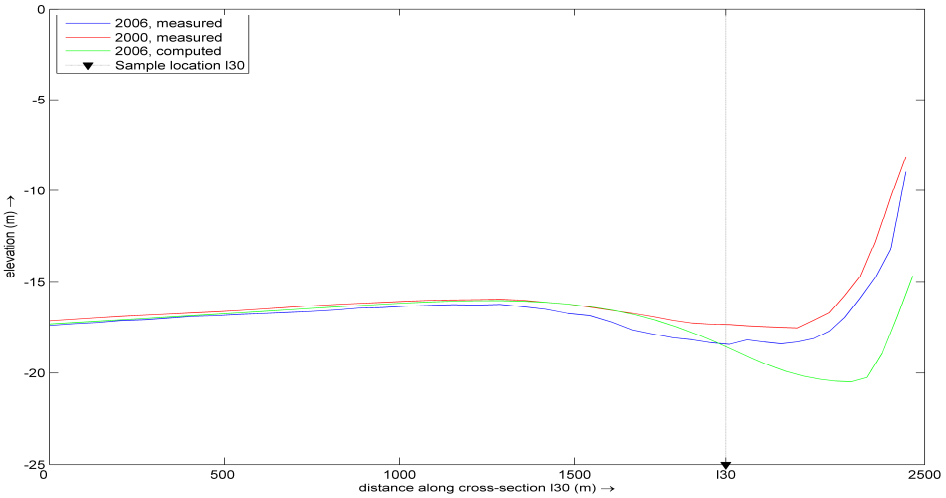

Figure 3.18 Cross section through sample point l30

3.3.5 Conclusion occurrence cohesive sediment around scour hole

From the previous two paragraphs some remarks can be made on the occurrence of clay layers in the area of the scour hole.

- From the erosion rates it can be concluded that there is a layer located between 16.5 and 17.5 meters below NAP which was hard to erode. Beneath this layer a less hard to erode layer exists.
- Two samples locations expose a clay layer, namely location b2 and l30. This is at depths of respectively 17.75 and 17.85 meters below NAP. These two locations are the only locations where the computed scour hole is overestimated.
- Surrounding locations like b3, b6, b9 and l24 do not show a clay layer at depths around 16.5 and 17.5 meters but neither at the depths at which the locations b2 and l30 do show clay. They start around 19 meters below NAP.
- Sample locations in front of the Slufter beach display a thin clay layer around 15 meters.
- Geotechnical analysis suggests that the clay is positioned higher when positioned more easterly.

The sand composition samples are all taken in 2005 and 2006. For the hindcast of the development of the scour hole we are in particular interested in the material which is scoured away. Two periods will be hindcasted, namely the period 1986-2000 and the period 2000-2006. Therefore the composition of the bottom in 1986 and 2000 is of interest. In this time material is eroded in the centre of the scour hole from 16 till 19 meters below NAP. So, actually the composition of the bottom between 16 till 19 meters in and around the scour hole is important.

It is clear that cohesive material is only exposed in the centre of the scour hole and directly around: The surrounding sample points do not show any clay at the surface. In the regarded time period, 1986-2006, there is not much material eroded away at these points. Therefore no clay is expected near the surface.

From sample locations b2 and l30 can be concluded that there exists clay at higher points than found in the samples surrounding the scour hole. This means that this clay layer either vanishes some distance from the scour hole or the clay layer descends. In both ways it is possible that the clay layer was considerably thicker in the centre of the scour hole and also extended between 16 till 19 meters below NAP. From a geological point of view it is also likely that the clay layer is positioned higher when located more easterly.

Spatial variation

In figure 3.14 (right) the bed level for the year 2006 is depicted. The scour hole is not totally regular. As the soil would be spatially identical the bottom of the scour hole would be regular or smooth. Now there are holes and humps at the bottom. This is because also spatially the clay has not everywhere the same composition and on some places will erode more easily than on other places. The extent of the clay layer which occurs at the surface of the bottom was probably growing in the time until the extent was that large that the clay layer was located to deep at the seaside.

3.4 Analysis soil composition MV2

In this paragraph the occurrence of cohesive layers in front of Maasvlakte 2 will be investigated. The position and the thickness are important for the extent of the scour hole.

The locations of the sample points are shown in figure 3.19. The points b6, b8, b12 and l32 are closest to the scour hole which will develop according to simulations in former models. Location l32 is located in the southern part of the expected scour hole (not in the deepest part). The locations b6, b8 and b12 are located eastward of the expected scour hole.

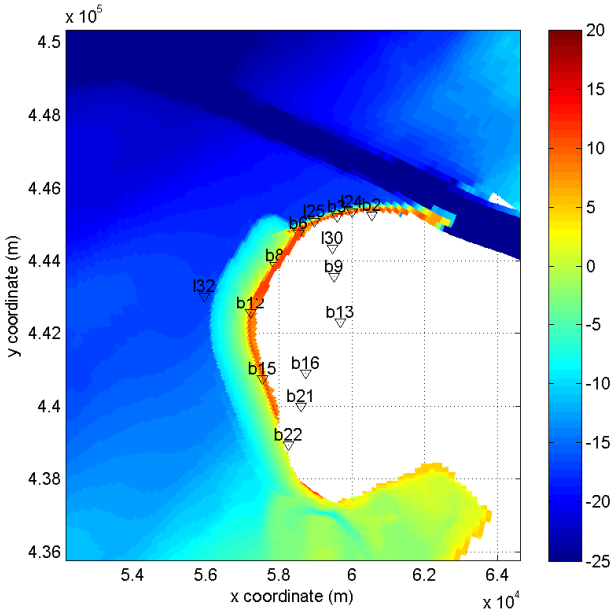

Figure 3.19 Sample locations

In figure 3.13 the locations of the clay layers are depicted for all the sample locations. The concerning locations are also displayed in table 3.2.

3.4.2 Vertical position clay layer

The vertical location where the clay layer starts is around 20 below NAP for all locations. As can be seen is the clay layer in location l32 located lower than in the other sample locations. This can be explained from a geotechnical point of view (appendix B).

Location l32 is considered as most important because of its location in the expected scour hole. Especially for the vertical location of the cohesive layers this sample is important because of the descending vertical location of the cohesive layer in seaward direction. The expected scour hole extents more seaward than sample point l32 is located. Therefore it is possible that the clay layer lies deeper than observed at sample point l32. Extrapolation of the clay depth from the sample points b13, b12 and l32 suggest that the maximum starting depth of the cohesive layer should not be below 22 meters below NAP.
The sample points b6 and b8 show a slightly higher located clay layer compared to sample points b12 and b13. It seems that the clay layer is located higher more northward. Therefore it is also possible that the clay layer is positioned

higher in the northern part of the expected location of the scour hole. It is not expected that the clay layer is located higher than in the sample points b6 and b8. The clay layer therefore is expected to start between 19 and 22 meters below NAP.

Table 3.2 Position clay layer in front of Maasvlakte 2

Location	Position in relation to NAP (m)		Thickness layer (m)	
	clay layer	sand with 10% clay	clay layer	sand with 10% clay
b6	18,55-22,16	-	3,61	-
b8	19,76-20,00	20,00-21,00	0,24	1
b12	20,23-21,69	-	1,46	-
l32	20,85-21,85	21,85-24,35	1	2,5

3.4.3 Thickness clay layer

The thickness of the clay layer has a high range for the four considered samples. If the sand with 10% clay content is also considered as a cohesive layer the thickness ranges from 1.24 to 3.61 meter. It is possible that the thickness declines in seaward direction considerably so that there is no cohesive layer left at the seaward side of the expected scour hole.

3.5 Accretion Maas trench and nourishment Slufter beach

The accretion of the trench of the Maas in reality is derived from dredging data. Here is assumed that only the accreted sand has been dredged. In table 3.3 the available dredge-data is depicted [source: R.C. Steijn, 2000 for the period 1985-2000 and H. Otten, RIKZ for the period 2000-2006]. The table shows the dredged material over the period 1985-2006 in the first 5 kilometres of the trench, measured from the most westerly point of the Noorderdam. The dredged material differs from year to year with a maximum of 3.255.000 m^3 in 1995 and a minimum of 936.000 m^3 in 1989. The average dredged material per year over the period 1985 -2000 is 1.622.133 m^3 and over the period 2000-2006 is 1.536.211 m^3. Especially the dredged material in 1995 is large. The extreme river discharge this year can be a reason for this. In 1996-1997 an experimental trench of 7 million m^3 is dredged in the trench of the Maas. This experimental trench is refilled in the years after 1996. A mean of 697.000 is accreted yearly in this trench. This is already added in table 3.3.

Table 3.3 Dredged volume 1985-2006

Dredging data 1985-2006	
Year	Dredged 0-5 km (m^3)
1985	1.809.000
1986	1.652.000
1987	1.669.000
1988	1.647.000
1989	936.000
1990	2.517.000
1991	1.043.000
1992	1.702.000
1993	1.087.000
1994	2.123.000
1995	3.255.000
1996	1.215.000
1997	1.180.000
1998	1.152.000
1999	1.345.000
2000	1.471.900
2001	1.792.930
2002	1.534.630
2003	1.999.570
2004	1.374.484
2005	1.551.604
2006	1.028.362
Mean '85 – '99	1.612.742
Mean without '95	1.505.500
Mean without '89	1.671.143
Mean '00 – '06	1.536.211

Nourishment

During the nineties there was nourishment at the Slufter beach. The mean nourishment volume was 728.000 m^3/year for the period 1990-1998 [Steijn, 2000].

3.6 Conclusions

In this paragraph the main findings which are done in this chapter are summarized. Also two hypotheses are posed which will be handled in the rest of this study.

3.6.1 Maasvlakte 1

Bathymetric data

From the analysis of the bathymetric data some important conclusions can be drawn:

- In contrast to what was suggested in former studies the scour hole did not reach equilibrium yet. The scour hole still develops.
- The erosion rate in the scour hole fluctuates. Three periods can be distinguished: (see also figure 3.5)

  1986-1989: high erosion in the whole area which is comparable with the computations done with non-cohesive material (chapter 4)

  1989-2000: Low erosion with more spatial variance

  2000-2006: higher erosion rate with a low spatial variance

Analysis sieve curves

The analysed sieve curves show a very wide range. Some of the samples contain a very high clay-content and are not considered for determining a representative curve. The representative particle size distribution is obtained by averaging the remaining curves (figure 3.12).

Comparison between samples from the bed level and slightly below gives in four of the five investigated locations a slightly coarser sample for the upper sample compared with the sample directly beneath. This can point out the armouring effect. But actually in the case of armouring a more clearly difference is expected. This does not directly imply that there is no armouring for two reasons: 1) An armour layer can be considerably smaller than the range where the sediment samples are taken in. 2) The armouring does not have to occur all the time, but only during certain flow.

Analysis soil composition and cohesive layers for the MV1-case

For the hindcast of MV1 it is difficult to determine what kind of sediment is scoured away in the period 1986-2006. There are four indicators which suggest that part of the erode material was cohesive material:

- Strong alternating erosion rate (paragraph 3.1) suggest difference in bed material
- An irregular bed level is observed (paragraph 3.1), which suggest a spatial variation of the bed material
- Clay is exposed at two locations close to the centre of the scour hole
- Geotechnical analysis suggests clay on higher positions in the area of interest (Appendix B)

Two hypotheses

There can be assumed that the large overestimating of the scour hole by the model is due to the composition of the bed material. It is not likely that this large difference with the reality can be explained by irregularities in the hydrodynamics.

For the composition of the eroded material of the scour hole there are two hypotheses.

1. There is only non-cohesive material exposed in the scour hole in the period 1986-2006. The overestimation of the scour hole by the models is due to two reasons. 1) The effect of armouring is not taken along. 2) As will be seen later in this study (chapter 6) smaller sediment diameter do not result in a larger but in a smaller scour hole. A large availability of small sediment particles in the system during several years is the reason of the strong alternating erosion rate. The material which is indicated as clay at the bed surface is not the suspected old clay but young clay or silt.
2. There is cohesive material exposed in the scour hole in the period 1986-2006. There are several layers with different clay content and therefore a different erosion rate is observed in this period.

Obviously there are many variations on these two hypotheses. But for simplicity these two hypotheses will be investigated separately in respectively chapter 6 and 7.

3.6.2 Maasvlakte 2

Sieve curves

Paragraph 3.2 showed that there was hardly spatial difference in the analysed sieve curves. Therefore the same representative sieve curve as used for the Maasvlakte 1 situation can be used for the Maasvlakte 2 situation.

Analysis soil composition and cohesive layers for the MV2-case

From four soil samples close to the expected scour hole in front of the Maasvlakte 2 there can be expected that a cohesive layer starts between 19 and 22 meters below NAP. The thickness of this cohesive layer has a high range (1.24 to 3.61 meter) but it is also possible that there is *no* cohesive layer in the most seaward area of the expected scour hole.

Chapter 4 MV1, tide only

For understanding the flow around the MV1 the case is first modelled without the forces of waves and wind. The results of this model can be used as a reference for the further cases in this study where step-by-step complexity will be added to the model.

First a short description of the hydrodynamic processes and the sediment transport by these processes will be given (4.1). In paragraph 4.2 the criteria which the simulations in this chapter are validated against are shown. in paragraph 4.2. Two periods are modelled with the tide only, the period 1986-2000 and 2000-2006. The model output will be compared with reality and analysed in paragraph 4.3. Paragraph 4.4 shows the conclusions of this chapter.

4.1 Hydrodynamic processes and sediment transport

Tidal forces generate a long-shore current. The direction of this current normally turns when going from ebbing tides to flooding tides and vice versa. Tidal forces are deterministic; they do not depend on weather or climate conditions. Once the tidal constituents (amplitude and phases) are known from measurements, tidal forces can be forecasted.

As described in chapter 2.4 these tidal forces are imposed at the open boundaries of the model by means of water levels. The sediment transport is calculated with the formula of Van Rijn (1993). This formula is based on the concept: S=v*c. (Sediment transport= flow velocity * sediment concentration). The transport of sediment is a combination of bed load and suspended load. Van Rijn distinguishes between sediment transport below the reference height that is treated as bed load transport and that above the reference height that is treated as suspended load.
For sediment transport in Delft3D the Online Morphology module is used. The transport is calculated at the same time as the flow by the advection diffusion solver in the flow module. Besides this the bottom transport is computed locally. Delft3D computes total change in sediment by summation of the change of the suspended load the change due to the suspended load correction vector and the change due to bed load. Suspended sediment exchange with the bed is implemented by means of computing sediment sources and sinks near the bottom of the flow by using a reference height and a reference concentration. Bed load transport is computed in vectors at the water level points and uses a different numerical scheme [Lesser et al., 2004]. The used time steps are equal but there is a significant difference in time scale between the flow and the morphology. Therefore a so called morphological factor can be used. This morphological factor simply increases the depth changes by multiplying with a constant factor n. This means that after a simulation over one time step the morphological changes has been modelled over n time steps. For formulae and further explanation is referred to the Delft3D flow manual and [Lesser et al.].

Tide driven flow pattern around the MV1
In figure 4.1 the flow pattern around Maasvlakte 1 are shown respectively for the flood and the ebb situation. In these figures the colour patches give the absolute value of the depth-averaged velocity and the vectors give the actual direction.
In front of the Zuiderdam (the breakwater around the Maasvlakte 1) acceleration and deceleration of the flow are clearly visible in the figures. It flows around the

hard construction of the Zuiderdam as can be seen with the vector arrows. This contraction of the flow happens for the ebb flow as well as for the flood flow. The highest flow velocity is directly in front of the Zuiderdam and is indicated with the darkest colour red. Just above the Zuiderdam the trench to the Euro-Maas decelerates the flow because of the larger water depth. Directly below the Zuiderdam, in front of the Slufter beach the 'normal' flow velocity occurs with decreasing flow velocity in the direction of the coast perpendicular on the streamlines.
In figure 4.2 the depth averaged flow velocity is shown for the contracted flow just in front of the Zuiderdam and just before the flow is accelerated directly below the Zuiderdam. In this figure can be seen that the maximum depth averaged velocity during flood is higher than during ebb. This is within the area of contraction and outside this area and is due to the asymmetry of the tide. This leads to a maximum ebb and maximum flood velocity in the contracted area of respectively 0.85 m/s and 1.1 m/s.

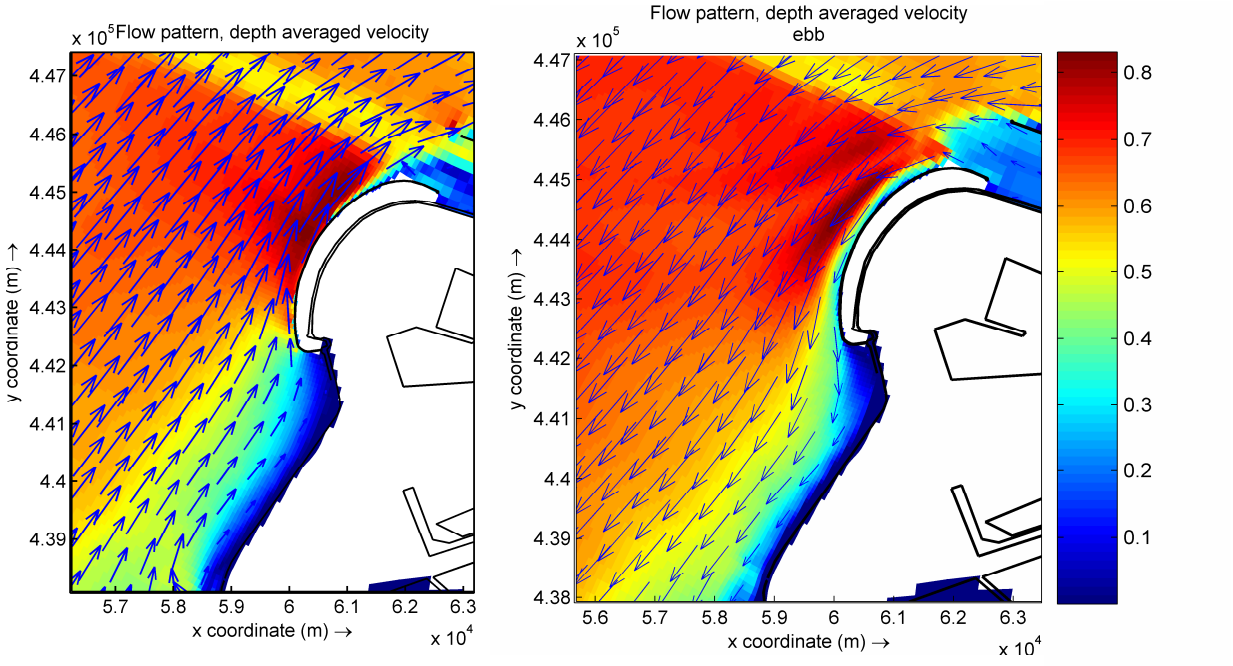

Figure 4.1 Flow pattern around the Maasvlakte 1

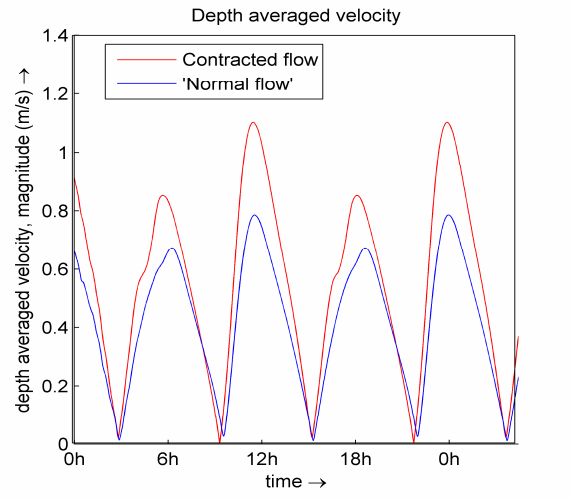

Figure 4.2 Depth averaged velocity

4.2 Validation flow model

This case, where no waves are present, will be validated against several criteria. Though there are certain shortcomings of the model, (besides the lack of waves there is also no sediment-nourishment mode incorporated) this model can be used as a reference model for the further cases where step-by-step complexity will be added to the model.

The following criteria are tested and analyzed for this case and will be tested for the next cases:

- Comparison of measured and calculated erosion and sedimentation pattern. In this way the development of the extent and the depth of the scour hole can be analyzed.
- Comparison of measured and calculated cross-sections on three places through the scour hole (see figure 4.5). In this way a good overview can be seen of the development of the depth of the scour hole in these cross-sections.
- Comparison of measured and calculated eroded volume
- Comparison of computed cumulative dredging demand in the trench of the Euro-Maas with the amount of dredged material in reality.

4.3 Simulation

By the beginning of this study complete bathymetric data of the area of interest was available for three years: 1986, 2000 and 2006. Therefore two simulations have been done: One for the period 1986-2000 and one for the period 2000-2006.

4.3.1 Cumulative erosion and sedimentation

In figure 4.3a the measured sedimentation-erosion for the period 1986-2000 is shown. In figure 4.3 b,c and d the computed sedimentation-erosion respectively 5, 10 and 14 years after 1986 are shown. In figure 4.4 the measured and computed sedimentation-erosion for the period 2000-2006 is shown.

In the measured sedimentation-erosion clearly a triangular shape in front of the northern part of the Zuiderdam with zero sedimentation-erosion can be seen. It is assumed that the bathymetrical data from 1986 of this area is not correct. Though only half of the scour hole now is covered with correct data, this data will be used for validation. As can be seen in the measured erosion 2000-2006 no triangle occurs and an erosion pattern as expected from the flow pattern as shown in figure 4.1 is observed. Because there is still erosion in the period 2000-2006 there can be concluded that also in reality probably no equilibrium for the scour hole is reached yet.

In reality there is erosion in front of the Zuiderdam. Though if this reality is compared with the computed erosion large differences occur. For both periods a large overestimation of the erosion is found.

The extent of the erosion seems to be quite similar if the measured erosion is compared with computed erosion. A slightly larger extent is found in reality. But especially the height of the erosion and therefore the depth of the scour hole differ a lot when the computations are compared with the measurements.

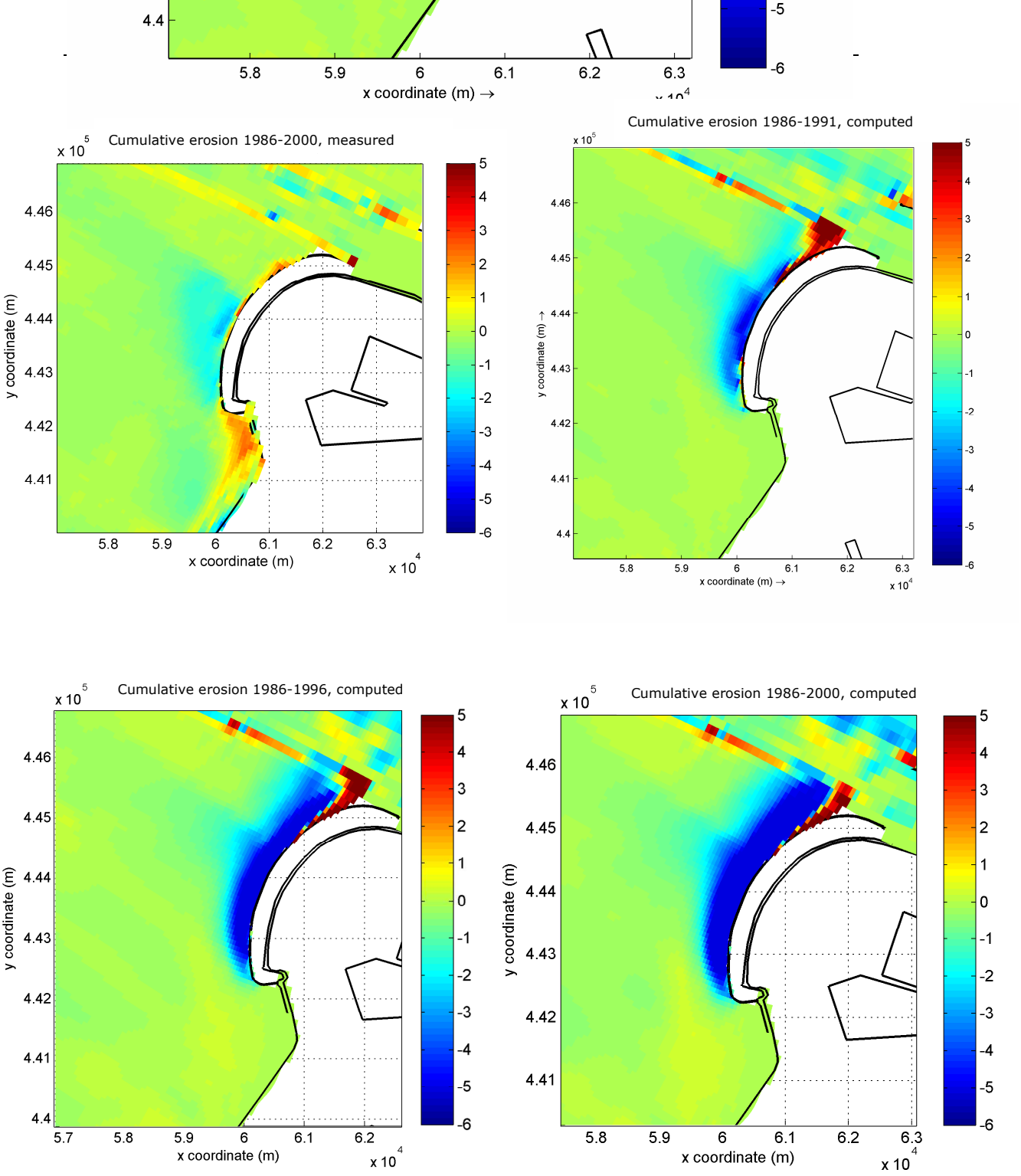

Figure 4.3 Measured and computed erosion 1986-2000

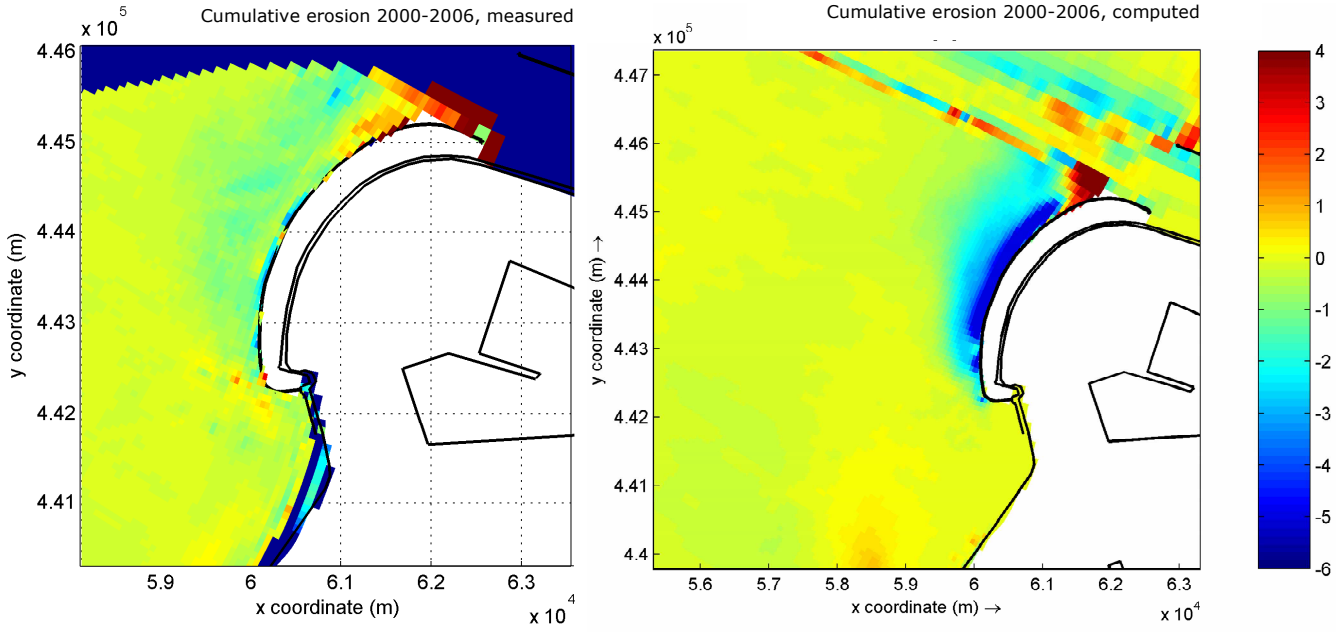

Figure 4.4 Measured and computed erosion 2000-2006

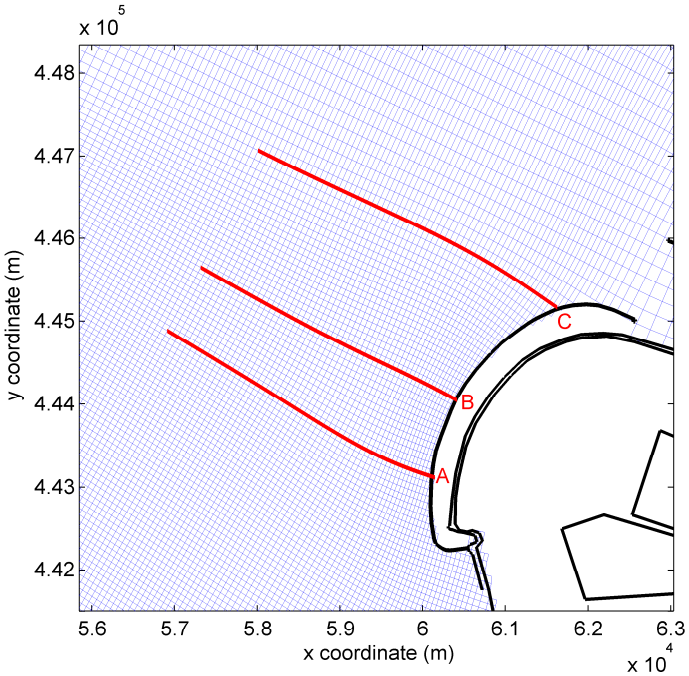

Figure 4.5 Location cross sections

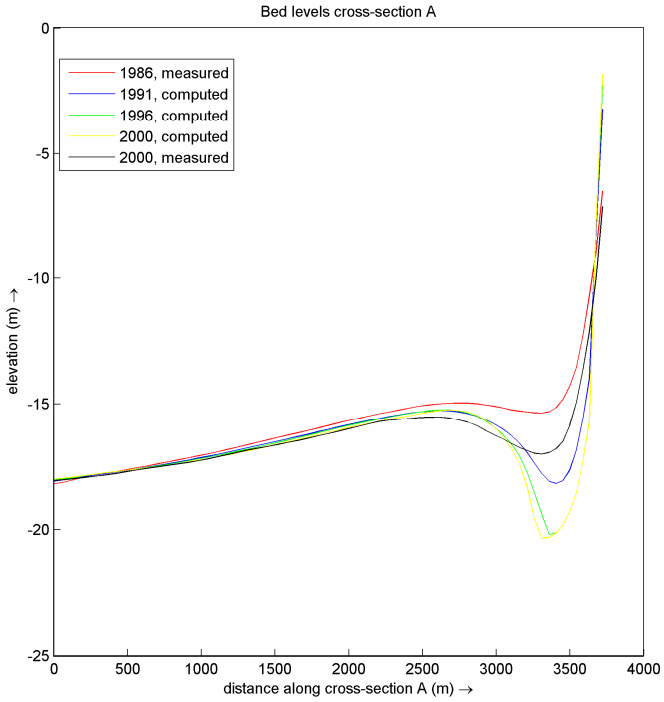

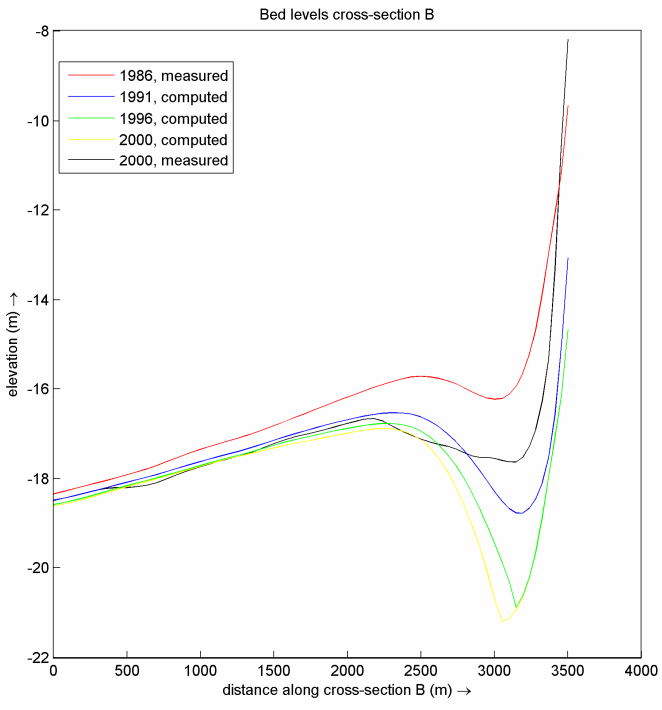

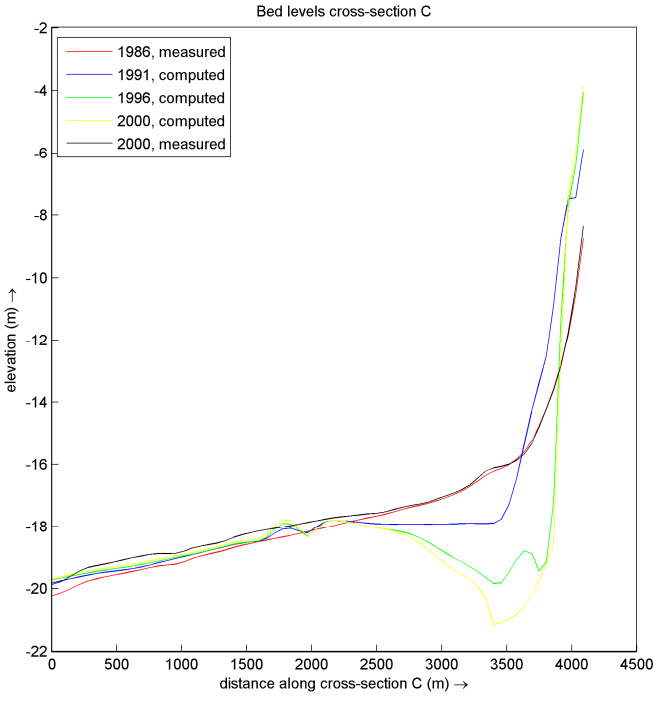

Figure 4.6 Bed levels cross-section A,B and C 1986-2000

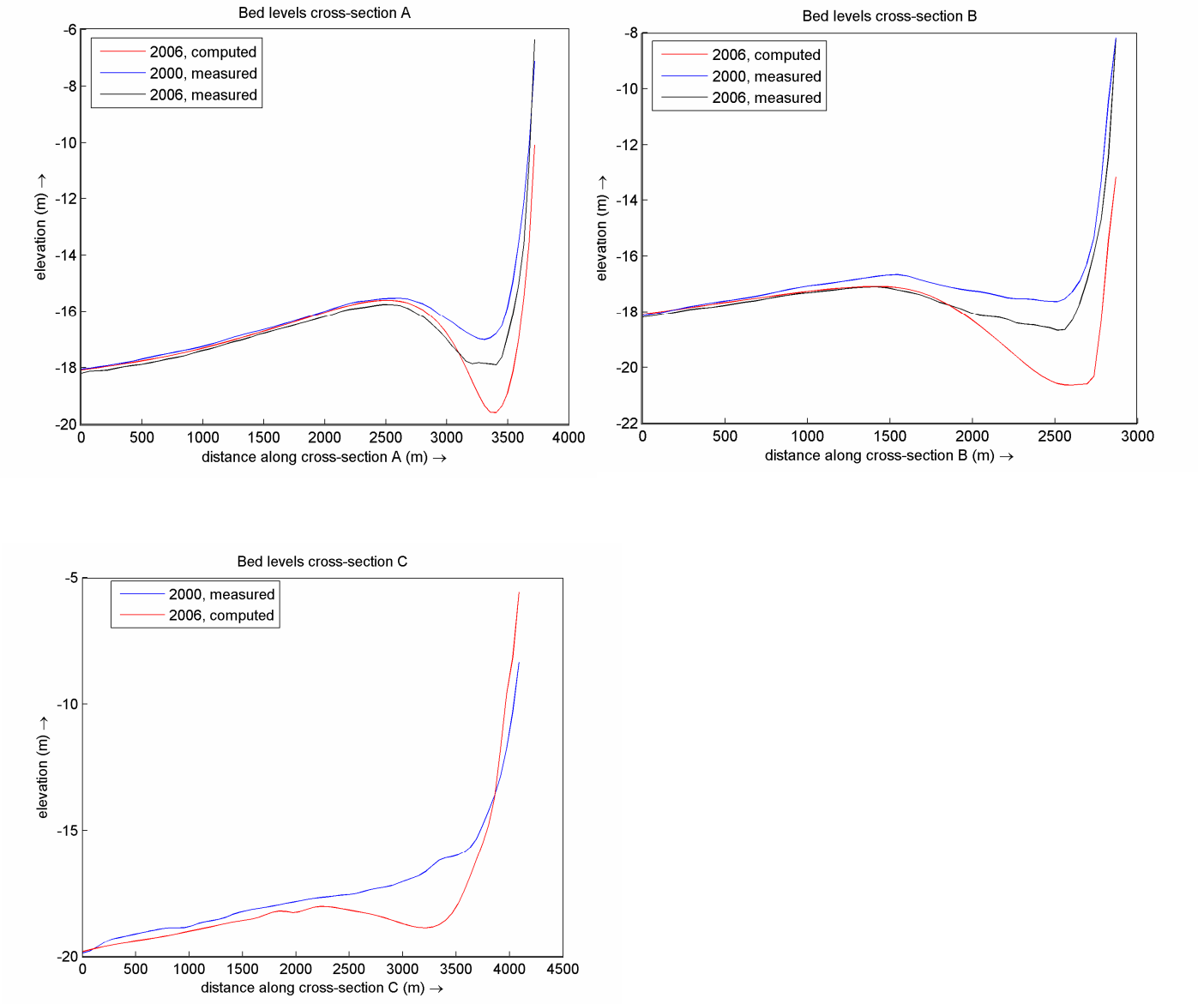

Figure 4.7 Bed levels cross-section A,B and C 2000-2006

4.3.2 Cross sections

In figure 4.6 and figure 4.7 three different cross sections are shown for respectively the period 1986-2000 and 2000-2006. The places of the cross-sections are shown in figure 4.5. Every figure includes the measured and the computed cross sections. In this figures clearly the difference can be seen in depth of the scour hole between the measurements and the computations. It can also be seen that there is hardly difference in the extent of the scour hole, the reality show a little wider extent. The extent of the scour hole is defined here as the area where descending of the seabed starts in the cross shore direction in the direction of the coast.

4.3.3 Eroded volume

The eroded volume is determined for the polygon which is shown in figure 4.8. This is only done for the period 2000-2006 because part of the 1986 data is incorrect. The volume which is eroded away in reality for the period 2000-2006

is: 3.80 * 10^6 m^3. The volume which is eroded away following from the computations is 8.40 * 10^6 m^3.

Also here a large overestimation of the erosion in the scour hole has been found when reality is compared with the model.

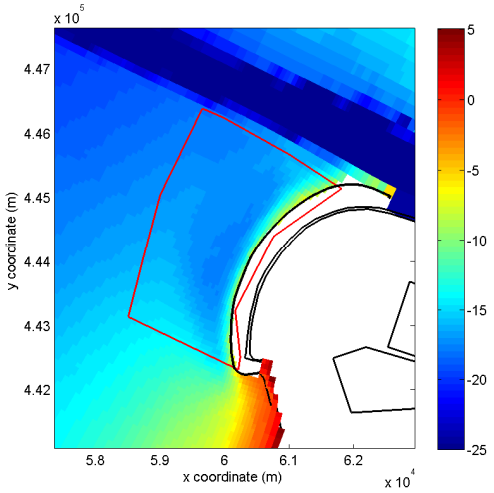

Figure 4.8 Measured bed 2000, polygon used for determination eroded volume

4.3.4 Accretion Maas-trench

In Delft3D the trench to the Maas is kept on a fixed depth. Sand that accretes in the trench is removed immediately. In this way the dredging works are schematized in the model. The material what has to be removed is kept up and so the dredged material is obtained.

In figure 4.11 several dredge compartments are shown. Each of these compartments is kept on a certain depth. For validation the compartments 2 and 3 are important. These compartments covers the area were the dredged material was determined (from the most westerly point of the Noorderdam to 5 km westerly).

In figure 4.9 and 4.10 the cumulative dredged material respectively for the period 1986-2000 and the period 2000-2006 is shown. The cumulative dredged material is shown for all the compartments together and the compartments 2 and 3. As can be seen the compartments which will be used for validation take up the greater part.

The dredging graph shows a gradually (step-by-step) growth. The steps upward are during slack water. So especially during slack water there is accretion in the trench. In dredge compartment 1 this step-by-step growth is not shown, therefore it can be concluded that the accretion in compartment 1 mainly comes from the river.

The year averaged dredged material is 1.6 *10^6 m^3 for the period 1986-2000 and 2.3 * 10^6 m^3 for the period 2000-2006.

In reality the averaged dredged material over the period 1985-1999 was 1.6 * 10^6 m^3. This agrees with the computed value for the period 1986-2000. For the period 2000-2006 a larger value is computed. The accretion of the accretion of the trench can give an overestimation in the model. This overestimation can be connected with the overestimation of the scour hole. A larger scour hole will entail a larger accretion. Therefore an overestimation of the scour hole will probably give an overestimation of the accretion.

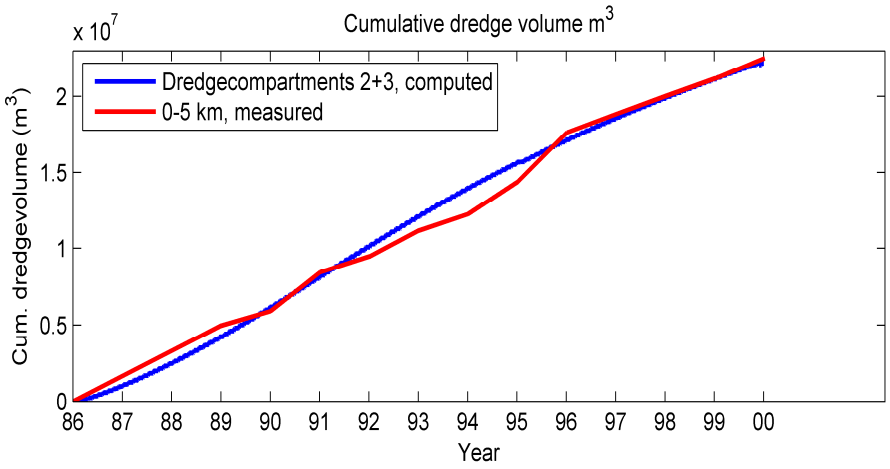

Figure 4.9 Cumulative dredged volume 1986-2000

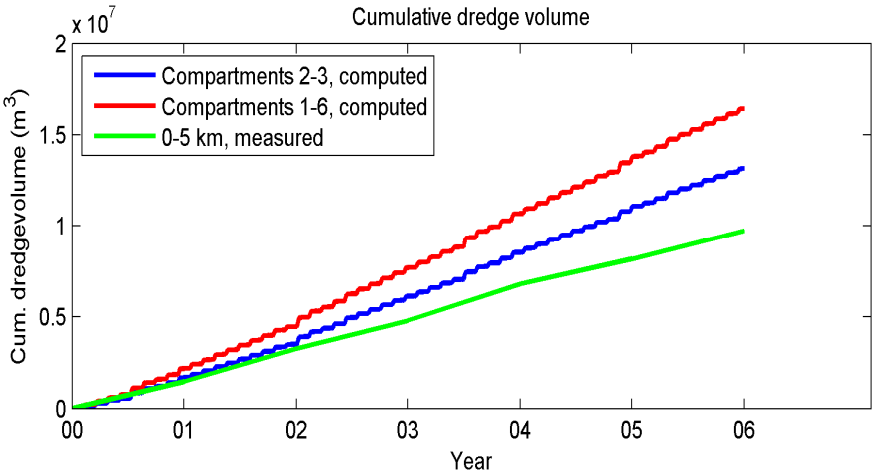

Figure 4.10 Cumulative dredged volume 2000-2006

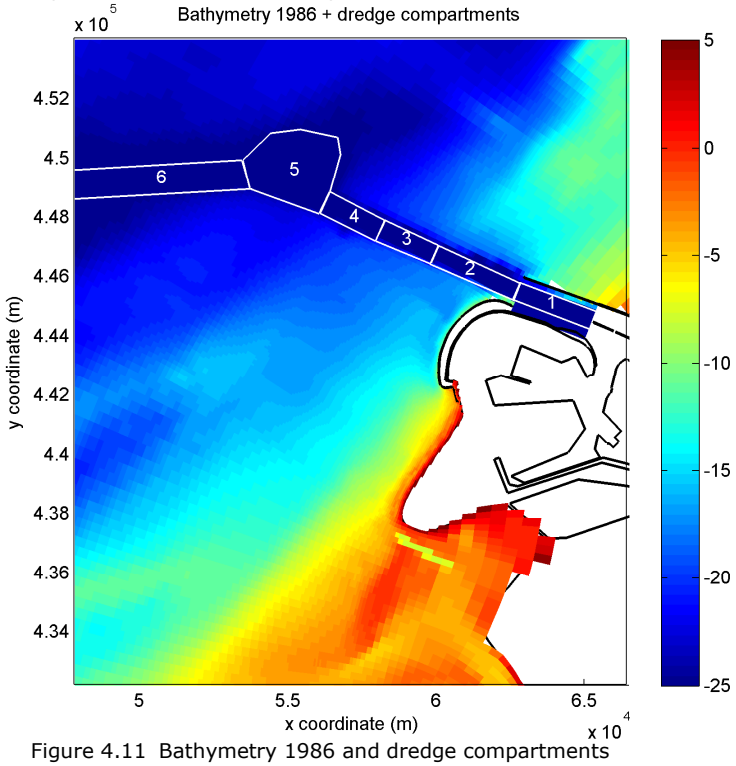

Figure 4.11 Bathymetry 1986 and dredge compartments

4.4 Conclusions

In this chapter the flow around the Maasvlakte 1 has been simulated and analysed. In this chapter there were no waves and uniform non-cohesive bed material (D50=0.200mm) has been applied. The simulations have been done to gain general insight of the flow around the Maasvlakte 1 and the results can be used as reference for the more complex simulations in the rest of this study.

Figure 4.1 clearly shows the contracted flow around the Maasvlakte 1 during ebb and flood. From this flow pattern a scour hole can be expected.

The scour hole has been simulated for two periods. Namely 1986-2000 and 2000-2006. For both periods the extent of the scour hole is comparable with the extent of the scour hole in reality. The developed depth on the other hand is overestimated. The computed scour hole depth develops about three times faster than the scour hole in reality.

The volume which is eroded out of the scour hole is double in the model compared to reality.

The computed accretion in the Maas trench is comparable with reality for the period 1986-2000 but slightly overestimated for the period 2000-2006.

Chapter 5 MV1: influence of waves on the scour hole

In the previous chapter the Maasvlakte 1 has been studies with tide only. In this chapter waves and wind will be added. The purpose of this chapter is to investigate the influence of the waves on the scour hole.

First a short introduction on waves will be given (5.1). The waves have a large influence on the occurring bed shear stress. Therefore the bed shear stresses following from current and waves are investigated in paragraph 5.2. The enhanced shear stresses by waves give a good vision on the influence of waves in the scour hole. After this first some simulations have been made with waves only so without the tide (5.3). This will give an idea of the wave induced currents. In paragraph 5.4 the waves will be combined with the tide. Two simulations have been made for respectively 1986-1991 and for 2000-2006. These two simulations will be analysed and compared with reality and with the case without waves (chapter 4). Paragraph 5.5 treats the connection between the size of the scour hole and the accretion in the Maas trench and will handle the nourishment at the Slufter beach. In paragraph 5.6 the conclusions are shown for this chapter.

5.1 Introduction waves

When a wave is completely sinusoidal the related water motion will stir up sediment and will bring sediment in suspension but the net transport will be zero. In real cases though, the waves can be cause of sediment transport.
Several mechanisms are therefore responsible [Van de Graaff, 2006]:

Wave asymmetry: This is caused by the non-sinusoidal character of the waves due to higher harmonics in the wave signal. Integration over the wave though will still give a net velocity of the water of zero. But since sediment transport is related to the flow velocity to a power larger than 1 more sediment is being moved in one direction. Therefore the net transport will be larger than zero.

Stokes drift: The horizontal movement of a water particle is in general larger higher in the water column than lower in the water column. A water particle under the top of the wave thus moves faster in the direction of wave propagation than a water particle under the trough of the wave runs backward. This makes that the orbital motion is not entirely closed over one wave period: the residual motion is called the Stokes drift. When waves propagate perpendicular to a coast the Stokes drift has to be compensated. This leads to return currents (undertow) close to the bed in the opposite direction as the Stokes drift that will give a seaward-directed sediment transport.

Currents do to breaking waves: When oblique incident waves break in the near shore zone, a complicated current pattern is generated in the surf zone consisting of a long shore current and an undertow current directed offshore. The generation of these currents can be explained by the radiation stress concept that describes the momentum fluxes associated with the waves. [Van Rijn, 1998]

The bed shear stress under tidal currents only is relatively small, which means that not much sediment will be in suspension, so that transport rates might be low as well. In the case of waves only, the bed shear stress may be increased significantly but since velocities are small, sediment transport rates remain small as well. In most cases, waves and currents are combined along coasts and the combination will give higher transports. The bed shear stress due to the combination of waves and current is even enhanced beyond the value would result from a linear addition. For sediment transport modelling the maximum bed shear-stress is important.

Waves are included in Delft3D-flow module by running the separate Delft3D wave-module SWAN. This Delft3D wave-module is assessed before running the flow-module. On a communication file the results of the wave simulation (Wave height, Wave period, wave direction, mass fluxes etc) are stored and can be used by the flow-module. The results from SWAN are used as follows: (1) Wave forcing due to braking waves is modelled as a shear stress at the water surface. (2) For the effect of the enhanced bed shear stress due to waves a model of Fredsoe is used. (3) Streaming, additional turbulence and wave induced mass flux. [Lesser, 2004]

5.2 Bed shear stresses

As stated before the bed shear stresses are of great importance on the sediment transport. Especially when waves and current are combined the sediment transports will become higher. The appearing bed shear stresses are used in the formula which determines the reference concentration in the Van Rijn transport formula and directly in the formula of Partheniades which will be used for cohesive sediment and will be treated later.

For 2D depth-averaged flow in Delft3D the bed shear stress from flow only is assumed to be given by a quadratic friction law:

$$\tau_c = \frac{\rho g U |U|}{C^2}$$

Where U is the depth-averaged velocity and C the Chezy coefficient. The shear stress from waves is calculated with:

$$\tau_w = \frac{1}{2}\rho f_w u_{orb}^2$$

Where f_w is the friction coefficient and u_{orb} the wave orbital velocity near the bottom. When waves and current are added the bed shear stress will be enhanced. This enhancement will be larger than the result of a linear addition. For sediment transport modelling the maximum bed shear stress is important. The current velocity and the turbulent diffusion are determined by the mean bed shear stress for combined waves and currents. Soulsby et al. (1993) fitted one standard formula to several of the existing models, each which their own fitting coefficients. The wave current interaction model of Fredsoe (1984) has been used in this study. The parameterization of Soulsby for the maximum bed shear stress and the mean bed shear stress are as follows:

$$\tau_{mean} = y(|\tau_c| + |\tau_w|) \quad \text{and} \quad \tau_{\max} = Y(|\tau_c| + |\tau_w|)$$

In figure 5.1 some values for y and Y are given for different angles between the waves and the current.

5.2.1 Bed shear stresses around MV1 due to current and waves

In figure 5.2 the maximum bed stresses τ_{cw} for combined waves and current are shown for cross section B as defined in figure 4.5. The shown bed shear stresses are the stresses during the maximum flood current. In the figure below (figure 5.3) a cross section of the bed level is shown. As can be seen in this figure the shear stresses are lowest at the seaside and increase in the direction of the coast. Some of them show a little decrease in the deeper part of the scour hole. This is because the shear stress due to waves depends on the water depth.

In this figure clearly waves from the north show higher shear stresses than waves from other directions which will be explained later. Of course waves with higher amplitude have higher maximum shear stresses.

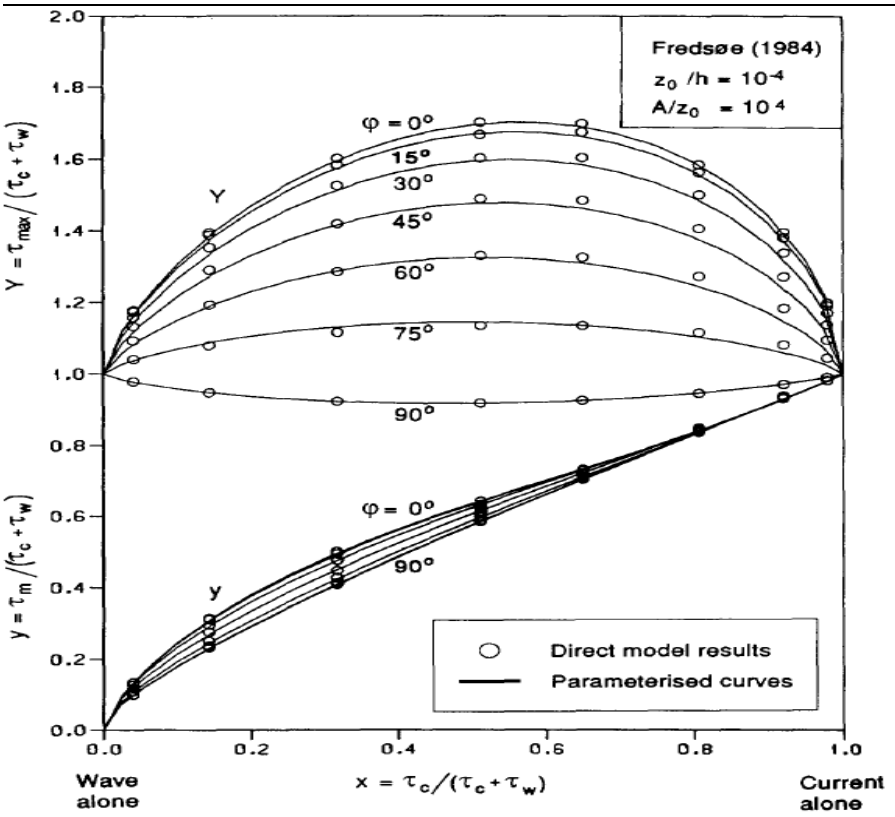

Figure 5.1 Coefficients for τ_{max} and τ_{mean}

In figure 5.4 a closer look is given at three wave conditions. Namely Z01, N09 and W00. The first two wave conditions are waves with a height of 1.05 meter and the directions are respectively from the South and the North. Wave condition W00 is taken as the reference case: A wave height of 0.1 meter will have no influence at the bed shear stresses.

As can be seen the maximum shear stress for wave condition Z01 is similar to the mean bed shear stress and similar to the bed shear stresses found for the reference case. This means that the waves have no influence on the bed shear stress. The maximum bed shear stress for wave condition N09 is higher than the mean shear stress. In figure 5.5 the wave height and the flow velocity in the middle of cross section B are shown, as can be seen the wave height fluctuates with the flow velocity. Opposing currents have a significant influence by steepening the waves even to the point of breaking. A following current enlarges the wave trough and thereby the wave length and reduces the wave height. This effect is so large that in the case of wave conditions Z01 and N09 the effect of the waves can be neglected in the case of following current and are of great importance with opposing currents.

For larger waves from the North and the South like Z02 the waves have always influence on the maximum bed shear stress, also with following current.

For wave directions other than north or south the influence on the wave height from the flow velocity is limited. Also the maximum shear stress is relatively smaller as also can be expected from figure 5.1: The wave direction makes a relatively large angle with the current.

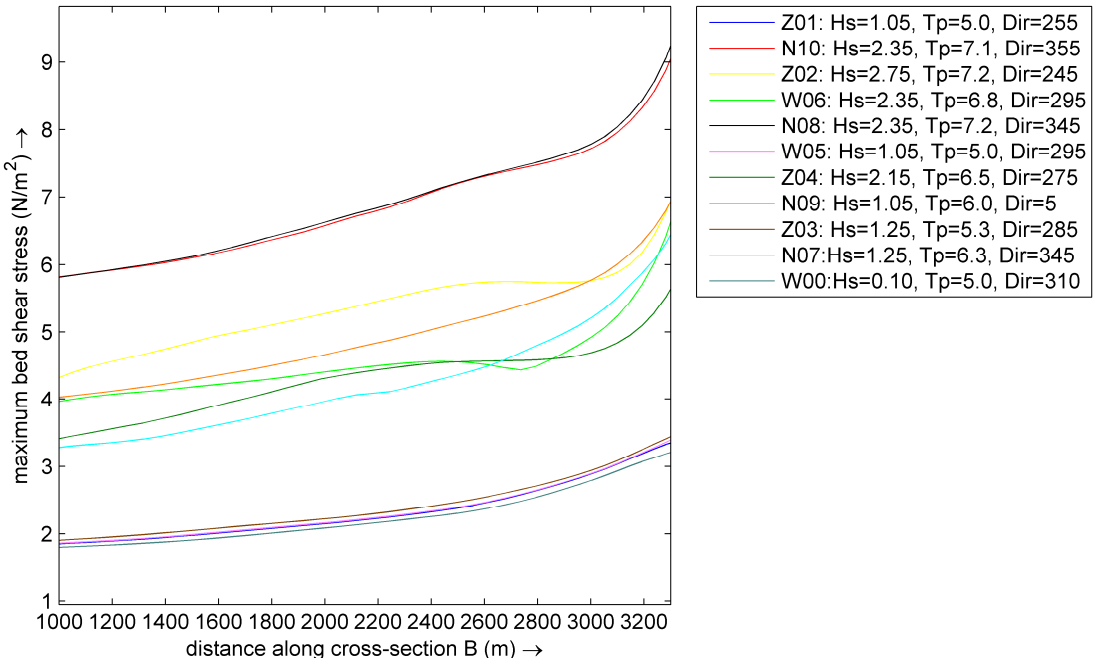

Figure 5.2 maximum bed shear stresses in cross-section B

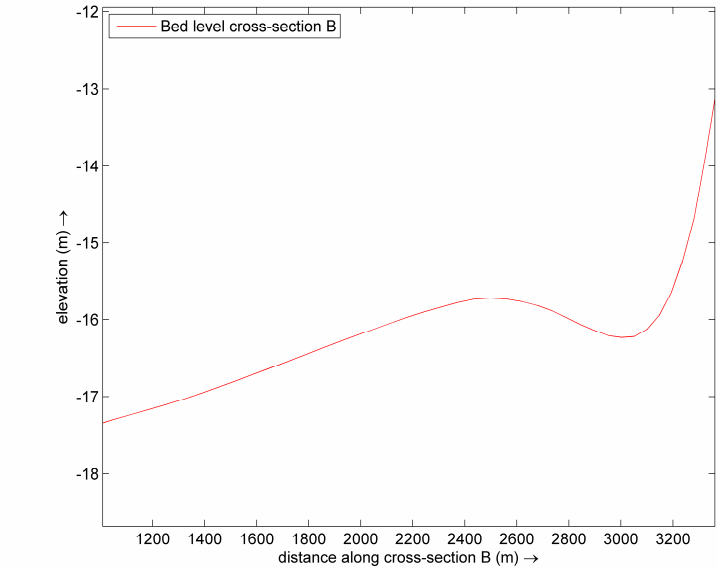

Figure 5.3 scour hole at cross-section B

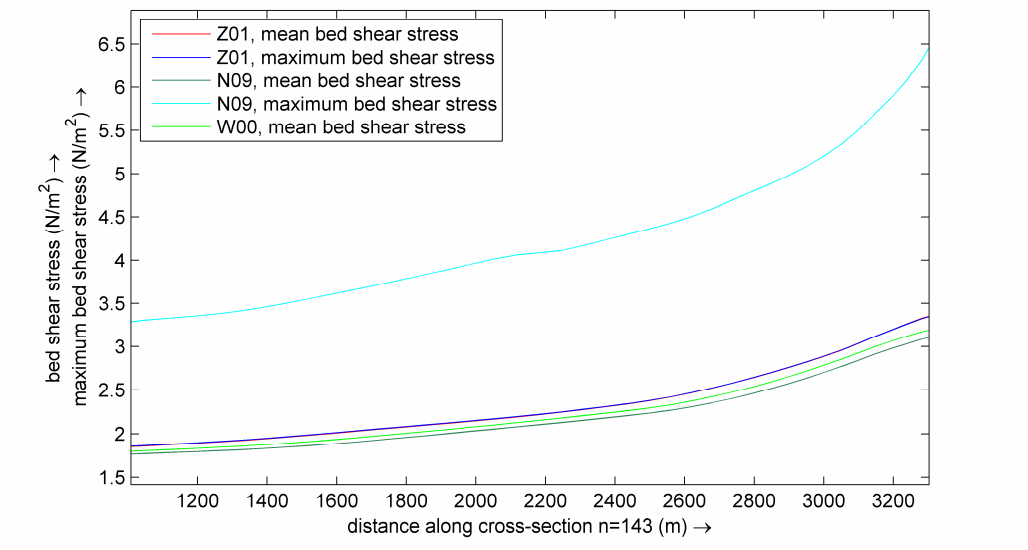

Figure 5.4 Bed shear stresses for three wave directions

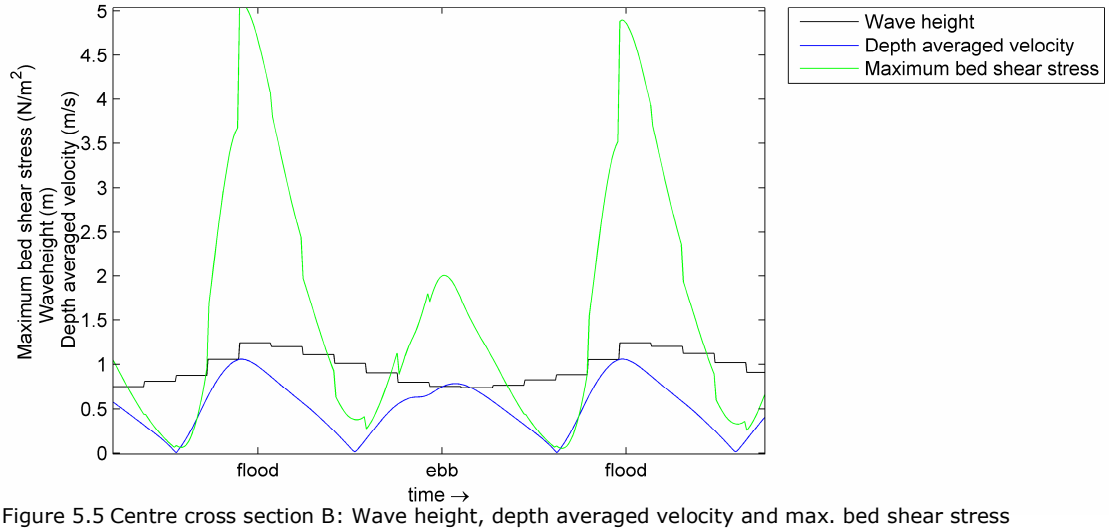

Figure 5.5 Centre cross section B: Wave height, depth averaged velocity and max. bed shear stress

5.2.2 Bed shear stress distribution

In figure 5.6 the distribution of the maximum shear stress is shown for the case without waves and for wave N09. This distribution is an indication for the extent of the scour hole.

In both figures (figure 5.6) the enhanced maximum bed shear stress in front of the Maasvlakte 1 can be seen. The figure shows that the maximum bed shear stresses in the whole area are larger when waves are added. In this particular case but this is also true for all larger waves (see figure 5.2).

As well as in figure 5.2 as in figure 5.6 can be seen that the maximum bed shear stresses for waves especially increase when close to the coast: The water depth is considerably smaller and therefore the bed-wave interaction increases.

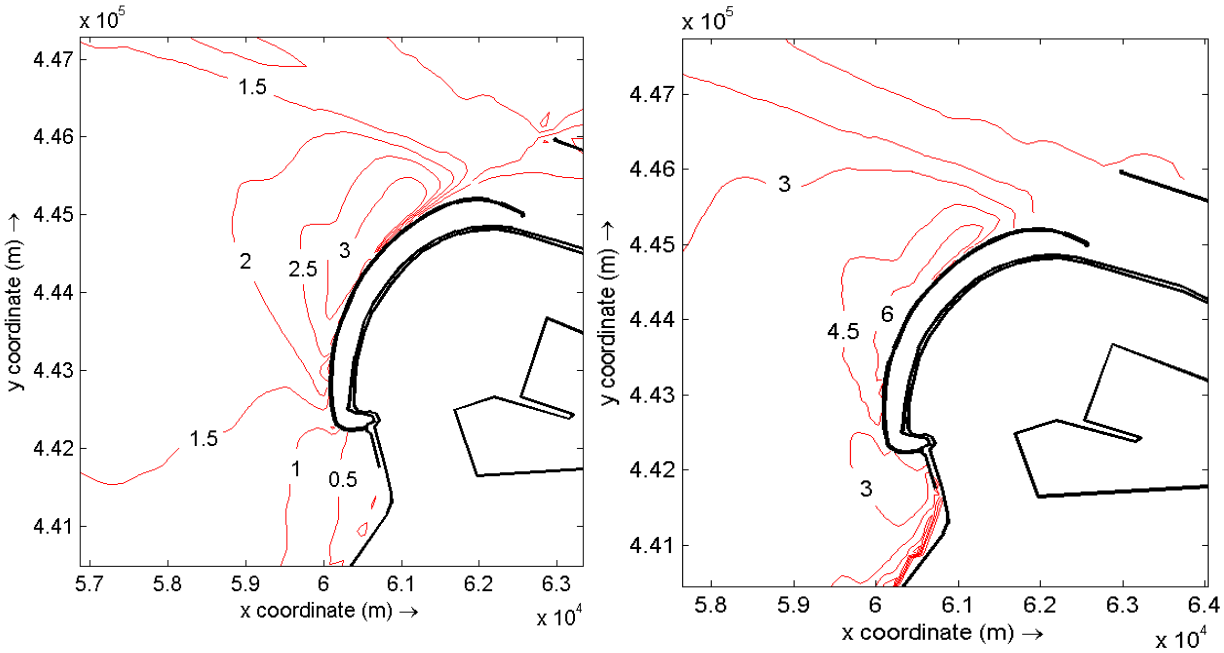

Figure 5.6 Maximum bed shear stress during maximum flood, no waves (left) and wave N09 (right)

5.2.3 Maximum bed shear stress versus scour hole

As clearly can be seen in figure 5.6 the maximum bed shear stress is enhanced at a large area when the situation without waves is compared to a situation with waves. But as can be seen in paragraph 5.4 there is only a deepening of the scour hole at a smaller area. Not only magnitude is important but also the direction and the gradient.

There also must be noted that not every wave has a deepening effect on the scour hole. Some waves will give sedimentation in the scour hole. The influence of the individual waves will not be further investigated in this study.

5.3 Waves only

For a general insight of the influence of the waves first all the wave conditions as shown in table 2.2 are modelled without any current. The resulting flow velocity and the sediment transport have been investigated. The two most extreme wave conditions are picked out and the sediment transport is depicted in Figure 5.7. As can be seen in the left figure, waves from the north, especially on the place of the scour hole there is no sediment transport. With waves from the south, figure 3b, this does not happen. As can be seen in both pictures there is only a very low sediment transport due to waves in front of the Zuiderdam. (order 10*-7 $m^3/s/m$). Just below the Zuiderdam, in front of the Slufter Beach, the waves are breaking and a wave driven current occurs. The sediment transport is there in order 10*-4.

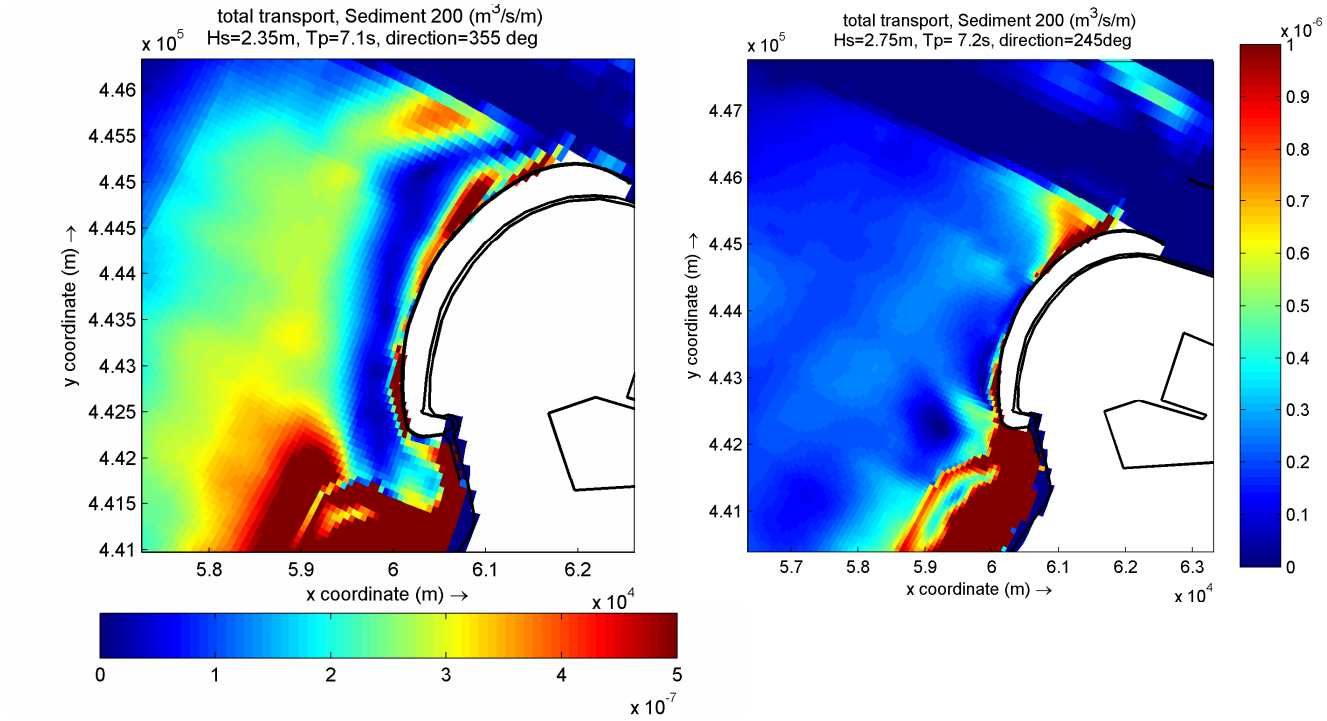

Figure 5.7 Total sediment transport for 2 wave conditions

5.4 Waves combined with flow

5.4.1 Model set up

In the online method in the Delft3D flow-module, the sediment transport and bottom updating are computed all at every time step. This does not take the difference in time scale between flow and morphology into consideration. Therefore the morphological factor is used. This factor n simply increases the depth changes by this factor. In this way after computation of one tidal cycle in fact n tidal cycles of morphology are modelled. This can only be done if nothing irreversible happens in one tidal cycle even if all the morphological changes are multiplied by the factor n. As shown in chapter 3 a morphological-factor of 100 is feasible for the flow.

When the annual occurrence duration of each wave as shown in table 2.2 was divided by 100 the wave classes were arranged one after the other in random order to make a 1-year time series. By doing so not every wave duration endures one complete tidal cycle. This is not desirable because waves during low water will give other results than during high water. Better is to have each wave during one complete tidal cycle. Making a time series longer than one year can do this. Disadvantage is that only a multiple of the duration of this time-series can be used. Another way is to use a morphological factor that varies with the wave condition, where a wave with low occurrence duration has a smaller morphological factor to obtain one complete tidal cycle in a 1-year time series. The wave conditions with low occurrence duration are the most extreme waves. With these waves something irreversible will happen earlier and a smaller morphological factor than 100 can be demanded. Therefore it is good to give a lower morphological factor to these waves.

The time set-up of the simulations is therefore as follows. Every wave has to run at least one tidal cycle; this resulted in varying morphological scale factor as shown in table 2.2. Also the number of tidal cycles for each run for a one-year-time series is depicted here. The flow model has to run 14 tidal cycles to attain one year of morphological changes. To model more than one year the same 14 tidal cycles is repeated to obtain the intended number of years.

Every 62 minutes the wave model is updated using the updated bathymetry and water levels from the flow model, after which the flow model ran with updated waves.

Again 2 periods were simulated: The period 2000-2006 and the period 1986-1991. The second period is not modelled for the 14 years as for the flow-only model. This was to limit the calculation time. Therefore it was assumed that effects of the waves also would be visible after a shorter time-span.

5.4.2 Cumulative erosion and sedimentation

In Figure 5.8 and figure 5.11 the cumulative erosion and sedimentation for 1986-1991 and 2000-2006 are shown. Very clearly the influence of the waves on the Slufter beach can be seen. With tide-only nothing happens here and by adding waves there is a lot of erosion and sedimentation. When the erosion in the scour hole is compared with the pictures without waves it can be concluded that the scour hole even gets deeper.

5.4.3 Cross sections

In figure 5.9 the cross-sections are shown. Also here can be seen that the erosion hole is getting deeper when waves are included. In every cross-section the waves cause a deeper scour hole. For the 1986-1991 case the extent of the scour hole is similar when waves or waves are not applied. For the 2000-2006 case though the extent in westerly direction is smaller if waves are applied compared with the case without waves.

5.4.4 Eroded volume

In table 5.1 the eroded volume out of the polygon as shown in figure 4.8 is shown for reality and for the computed cases including waves and without waves. As can be seen in this table is also the eroded volume out of the scour larger for the case including waves when compared to the case without waves. Compared to reality the eroded volume is nearly two and a half times larger.

Table 5.1 Eroded volume 2000-2006, reality and computed

	Reality	Computed without waves	Computed including waves
Eroded volume [m^3]	3,80E+06	8,40E+06	9,30E+06

5.4.5 Accretion Maas trench

Including waves also causes a larger accretion in the Maas trench as is depicted in figure 5.10 and figure 5.13 (respectively 1986-1991 and 2000-2006). In the cases without waves the accretion in the model was comparable with reality. When waves are added the accretion in the Maas trench is considerably higher. Especially in the 2000-2006 period the computed accretion is nearly double of the measured accretion. The yearly accretion in the model is roughly the same for both periods.

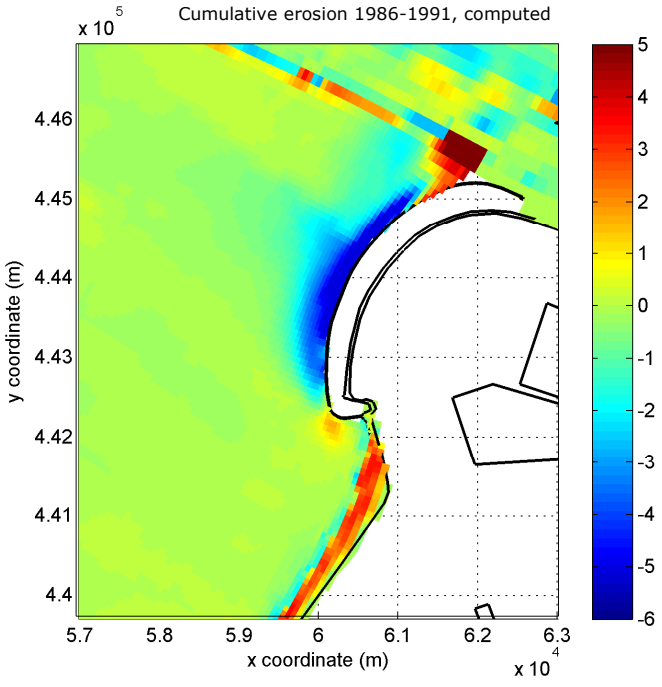

Figure 5.8 Cumulative computed erosion 1986-1991

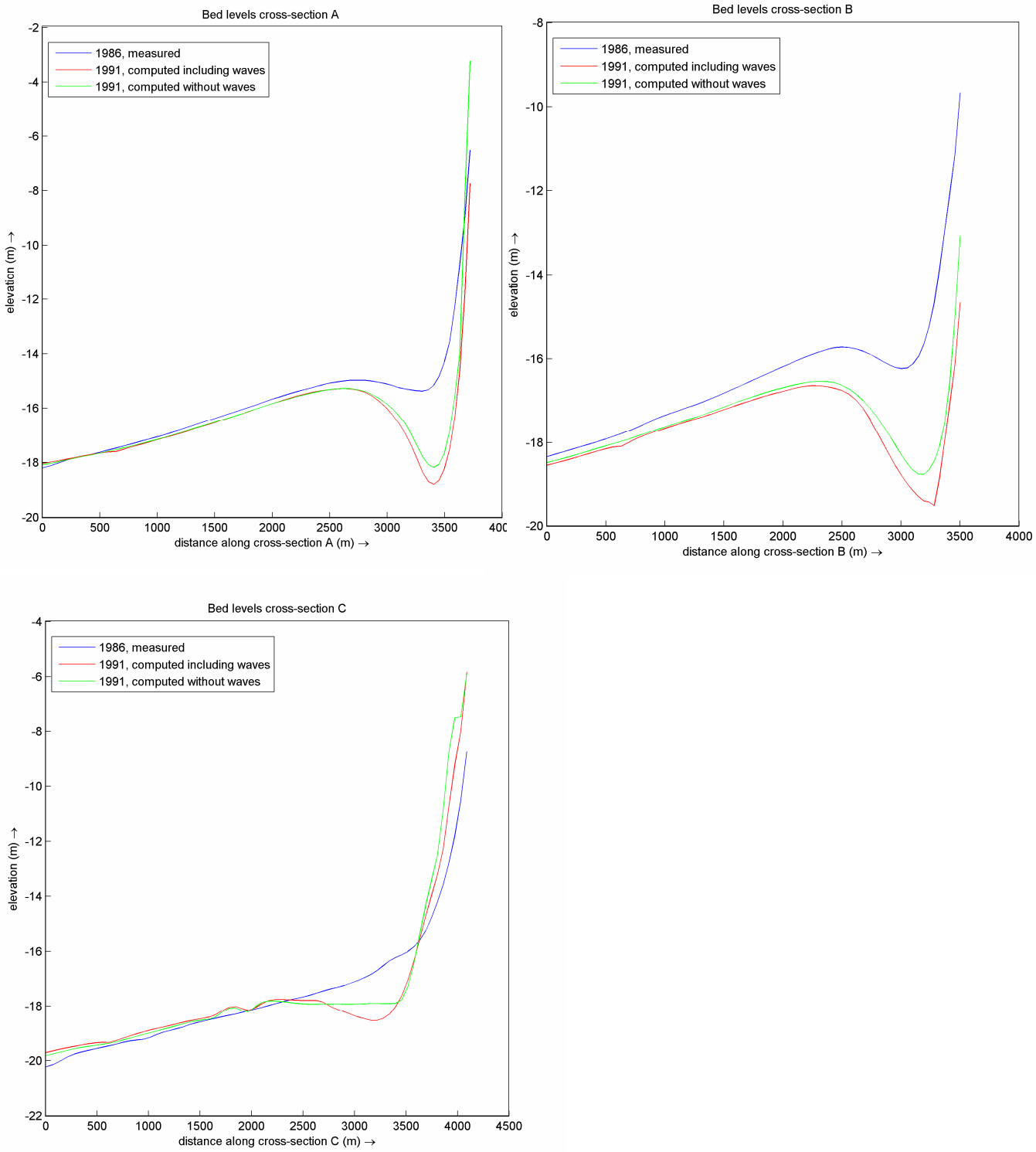

Figure 5.9 Cross sections

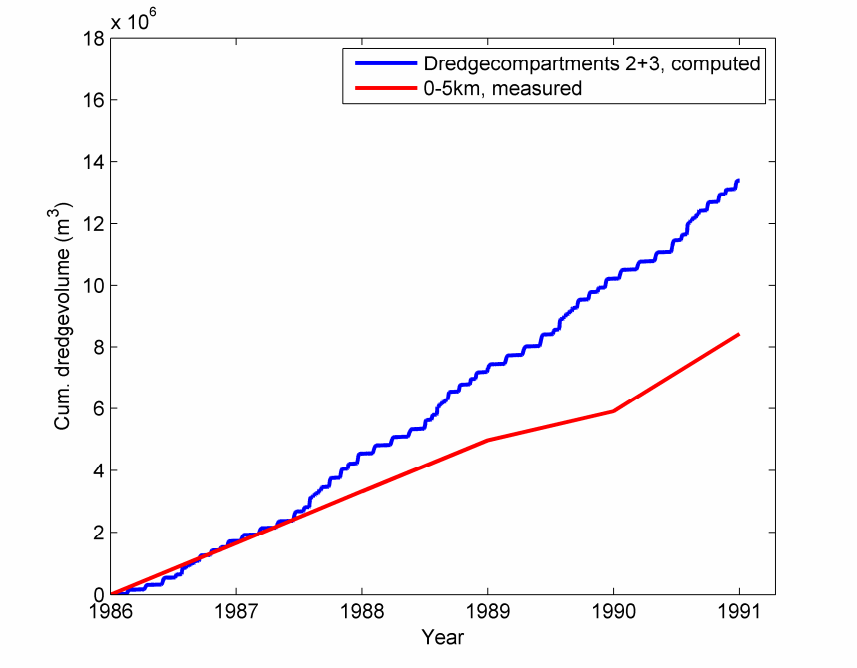

Figure 5.10 Cumulative dredge volume 1986-1991

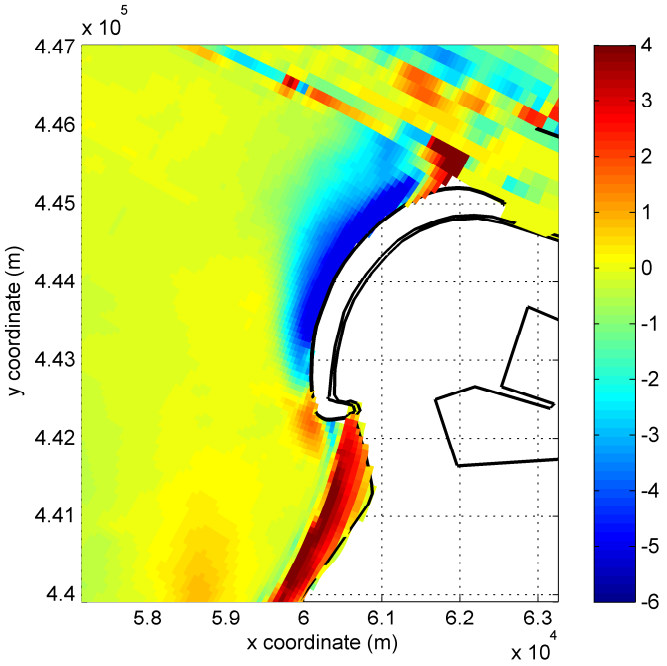

Figure 5.11 Cumulative computed erosion 2000-2006, waves included

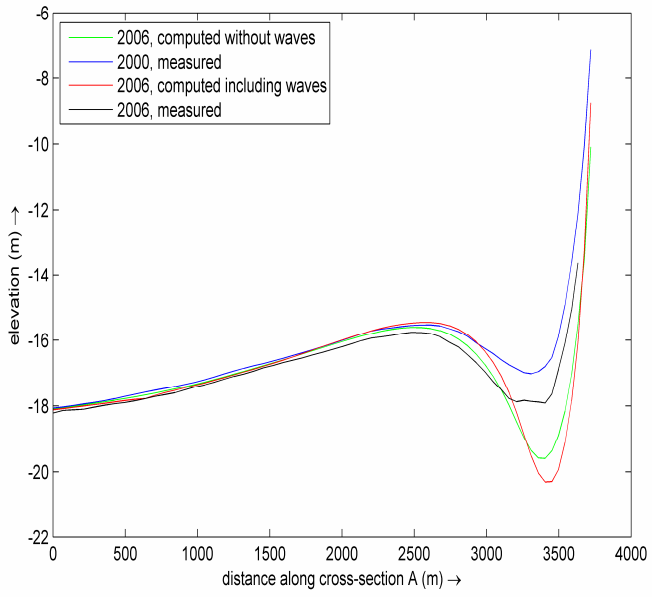

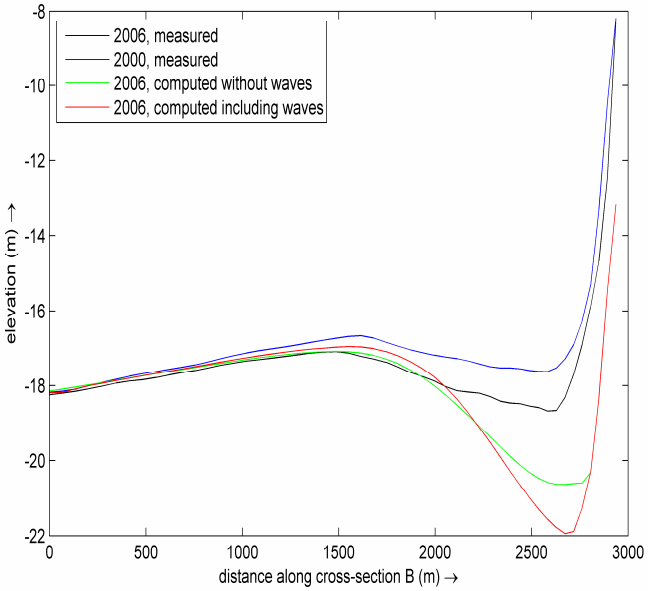

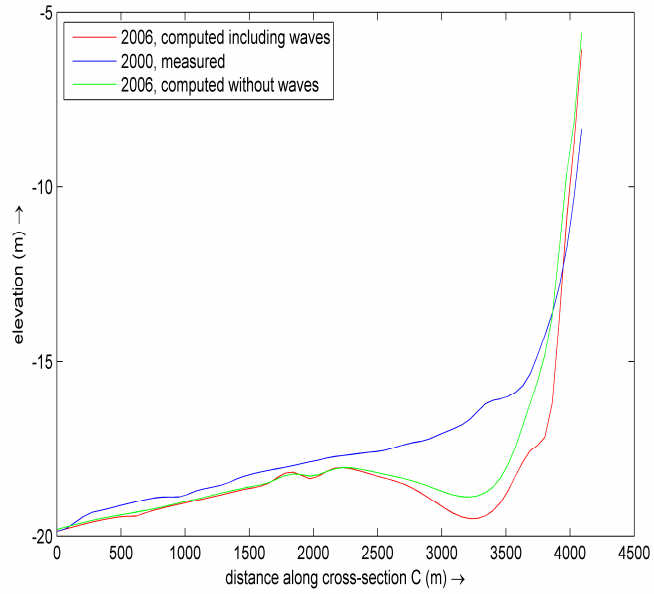

Figure 5.12 Bed levels cross section A, B and C for 2000-2006

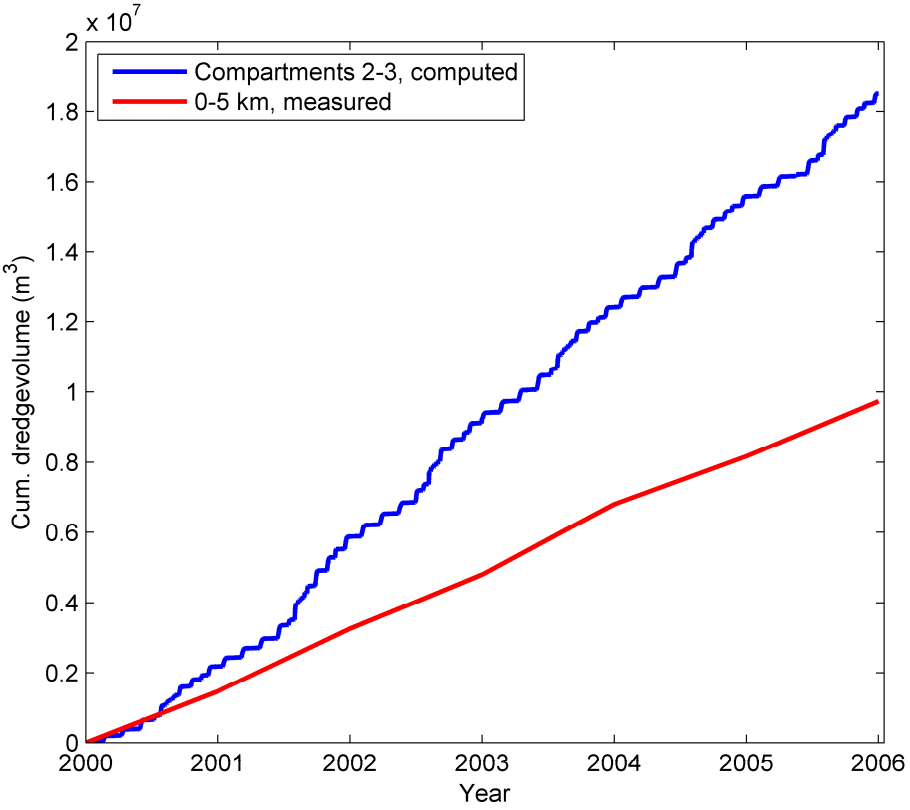

Figure 5.13 Cumulative dredged volume 2000-2006

5.5 Morphological interactions

5.5.1 Eroded volume versus accretion Maas trench

In the case of waves there is a larger volume eroded than in the case without waves. There was also a larger accretion in the Maas trench. Part of the material which eroded out of the scour hole will accrete in the Maas trench. Therefore there is a connection between the erosion out of the scour hole and the accretion in the Maas trench.

For the 2000-2006 period reality and computations can be compared. Comparison of the case including waves with reality shows that there eroded 5.5 * 10^6 m^3 sediment more out of the scour hole and that there was 8.9 * 10^6 m^3 more accretion in the Maas trench.

Comparison of the case including waves with the case without waves shows that there eroded 0.9 * 10^6 m^3 sediment more out of the scour hole and that there was 4.3 * 10^6 m^3 more accretion in the Maas trench.

These two comparisons show that larger erosion in the scour hole does cause a larger accretion in the Maas trench. But it also shows that the increase of the accretion in the Maas trench is larger than the increase of the erosion in the scour hole. It can be concluded that the overestimation of the accretion in the Maas trench is merely partly due to the overestimation of the scour hole.

5.5.2 Nourishment

As posed in paragraph 3.5 there is yearly nourishment at the Slufter beach. The volume of this nourishment was 728.000 m^3/year. The average erosion in the scour hole in the period 2000-2006 is 633.000 m^3/year. In this chapter yearly erosion out of the scour hole was found of 1550.000 m^3/year. So even if all nourished sediment is deposited in the scour hole there is still an overestimation of the scour hole.

In reality there is erosion at the Slufter beach, in this model, where the focus is on the scour hole, there is sedimentation at the Slufter beach. It is possible to implement a nourishment mode for the actual case (one layer, uniform sediment). In this mode the Slufter beach profile will be kept in the initial profile by nourishing after each computation step. Because there is no erosion at the Slufter in the current model this will only have a minor effect.

The nourishment mode is not yet implemented in the model for simulations with multiple fractions and layers. Because the current case will be used as a reference for the next chapters the nourishment mode was not implemented in the current chapter.

Only a minor part of the nourishment will end up in the scour hole, therefore it is clear that when nourishment is included there should still be a large overestimation of the scour hole.

Therefore the model without nourishment mode will be sufficient for investigating the influence of different bed compositions on the scour hole.

5.6 Conclusions

Bed shear stresses

As can be seen in figure 5.2 the maximum bed shear stresses are enhanced due to the waves. The smaller waves do not have influence on the bed shear stress. The maximum bed shear stresses due to currents and waves especially increase when close to the coast.

Waves only

From the simulations were only waves were included can be concluded that there is hardly wave driven current in front of the Maasvlakte 1 construction. In front of the Slufter beach (just below the Maasvlakte 1) the waves are breaking and a wave driven current occurs.

Waves combined with flow

Two periods have been simulated for the case where the waves and the tide are combined. Namely 1986-1991 and 2000-2006.

The computed patterns, depth and accretion in the Maas trench were compared with the case without waves and with reality.

The computed extent in this chapter is comparable with reality and the computations in chapter 4 (the case without waves). Only small differences occur: For the 1986-1991 period the computed extent is slightly wider compared with the computed case without waves. For the period 2000-2006 the computed extent with waves is smaller compared with the case without waves and therefore also smaller when compared with reality.

The computed depth is for both periods larger when compared to the case without waves and therefore also considerably larger when compared with reality. The computed scour hole depth develops about 3.5 to 4 times faster compared with reality for the period 2000-2006. The case without waves developed 3 times faster.

The eroded volume out of the scour hole is 2.5 times larger than in reality and are also slightly larger than in the case without waves as can be seen in table 5.1.

For the case without waves the accretion in the Maas trench was comparable with reality. For the case including waves there is an overestimation of more than 50% for the period 1986-1991 and almost 100% for the period 2000-2006.

Because part of the eroded material out of the scour hole ends up in the Maas trench there is more accretion when there erodes more material out of the scour hole. The accretion in the Maas trench increases more than the increase of the volume which erodes out of the scour hole. Therefore is the overestimation of the accretion in the Maas trench not only due to the overestimation of the scour hole.

There is no nourishment mode included in the current study. If this nourishment mode would be included there would still be a large overestimation of the scour hole. Therefore a model without a nourishment mode will be sufficient to investigate the influence of different soil compositions in the scour hole.

Chapter 6 MV1: Armouring non-cohesive fractions

Natural seabed sediments are non-uniform and therefore natural sorting of bed sediments occurs. The finer sediment will erode and the coarser material will stay behind forming an armour layer on the surface of the seabed. For erosion of this coarser material higher flow velocity is required and therefore the morphological changes will be smaller which may result in a reduction of the scour hole. This effect of armouring can be simulated in Delft3D by distinguishing several sediment fractions and bottom layers.

The aim of this chapter is to make a new hindcast of the Maasvlakte 1 case where the effect of armouring is included by implementing more than one fraction (graded sediment). Aim is to determine a certain bandwidth resulting from the bandwidth of the sieve curves as shown in chapter 3. The used parameters and the determined bandwidth can be used for the Maasvlakte 2 case.

In this chapter several sediment fractions and bed layers will be applied. Each layer contains up to five fractions. The composition of the different layers can differ. Initially the sediment composition of the bed will be spatially uniform.

First uniform non-graded fractions will be investigated. As in the previous chapters there is one layer and one fraction. Several simulations with different D50's will be made to investigate the effect of the grain size on the scour hole (paragraph 6.1).

In chapter 3 the available sieve curves were analysed and a representative curve was determined. In paragraph 6.2 this representative curve will be schematized such that it can be used in the Delft3D model.

In paragraph 6.3 simulations will be done with a model were five sediment fractions and several bed layers are implemented. In paragraph 6.4 the armouring effect in these simulations will be highlighted.

Paragraph 6.5 contains the conclusions of this chapter.

6.1 Uniform fractions with different grain sizes

Further in this chapter more than one fraction and several layers will be added in the model. The added fractions are relatively small and relatively large compared to the so far used D50. Therefore the influence of the grain-size on the sediment-transport shall be investigated in this paragraph. In all the simulations in this paragraph the sediment is uniform (non-graded): There is one layer and one D50.

As known from literature the grain-size has a great influence on the suspended sediment-transport and a relatively small influence on the bed-transport [L.C. van Rijn and S. Boer, 2005]. The effect of the sediment size is largest at low current velocities and decreasing if the velocity increases.

6.1.1 Uniform fraction without waves

In figure 6.1 the suspended transport in the scour hole is shown for relatively fine and coarse sediment. Very clearly the higher transport for fine sediment is observed in this figure. Also a smaller threshold for motion can be seen for the finer sediment.

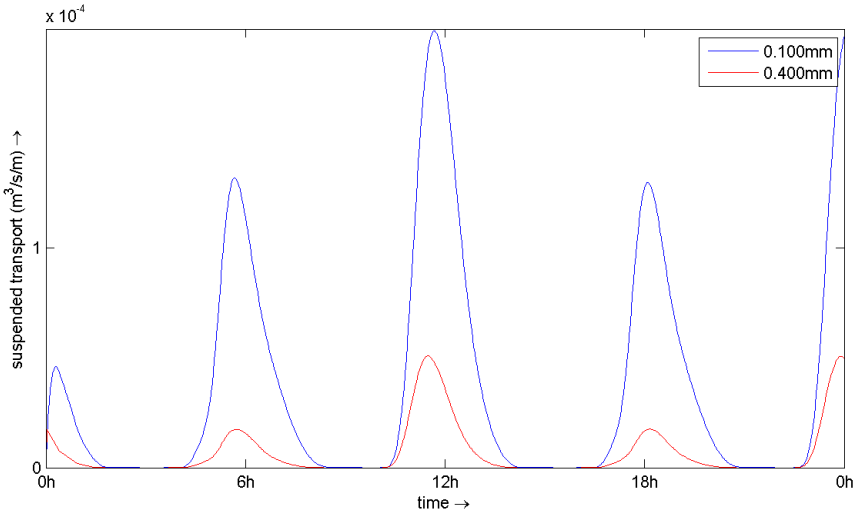

Figure 6.1 Suspended transport in the scour hole for fine and coarse sediment

The flow model, without waves, is executed with the following D50's: 100, 160, 240 and 400µm. In figure 6.2 the bed level in cross section B after 5 years is shown for these different fractions. As expected the smaller grain sizes show more erosion and also more accretion in the Maas trench (table 6.1).

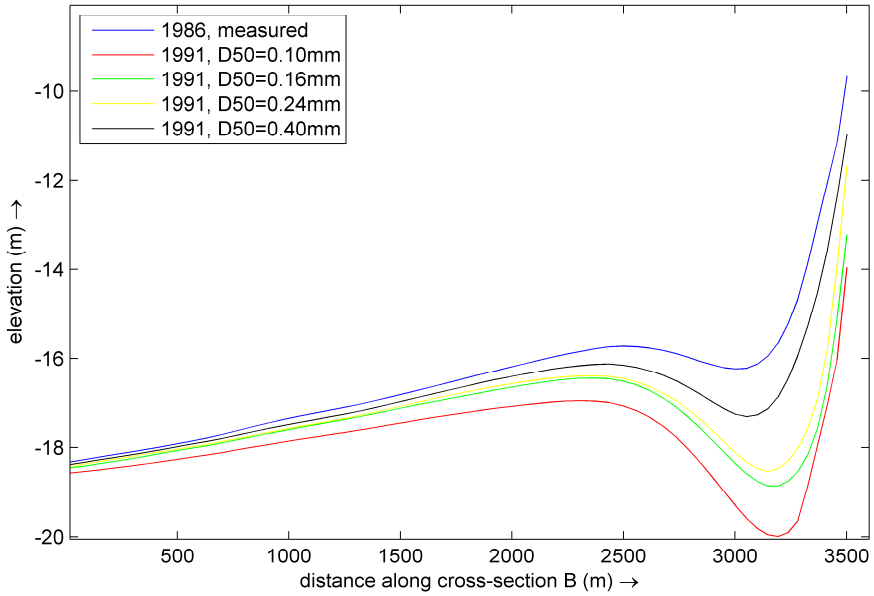

Figure 6.2 Bed level cross section B after 5 years for different uniform fractions

Table 6.1 Computed average dredge volume for different fractions

D50 (mm)	Averaged dredged volume (year)
0,100	1,90E+06
0,160	1,88E+06
0,200	1,60E+06
0,240	1,40E+06
0,400	5,50E+05

6.1.2 Uniform fraction including waves

Close to the bed the sediment concentrations are higher for coarse sediment compared with fine sediment. This is because the bed ripples are larger and steeper and so the particles are lifted easier. Higher in the water column the concentration of the fine sediment is higher. This is due to the lower fall velocity for fine sediment.

Suspended transport increases considerable when waves are added but this effect diminishes relatively when the current velocity increases [Van Rijn, 1993]. [L.C. van Rijn and S. Boer, 2005] showed that for waves (Hs=0.075 and 0.15m.) the factor between sediment transport for D50=0.100mm and D50=0.200mm is independent of the current velocity.

In figure 6.3 and figure 6.4 respectively the cumulative erosion and the bed level in cross section B (figure 4.5) are shown for the year 1991 after 5 years of simulation starting with the bathymetry of 1986 for the relatively fine uniform sediment of 0.100mm. Compared to the case where larger sediment particles were used the extent of the scour is considerably larger but the maximum depth is smaller as well can be seen in the cross section. The reason for this is that the difference in gradient in the sediment transport is smaller. Already with smaller flow velocities the sediment transport is relatively high. Therefore the increase in sediment transport with increasing velocity is relatively smaller. Because of that the extent of the scour hole is larger but less deep. Another reason of the smaller scour hole in case of smaller grain size can be the bed slope effects:

smaller grains roll easier in the scour hole and therefore the scour hole will become less deep.
For fractions larger than 0.100 mm the depth and extent of the scour hole decreases with increasing particle size. This is similar to the cases without waves.

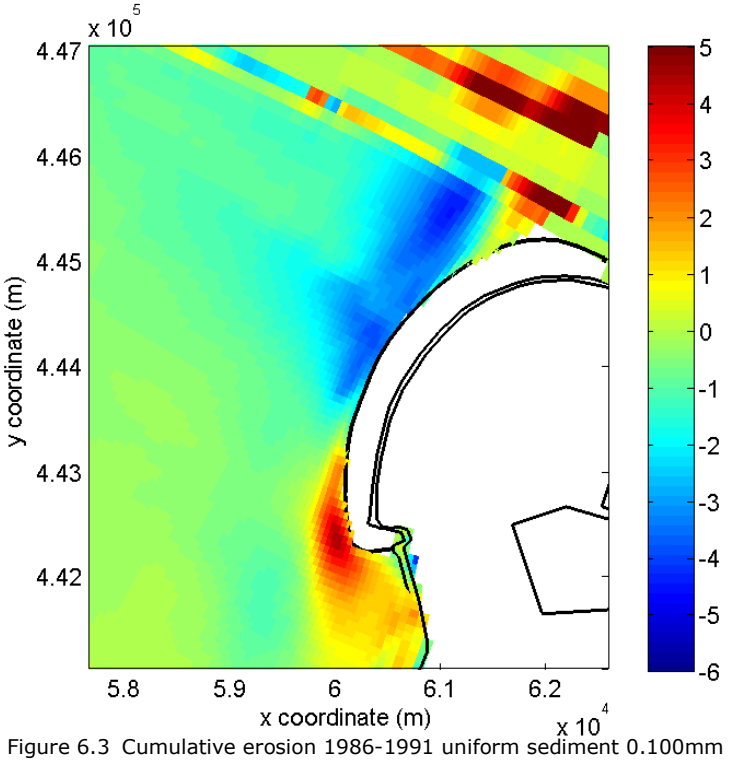

Figure 6.3 Cumulative erosion 1986-1991 uniform sediment 0.100mm

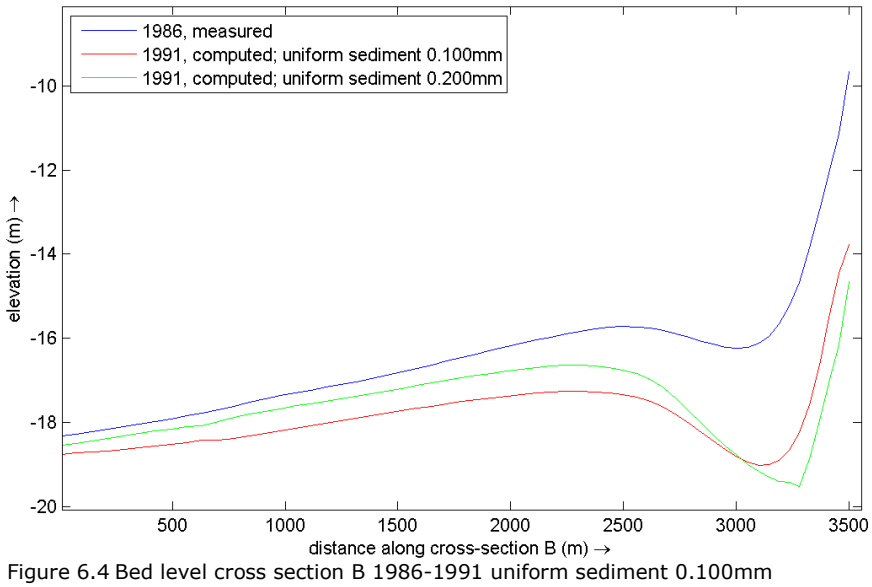

Figure 6.4 Bed level cross section B 1986-1991 uniform sediment 0.100mm

6.2 Schematized sieve curve

In paragraph 3.2 the available sieve curves were analysed. From the analysed sieve curves a representative curve was obtained. The obtained curve has a D50 of 0.185 mm and a D90/D10 of 5. In all the former studies except in [Elias 2006] a D50 of 0.160mm has been used. This value was a representative value for the complete model area. This value can vary locally and therefore another value can be found in the area of interest. In [Elias 2006] where also five fractions were used a value for the D50 of 0.200 mm has been found. In this study only the Maasvlakte 2 case has been investigated, in that case a smaller scour hole was found because of the larger D50. Therefore a smaller scour hole is expected for the Maasvlakte 1 case as well.

The maximum number of fractions that can be implemented in the Delft3D model is 5. Therefore the representative sieve curves have to be translated into 5 fractions. This schematization of the representative curve is shown in figure 6.5 and table 6.2. This 'best fit' of the representative particle size distribution will be used in the first computations where the multiple fractions will be implemented in the model. But as stated before, the range of the sieve curves is very large. Therefore it is recommendable to test the sensibility of this representative particle size distribution. This can be done by modelling the model with finer and coarser distributions. Besides this testing of the grading is advisable.

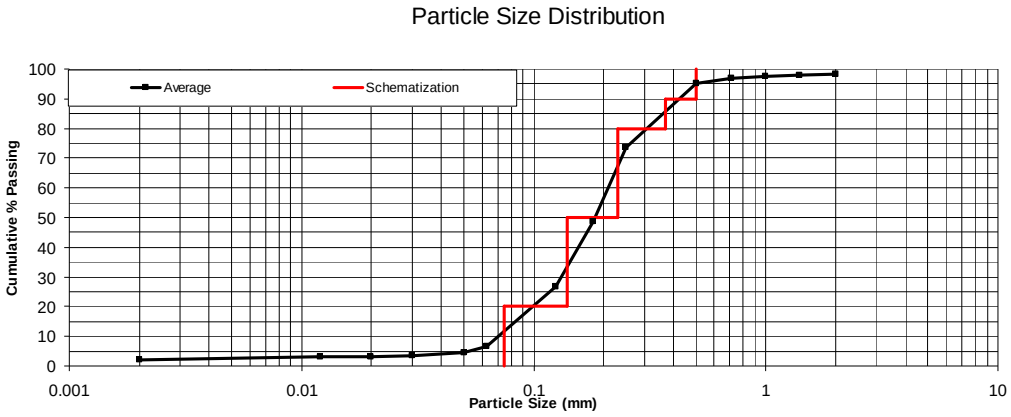

Figure 6.5 Schematization mean sieve curve

Table 6.2 Schematization sediment fractions

Fraction	D50 (mm)	Distribution(%)
1	0,075	20
2	0,14	30
3	0,23	30
4	0,35	10
5	0,50	10

Beside the best fit of the average curve, other schematizations have to be obtained to investigate the sensitivity. In table 6.3 the other fraction-distributions that will be modelled are shown.

Table 6.3 Fraction distributions

Distribution (%)	**run1**	**run2**	**run3**	**run4**	**run5**
	D50[mm]	D50[mm]	D50[mm]	D50[mm]	D50[mm]
20	0,100	0,100	0,100	0,100	0,100
30	0,171	0,115	0,140	0,150	0,110
30	0,242	0,185	0,230	0,180	0,300
10	0,347	0,200	0,350	0,200	0,400
10	0,487	0,300	0,500	0,250	0,500
Average D50 [mm]	0,206	0,153	0,185	0,165	0,205
D90/D10	4,9	3,0	5,0	2,5	5,0

The distribution used in run 1 is identical to the distribution used in [Elias 2006]. The distribution used in run 3 is the best fit from the sieve analysis. The other three runs are chosen such that the sensitivity of the D50 and the sensitivity of the grading can be examined. There must be noted that it was not possible to execute simulations with fractions smaller than 0.100mm.

In the simulations the distribution of the fractions will be initially *spatially* uniform. In reality this is not true. The sediment samples are taken in the area of interest and represent that specific area. In the area of interest there was hardly spatial difference (chapter 3). Spatial difference at a larger scale has not been investigated, but can be partly cause of the overestimation of the accretion in the Maas trench.

6.3 Simulation with several fractions and multiple layers

6.3.1 Implementation in Delft3D

In the previous chapters a uniform bed with one sediment layer was used. The thickness of this sediment layer was set to 5 meters and the median sediment diameter (D50) was 0.200mm. The erosion of this sediment layer was possible until this layer was fully eroded. To investigate the effect of armouring another bed composition model is used. In this model a number of layers can be included and several sediment fractions will be used instead of one fraction. Each fraction has its own median sediment diameter and accompanying reference concentrations, erosion rates and sediment transport rates. Each layer is bookkeeping to keep track of sediment deposits. The erosion rates, the reference concentrations and the sediment transport rates are proportional to the availability of the sediment fraction considered in the top-most layer of the bed-stratigraphy. In the present case there is no hiding and exposure correction which means that finer particles cannot hide behind coarser sediments and coarser sediments are not extra exposed to the flow.

A distinction can be made between the defined layers (figure 6.6):

1. One transport/ active layer: This layer is the topmost layer. This layer is always present. The thickness of the layer is a user defined constant in this study.
2. Bookkeeping layers: These layers are filled up to a user-defined maximum thickness, if this threshold is exceeded a new layer is created. The initial number and thicknesses of the bookkeeping layers is user defined. If the creation of a new layer would exceed the maximum number of layers specified, layers at the bottom of the stratigraphy stack will be merged.
3. Base layer: This is the undermost layer. Everything what does not fit in the other layers will go to this layer.

The initial stratification, the total number of layers, can be specified. Also the initial fraction distribution and the thickness for each layer can be specified.

Deposition of sediment
For visualization see figure 6.6 (left). Deposited sediments are initially added to the top-most layer (1). After mixing in the top layer (2), the sediments are pushed towards the bookkeeping layers beneath it in the fraction distribution as in the transport layer (3).

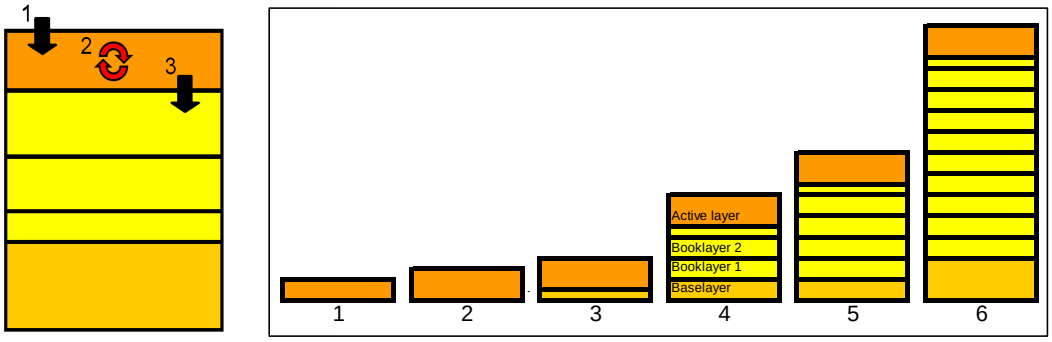

Figure 6.6 Visualization deposition of sediment in multiple layer model

Figure 6.6 (right) shows the development of the stratification during sedimentation. First the active layer is filled (1,2). The layer under the active

layer is partly filled (3). Extra layers are created when the underlayers are filled up to the user defined maximum thickness (4,5). When the user-defined maximum number of layers would be exceeded the layers at the bottom of the stratigraphy stack will be merged (6).

Erosion of sediment
For visualisation see figure 6.7 (left). Only the sediments in the top-most layer are available for erosion. In one computational step maximal the available sediment in the active layer can be eroded. After sediment is eroded from the active layer (1) this layer will be replenished from the layer below with the fraction distribution as in this underlying layer (2). The thickness of the active layer will be kept constant.

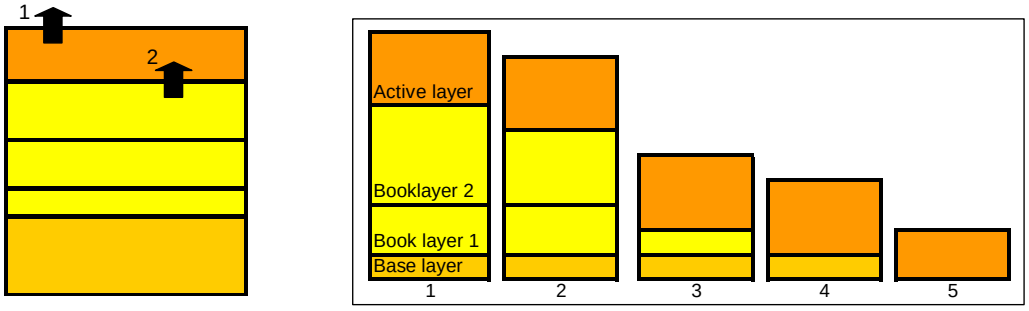

Figure 6.7 Visualization erosion of sediment in multiple layer model

Figure 6.7 (right) shows the development of the stratification during erosion. Erosion of the active layer is replenished from the layer below (1 and 2). When an underlayer is completely eroded, replenishment will be done by the next underlying layer (3). This will continue till all layers are eroded. Hereafter the active layer is not replenished anymore (5).

6.3.2 Executed simulations

Analogous to [Elias 2006] five layers of three meters with graded sediment are applied in this study. Graded sediment stands for more than one fraction. Each layer contains five fractions. Five simulations were executed. Each simulation is executed with a different fraction distribution. The five fractions distributions were shown in table 6.3. In each simulation was the initial fraction distributions equal for each layer. As stated before the fraction distributions of *run 1* and *run 2* are best fitting sieve curves and the other distributions are chosen such that the sensitivity of the D50 and the grading can be examined. In these simulations waves were involved.

Aim of the simulations is to investigate the influence of graded sediment on the extent and the depth of the scour hole. Further more the bandwidth of the large range for D50 and grading has to be determined. The effect of armouring has to be indicated from the simulation results. Finally, the simulation results should lead to a parameter configuration which can be used for the Maasvlakte 2 case.

6.3.3 Cumulative erosion and sedimentation

Figure 6.8 shows the spatial cumulative erosion for the five different fraction distributions as presented in the previous paragraph. The presented cumulative

erosion is after 5 years of simulation starting with the bathymetric data of 1986. For comparison the cumulative erosion after 5 years for uniform sediment of 0.200 mm is added to the figure as well. The erosion pattern of the uniform sediment was reasonably identical to the erosion in reality. Globally the extent of the scour hole is identical for the graded and the uniform simulations. Locally a few differences can be found for the erosion pattern. *Run 2* and *4* give larger erosions in the northern part while *run 1, 3* and *5* give identical erosions in this part. In the middle part all the runs give a comparable extent of the scour hole.

The scour hole extends less at the southern side of the scour hole and the accretion just below the Zuiderdam is larger for all graded sediment simulations.

6.3.4 Cross sections

The maximum scour hole depth is shown in figure 6.9 and 6.10 for respectively cross sections A and B (as defined in figure 4.5). In both figures it can be seen that all the simulations with graded sediment result in less deep scour holes. Especially in cross section A the reduction of the depth of the scour hole is substantial. While in cross section B, which is closer to the centre of the scour hole, the reduction is less.

Run 5 gives a distinctly less deep scour hole than the other graded sediments. *Run 4* gives in both cross sections the minimum reduction. *Run 1, 2* and *3* are very close in cross section A. In cross section B though the reduction of these runs varies merely slightly.

The depth and the extent of the scour hole differ for the various fraction distributions. This can be partly explained by the difference in D50 and other sediment characteristics. A smaller D50 would give larger erosion as already treated in paragraph 6.1. *Run 1* and *run 5* give less erosion than the other runs because of the larger D50. Run 5 has on its turn smaller erosion than *run 1* though they have the same D50. A closer look at the distribution shows that *run 5* has a larger D60, D70, D80 and D90 which explains the difference between *run 1* and *run 5*.

The D50 of *run 2, 3* and *4* is smaller compared with the uniform sediment. The erosion is smaller though. This difference will be explained later. Again the difference between *run 2, 3* and *4* can be explained by difference in distribution.

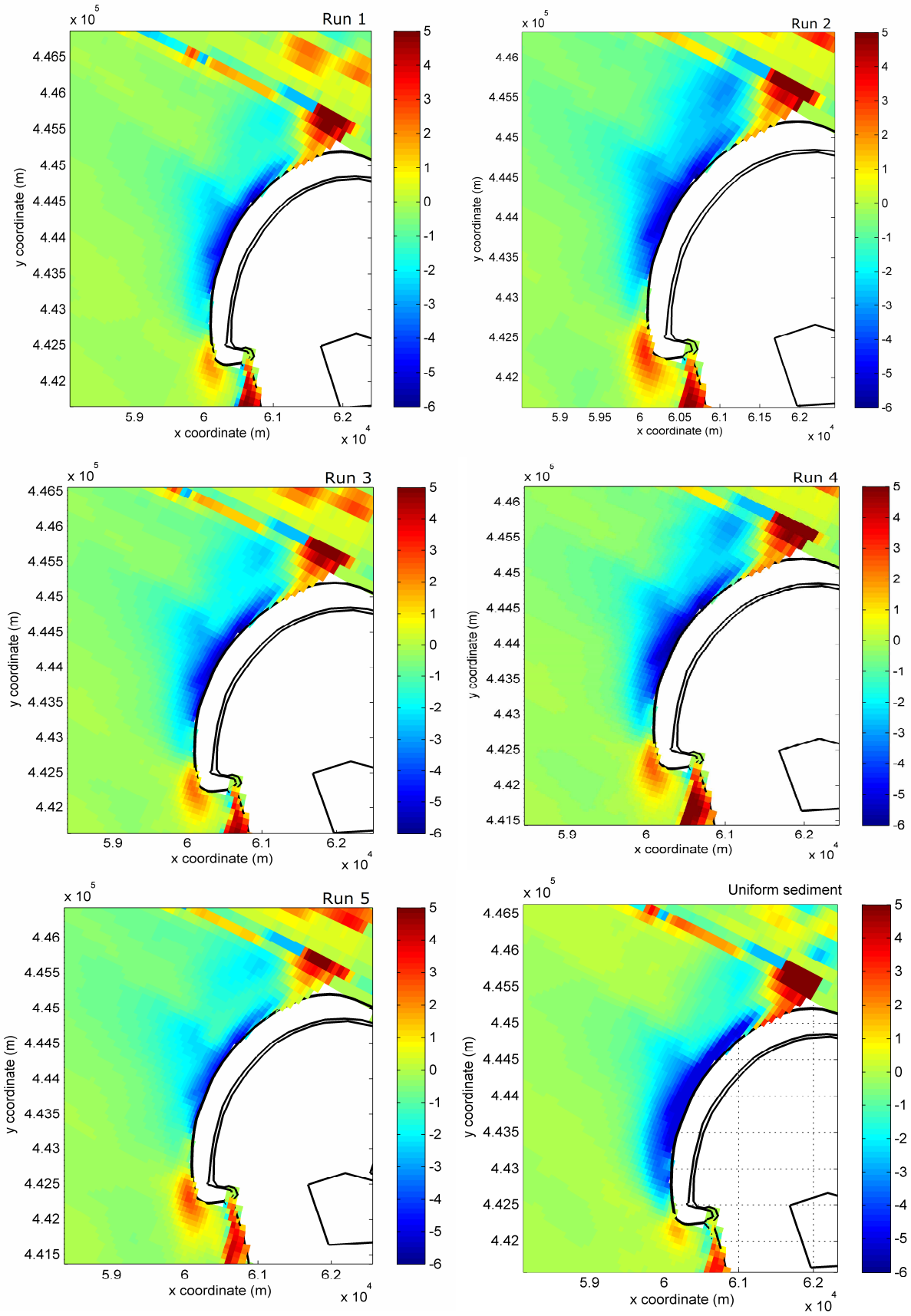

Figure 6.8 Cumulative erosion run 1–5 and uniform sediment of 0.2mm

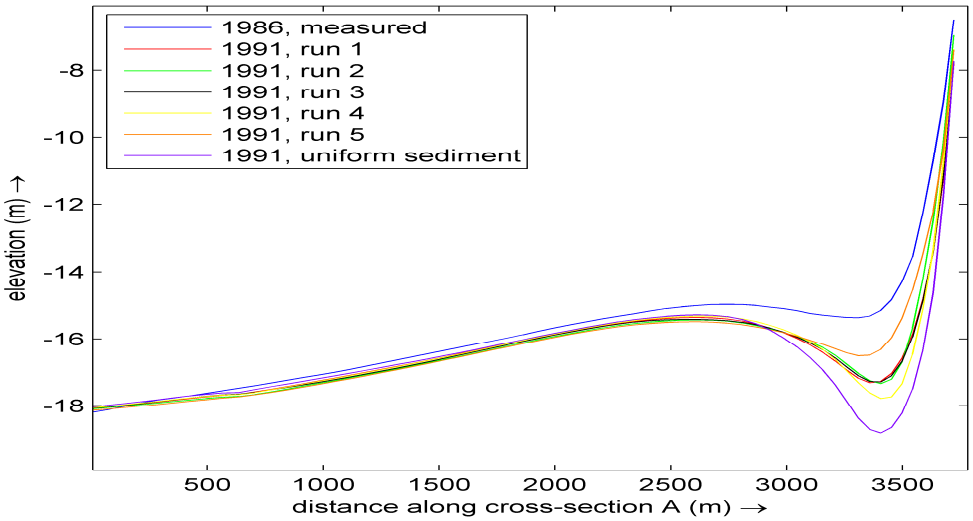

Figure 6.9 Bed levels cross section A 1986-1991 for different fraction distributions

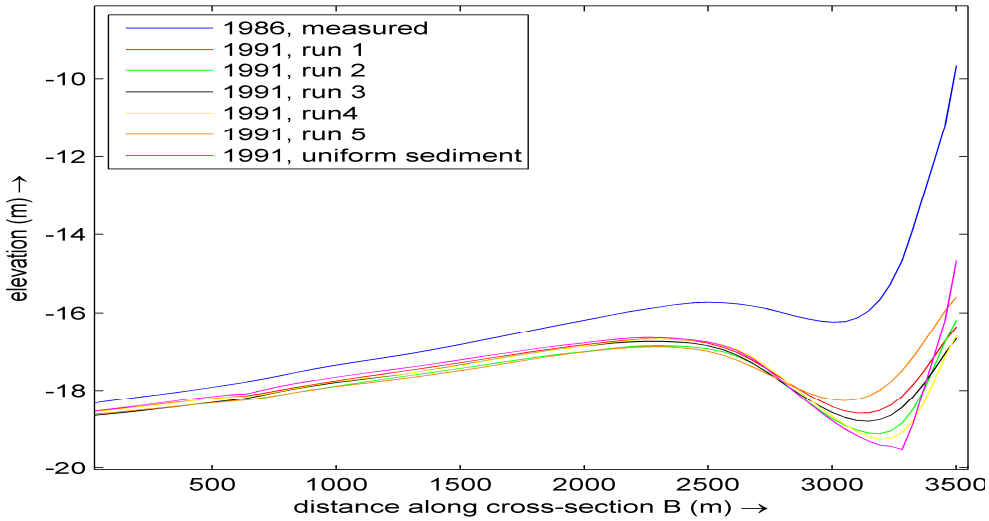

Figure 6.10 Bed levels cross section B 1986-1991 for different fraction distributions

6.3.5 Accretion in the Maas trench

In figure 6.11 the accretion in the Maas trench is given. As discussed in chapter 5 there was already an overestimation of the effort for dredging in the model compared with reality for uniform sediment. As can be seen in this figure there is a larger overestimation for the simulations with graded sediment. As posed in paragraph 6.1 there is a larger accretion for fine sediment. So because of the presence of relatively fine material in the graded sediment a larger accretion is explained. As can be seen the runs with the largest amount of fine material have the largest accretion in the Maas trench.

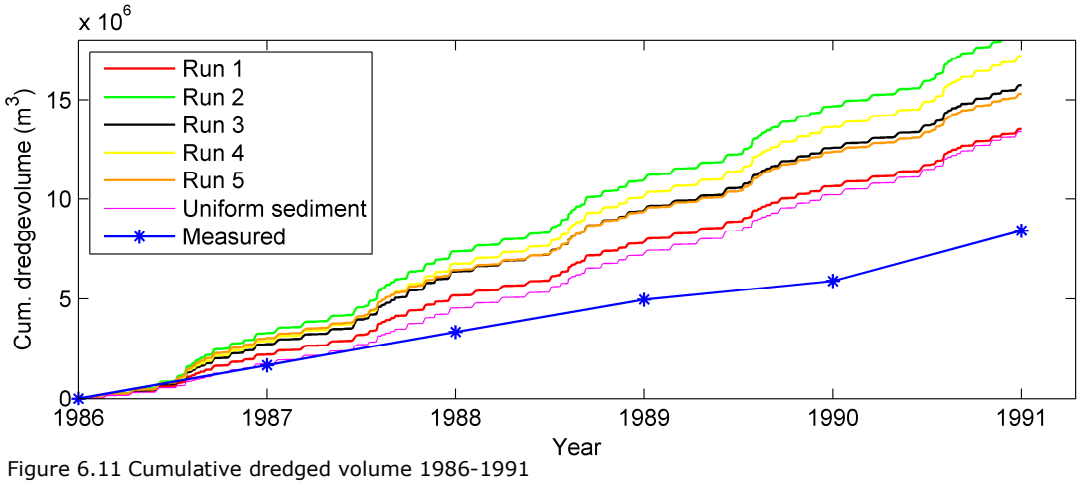

Figure 6.11 Cumulative dredged volume 1986-1991

6.3.6 Eroded volume

In table 6.4 the eroded volume out of the polygon as shown in figure 4.8 is shown for the simulated runs. The eroded volume is larger for the runs with the larger erosion depth and extent as discussed in the former paragraph.

Table 6.4 Eroded volume and accretion Maas trench, computed 1986-1991

	Eroded volume [m^3]	Accreted volume [m^3]
Run 1	6,80E+06	1,35E+07
Run 2	8,30E+06	1,84E+07
Run 3	7,70E+06	1,57E+07
Run 4	8,00E+06	1,72E+07
Run 5	6,80E+06	1,53E+07
Uniform sediment	8,80E+06	1,34E+07

Mutual comparison of the graded sediment simulations show that a larger eroded volume cause a larger accretion in the Maas trench. Run 1 shows the smallest eroded volume and the smallest accretion. The other four runs show relatively to run 1 more accretion than erosion out of the scour hole as can be seen in table 6.5. This points out that the increase in accretion is not only due to a larger scour hole.

Table 6.5 Eroded volume and accretion Maas trench relatively to run 1

	Accreted volume [m^3] relatively to run 1	Eroded volume [m^3] relatively to run 1
Run 1	0,00E+00	0,00E+00
Run 2	4,90E+06	1,50E+06
Run 3	2,20E+06	9,00E+05
Run 4	3,70E+06	1,20E+06
Run 5	1,80E+06	0,00E+00

6.3.7 Erosion rate

In figure 6.12 the erosion is given in the middle of cross section B (figure 4.5) for the five runs with graded sediment and uniform sediment. The simulations with graded sediment show initially fast erosion. This is because of the easily eroded fine sediment. As the fine sediment is eroded the soil composition in the scour hole becomes coarser and the erosion rate decreases. The uniform sediment shows a constant erosion rate in time. The change in rate of erosion as

can be seen in the figure is due to waves. Although the same wave conditions and the same sequence of wave conditions is applied for uniform and graded sediment there is a difference in the erosion rate. For uniform sediment very clearly the erosion rate increased when waves are applied. For graded sediment a minor increase occurs.

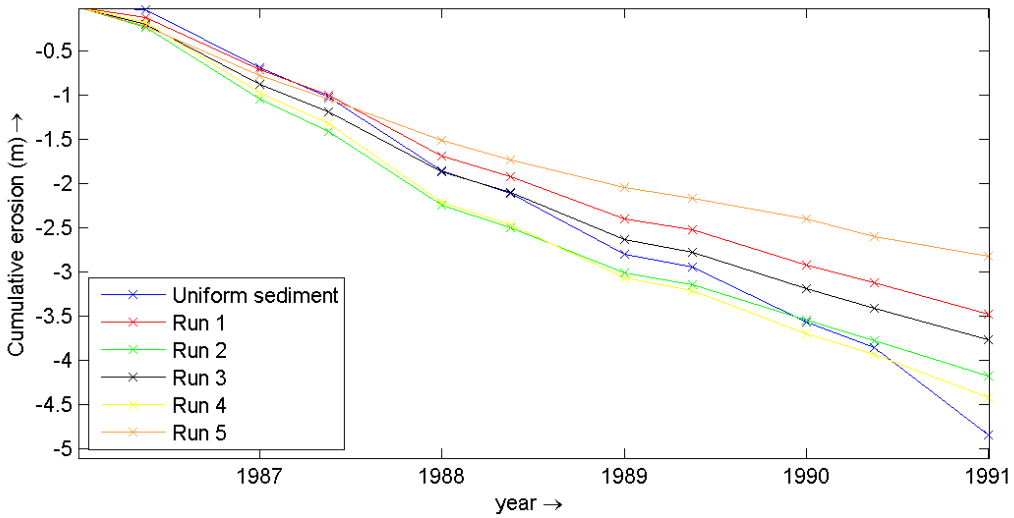

Figure 6.12 Decreasing erosion rate for graded sediment

Run 3, 12 year simulation

For run 3 a simulation of 12 years has been executed. In this way the erosion rate and the accretion in the Maas trench after the erosion of the fine sediments can be better determined. Both the accretion in the Maas and the erosion for a point show a slightly decrease after 3 years. After this period the erosion rate and the accretion rate are only slightly decreasing as can be seen in figure 6.13 and figure 6.14.

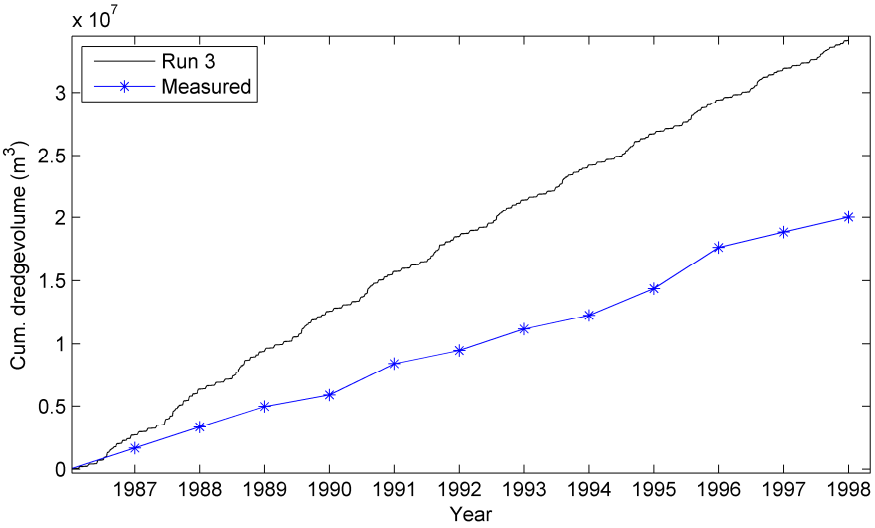

Figure 6.13 Cumulative dredge volume run 3 after 12 years

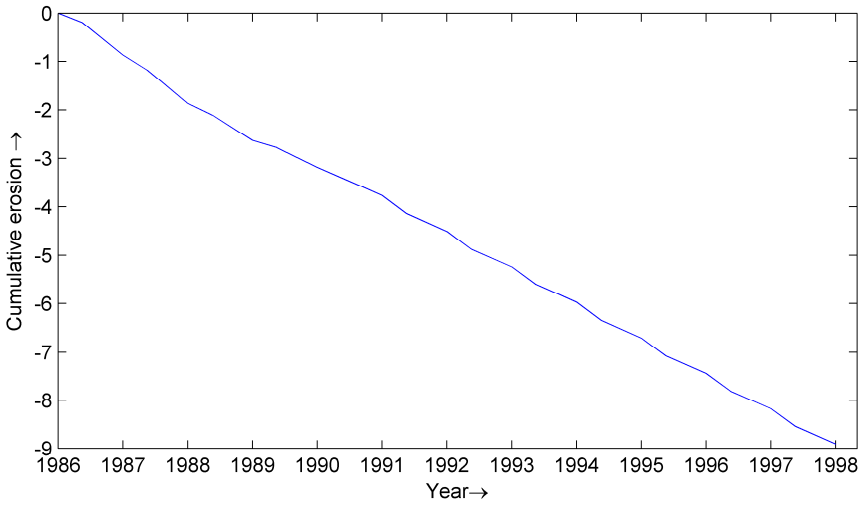

Figure 6.14 Erosion run 3 for 12 years

6.4 Armouring

The fine sediment will erode faster than the coarse sediment. The material eroded in the transport layer will be replenished from below. The distribution of the replenishment is equal to the distribution of the layer below, which initially has the same distribution as the transport layer. In this way the eroded fine sediment is replaced by sediment which is less fine. Therefore the distribution in the transport layer is getting coarser and coarser.

In figure 6.15 the distribution of the different fractions in the transport layer along cross section B is shown for the five runs. In the figure right below the position in the scour hole can be seen. The blue lines indicate the initial sediment distribution for each sediment fraction. (The initial distribution was: Fraction 1: 20%, fraction 2: 30%, fraction 3: 30%, fraction 4: 10%, fraction 5, 10%)

In general the finer sediments are eroded and give a lower content in the cross section. The content of the coarser sediments therefore becomes higher. The proportion fine/coarse sediments becomes lower and therefore also the D50 in the transport layer increases as can be seen in figure 6.14.

A closer look at *run 1* in figure 6.15 shows a higher content of fraction 4 and fraction 5 as expected because these fractions will erode less. There is a lower content for fractions 1, 2 and 3. The maximum coarsening is not in the deepest point in the scour hole but on the point with the largest erosion which is actually closer to the coast. The highest content reduction is found for fraction 2 with a maximum content decrease from 30% to 21.5% which is a reduction of 28% for this sediment. (The erosion is proportional to the availability of sediment in the transport layer. Therefore the reduction for each individual sediment is of concern.) The smallest fraction content is reduced from 20% to 17%, which is a reduction of 15%. Besides a larger extent of the reduction for fraction 1 an increase of this content is found near the coastline.

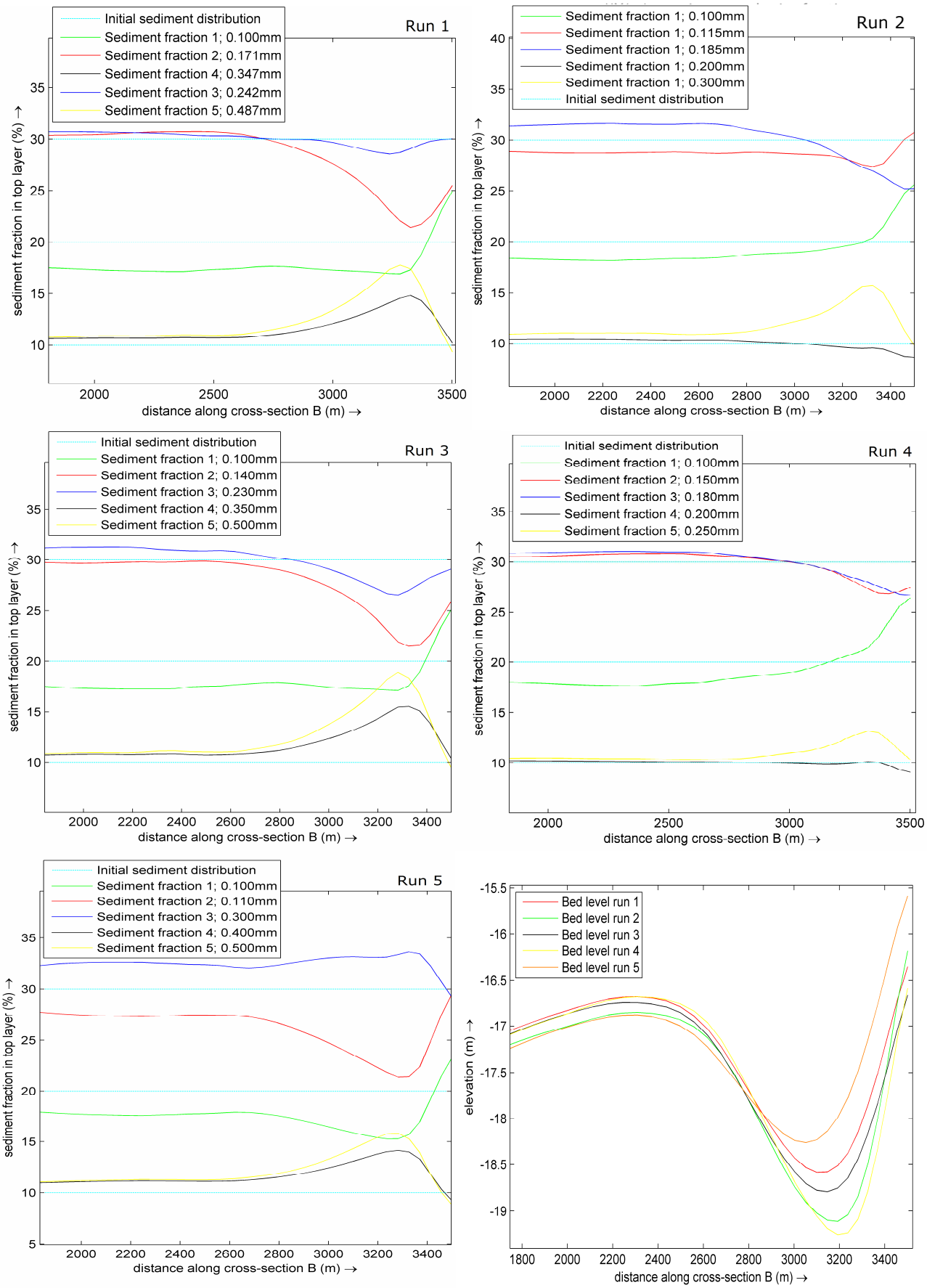

Figure 6.15 Sediment fraction distribution in cross section B after 5 years for run 1-5. The figure right below shows the position in the scour hole.

The other simulation runs show the same results: a content decrease for the small sediment fractions and a content increase for the large sediment fractions. Also every run demonstrates over a large extent a relatively low content reduction and a content increase near the coastline for the smallest sediment fraction. There is a difference in this runs for the fractions 2, 3 and 4. There content can increasing or decrease. Depending on the composition of the run and the D50 of the fraction the fractions have the function of armour or armoured.

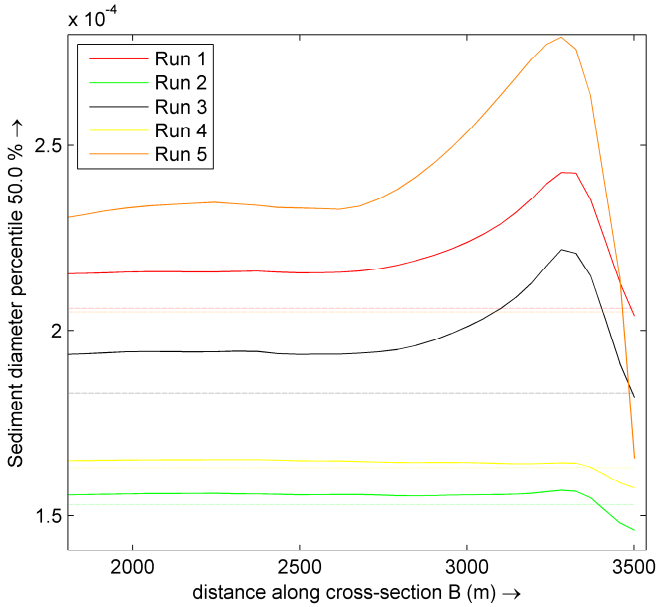

Figure 6.16 D50 distribution along cross section B

Figure 6.16 displays the D50 distribution along cross section B and figure 6.17 shows the distribution for the whole area of interest. Run 1, 3 and 5 show a large increase of the D50 at the place of the scour hole which has a similar pattern of erosion. Run 2 and 4 show less or no increasing D50. This is due to the fine sediments which show less erosion depth as seen in paragraph 6.1. The increase of the D50 shows the effect of armouring.

Run 2 and 4 are the runs with lowest D90/D10. With a large D90/D10 ratio armouring will happen easier. In the model can be seen that the D50 has only a low increase. Figure 6.15 shows an increase of the content of the largest fractions. But since there is only a little difference in D50 for the different fractions (low D90/D10) the fraction distribution changes but the effect on the D50 is small.

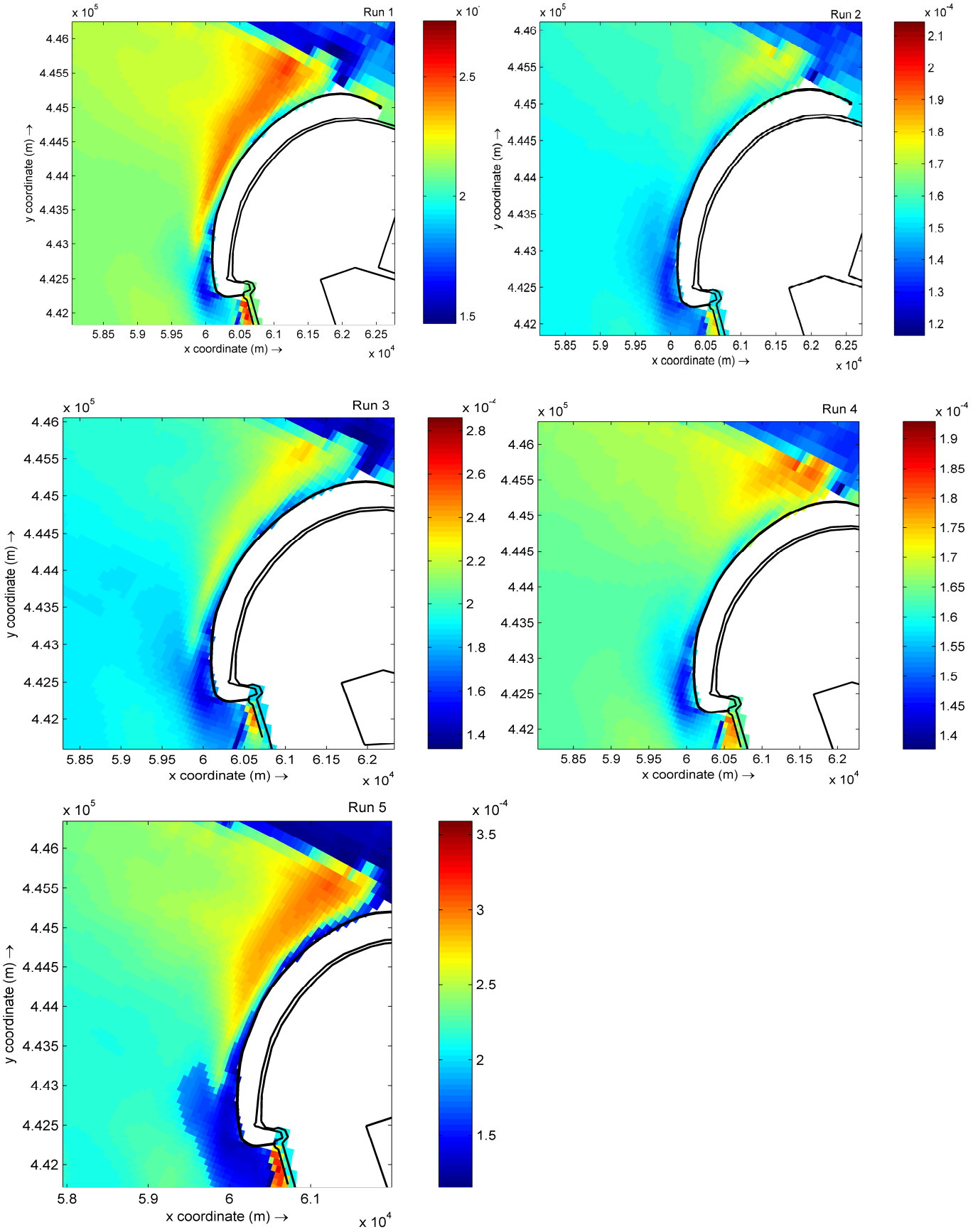

Figure 6.17 , D50 distribution top layer around scour hole for run 1-5

6.5 Conclusions

6.5.1 Uniform fractions

Several runs have been made with a single layer and spatial and depth uniform sediment. There was variation in the D50 for the different simulations. From the simulations (waves were included) it is concluded that for the smallest sediment fraction used in this chapter (100 μm) the depth of the scour hole is smaller but the extent is considerably larger. The other investigated sediments were larger than 100 μm and showed a decreasing scour depth and a decreasing extent for an increasing particle size.

The accretion in the Maas trench increases with a decreasing particle size. Because there is more sediment transport with smaller particles there will be more accretion.

6.5.2 Implementing several fractions and multiple layers

Five simulations have been performed to investigate the influence of graded sediment. All performed runs show clearly a decrease of the erosion compared with the uniform sediment run. The displayed erosion pattern is similar.

There are two reasons for the decrease of the erosion:

1. Armouring: the transport layer coarsens because the relatively fine material eroded faster. This relatively courser layer causes a decrease of the erosion.
2. The finest sediments (100 μm) cause a decrease of the maximum erosion depth as shown in paragraph 6.1.

Simulations with uniform sediment (non-graded) of 200 μm already showed an overestimation of the accretion in the Maas trench. All the simulations with graded sediment show an even larger accretion. The volume what is eroded out of the scour hole is smaller compared to the case with uniform sediment. The larger accretion is due to the small fractions which cause a relatively high accretion in the Maas trench. When the five simulations with graded sediment are mutually compared a larger accretion is found when a larger volume is eroded out of the scour hole. Not the complete increase of accretion can be clarified with the larger volume which is eroded out of the scour hole.

All the graded sediment simulations show a decreasing erosion rate because the availability of the easily eroding fine sediment is decreasing and the content of the hard to erode larger sediment is larger.

Armouring
The armouring effect is observed well in the model. In and around the scour hole an increase of the content of the larger sediment fractions is found and a decrease for the smaller sediment fractions (except for the smallest particles, 100 μm). The armouring effect depends on the ratio D90/D10. A high value for this rate gives more armouring.

Quantification
The best fit of the analysed sieve curves has been used in run 3. The same fraction distribution will be used in the Maasvlakte 2 case. Investigation of the deepest point of the scour hole shows 25% reduction of the erosion depth. This is far below what is needed to give the same erosion depth as found in reality which is a reduction of 60%. This 60% needed reduction only counts for the first years after 1986. After 1990 even less erosion is observed as shown in chapter 2. The other runs with graded sediment give 29%, 13%, 8% and 39% reduction for respectively run 1, 2, 4 and 5. So because of the wide range in sieve curves there is also a wide range in the reduction of the erosion in the scour hole. But even in run 5 the reduction is not enough to approach the erosion found in reality.

Chapter 7 MV1: Cohesive sediment

In the area of interest certain clay layers have been found. Because of the cohesiveness of clay a lower erosion rate is expected and therefore the development of the scour hole will be limited. This can be the explanation of the overestimation of the scour hole by the model when only non-cohesive sediment is considered. The area around the scour hole is a former complex estuarine system, composed of highly mobile tidal channels and tidal flats which have resulted in a highly stratified bottom. In such a stratified system the erosion rate can fluctuate extremely. Sand erodes relatively fast, but when a clay layer has been reached the erosion rate can reduce strongly and in some cases reduce to zero. When a thin layer of clay is eroded away an erosion hole can develop relatively easy again, until a next clay layer will be reached.

The aim of this chapter is to make a new hindcast of the Maasvlakte 1 case where cohesive sediment is implemented. The results will be compared with the case where uniform sediment is simulated and with reality. Aim is to calibrate the concerning parameters such that these can be used for the Maasvlakte 2 case.

In this chapter first a short introduction will be given on the physical aspects of cohesive sediment (7.1). From the data analysis in chapter 3 a schematization for the model will be made (7.2). In paragraph 7.3 the parameter setting concerning cohesive sediment will be determined. Hereafter these parameters will be tested (7.4) in several simulations with uniform (non-graded) cohesive sediment (the complete model area is covered with the same cohesive sediment, no variation in vertical direction). In paragraph 7.5 three different schematizations will be simulated. In the first schematization a thick clay layer lies parallel to the surface where in schematization 2 a thick layer is defined on a certain depth. The first 2 schematizations where started at the 1986-bathymetry. The third schematization is started at the 2000-bathymetry. In this schematization the effect of a thin layer is investigated.

In paragraph 7.6 the conclusions for this chapter will be given. This chapter ends with general conclusion about the Maasvlakte 1 simulations.

7.1 Introduction to cohesive sediment

For low sediment concentrations, silt and clay are only transported in suspension. For high concentrations, silt and clay can also be transported as fluid mud in a layer near the bed. In that case, the fluid mud will act as a viscous layer on top of the bed, blocking exchange of sand between the bed and the water column.

For clay content of less than 5-10% the bed behaves more or less non-cohesive. In that case sand and mud erode more or less independent, so the normal formulations for the bed erosion can be used. For clay content exceeding 5-10% the bed behaves cohesively. The sand and mud particles are eroded simultaneously.

In sediment transport modelling, the exchange processes between water column and bed layer are often assumed to be governed by the critical bed shear stress of the bed material and the actual occurring bed shear stresses. For actual bed shear stresses larger than the critical bed shear stress of the bed material, the grains can be eroded, whereas for actual bed shear stresses smaller than the critical bed shear stress of the bed material, the grains can settle. [Van de Graaff, 2006]

For non-cohesive material the critical bed shear stress $\tau_{b,cr}$ is for erosion equal to the critical bed shear stress for sedimentation. For cohesive material, where there is a strong binding force between the particles, this is not the case. The critical bed shear stress for erosion is larger than the critical bed shear stress for sedimentation. This implies that for a range of actual bed shear stresses, there is no exchange with the bottom layer in case of cohesive sediments. [Van Ledden, 2003]

Erosion of cohesive sediments

The erosion rates of different beds, ranging from old, well consolidated deposits to fresh soft deposits, may vary by several orders of magnitude, depending on among other things the stress history. In general only a few millimetres will erode in one tidal cycle. But when mixed over the water column, the eroded sediment may increase the local suspended sediment concentration by tens to hundreds of mg/l. Here large gradients in physical-chemical properties may occur, affecting the erodibility of sediment deposits. This explains once more the large range of the rate of erosion. [Winterwerp and Van Kesteren, 2004]

[Winterwerp and Van Kesteren, 2004] distinguishes four modes of erosion: Entrainment, floc erosion, surface erosion and mass erosion. The entrainment occurs when the mud is so soft that it behaves as a viscous fluid. Floc erosion happens when flocs at the bed surface are individually disrupted by the water movement. This may occur when the flow induced bed shear stresses exceed the strength of the flocs or the adhesion of flocs to the bed. The floc strength and adhesion may decrease in time by cyclical stresses. Surface erosion happens when eroded sediment particles are replaced by water and the top of the bed liquefies. In the case of mass erosion lumps of material are removed when the external stresses exceed the undrained shear stresses of the bed.

Partheniades [Winterwerp and Van Kesteren, 2004] was the first to carry out erosion experiments on marine cohesive sediments in a systematic way. He developed a formula which is still widely used:

$$E = M*(\tau_0 - \tau_e) \text{ for } (\tau_0 > \tau_e)$$
$$E = 0 \qquad \text{for } (\tau_0 \le \tau_e)$$

where:
$E = \text{erosion flux } \left[\text{kg/m}^2/s\right]$
$M = \text{erosion parameter } \left[\text{kg/m}^2/s\right]$
$\tau_0 = \text{bed shear stress due to current and waves} \left[\text{N/m}^2\right]$
$\tau_e = \text{critical shear stress for erosion} \left[\text{N/m}^2\right]$

This formula is also used in the Delft3D model and therefore used in this study.

7.2 Schematization of stratified bottom for the model

Four indicators were shown in chapter 3 which suggests that part of the eroded material in the scour hole was cohesive material:

- Strong alternating erosion rate (paragraph 3.1) suggests difference in bed material
- An irregular bed level is observed (paragraph 3.1), which suggests a spatial variation of the bed material
- Clay is exposed at two locations close to the centre of the scour hole
- Geotechnical analysis suggests clay on higher positions in the area of interest (Appendix B)

From these indicators the following hypotheses followed:

There is cohesive material exposed in the scour hole in the period 1986-2006. There are several layers with different clay content and therefore a different erosion rate is observed in this period.

From the sediment samples and on basis of the geotechnical setting there can be concluded that the system is highly stratified. Different layers with different clay content, pure non-cohesive layers and also peat are observed. For the hindcast of the Maasvlakte 1 model it is important what kind of material is eroded out of the scour hole. There is no information about the exact stratification than the erosion rate. Three periods were distinguished in chapter 3:

- 1986-1989: high erosion in the whole area which is comparable with the computations done with non-cohesive material (chapter 4)
- 1989-2000: Low erosion with more spatial variance
- 2000-2006: higher erosion rate with a low spatial variance

The following can be concluded concerning the soil composition. The soil which is eroded in the period 1986-1989 eroded relatively easily so actually no clay content is expected.

In the period 1989-2000 only a few decimetres eroded in the centre of the scour hole. For some periods hardly any erosion is found. Much of the material which is eroded in this period seems difficult to erode. Therefore high clay content is expected.

In the period 2000-2006 no intermediate bathymetric data is available. The average erosion rate is higher that in the period before but lower than expected with merely non-cohesive material. Therefore it is expected there is still some clay content in the eroded material in this period. It can also mean that the first years after 2000 the last part of a clay layer is eroded and after this the relatively fast erosion of a sand layer has been started.

In the Delft3D model different layers can be implemented. Therefore it is possible to implement the observed stratified bed. In the area outside the scour hole merely non-cohesive material is exposed.

For the period 1986-1989 no clay content is expected. In this period an erosion rate of around 0.5 meter/year occurs. Therefore a cover of the whole area of 1.5 meter will be given. Under this 1.5 meter of sand 1 meter hard to erode clay is expected in the place of the scour hole. This will be implemented in the whole

area though this clay does not exist everywhere. This will not give an error because in the area besides the scour hole the sand cover of 1.5 meter will probably not erode at all. This meter of clay eroded according to the measurements in the period 1989-2000.

The period 2000-2006 was from the beginning in this study computed separately from the period 1986-2000. This will also be done in this chapter. Therefore locally, at the place of the scour hole, a clay layer will be defined. There is a lower erosion rate than in the period 1989-2000. Therefore here a lower erosion parameter (next paragraph) will be applied for this case.

7.3 Parameter setting

In Delft3D for cohesive sediment fractions the fluxes the erosion fluxes are calculated with the Partheniades-Krone formulations as derived by Partheniades in 1965 [Delft3D-Flow manual].

$$E = M*(\tau_0 - \tau_e) \text{ for } (\tau_0 > \tau_e)$$
$$E = 0 \qquad \text{for } (\tau_0 \le \tau_e)$$

where:
$E = \text{erosion flux } \left[\text{kg/m}^2/s\right]$
$M = \text{erosion parameter } \left[\text{kg/m}^2/s\right]$
$\tau_0 = \text{bed shear stress due to current and waves} \left[\text{N/m}^2\right]$
$\tau_e = \text{critical shear stress for erosion} \left[\text{N/m}^2\right]$

The erosion parameter M and the critical shear stress for erosion τ_e have to be defined for the model. Both parameters have a large range and are usually determined by calibration.

[Winterwerp and Van Kesteren, 2004] and [Whitehouse et al., 2000] give some formula for these parameters and values which are found in other cases. This is further elaborated in appendix D.

The ranges which are found are rather large: 1.0 – 2.5 Pa. for the critical shear stress and $1*10^{-4}$ to $1*10^{-6}$ m/Pa/s. for the erosion parameter.

7.3.1 τ_e versus M

When distinction is made in four modes, two different values for τ_e and M will be found for the governing two erosion modes. For floc erosion a relatively low τ_e and M. For surface erosion a relatively high τ_e and M.

The actual extent of consolidation in the area of interest determines the values of these parameters. When the stratified system which has been formed in the Holocene is strongly overconsolidated the old clay has to swell first before it can erode.

The critical shear stress τ_e is coupled to the erosion parameter M depending on the erosion mode: an old layer which is hard to erode will have a high critical shear stress and a low erosion parameter while a fresh layer which just deposited will have a relatively low critical shear stress and a high erosion parameter M.

When computations are made to determine the equilibrium the relation between the critical shear stress and the apparent shear stress is important. When the rate of erosion is important the value for M is very important. For the extent of the erosion again the critical shear stress becomes important.

In the Maasvlakte 1 case the rate of erosion is very important for the hindcast of the scour hole. No equilibrium is reached yet and therefore the relation τ_e versus τ_{cw} becomes less important.

For the Maasvlakte 2 case the equilibrium state of the scour hole becomes more important and therefore also the relation τ_e versus τ_{cw}.

In the area of interest in case of Maasvlakte 1 distinction has to be made between erosion of the old Holocene clay layer and fresh clay. The old clay will have a high critical shear stress and a low erosion parameter M. When this clay is eroded and settled again it will not have the same parameters as before. This fresh clay can come out of the scour hole but can also come from other places in the system. The critical shear stress is considerably lower and the erosion parameter is considerably higher for this fresh clay.

In the Delft3D-model it is not possible to define different parameters for old clay and fresh clay. The freshly deposited clay will have the same parameters as the old clay. This problem can be circumvented by setting the critical shear stress for deposition on 10^{-6} Pa. In this way the once eroded clay will not settle and will therefore not receive the wrong erosion parameters. The critical shear stress for erosion and deposition can be spatially defined. By doing this the clay can be defined as old clay in the scour hole and as fresh clay in the rest of the model area.

The cyclic load of waves can accelerate the process of swelling in case of the overconsolidated old clay. The waves influence by way of the enhancement of the bed shear stress caused by wave-current interaction. As can be seen in figure 5.2 the waves influence the maximum bed shear stress. The actual cyclic load which would accelerate the swelling of the clay is not incorporated in the Delft3D model. This should be discounted in the erosion parameter M: a higher value for this parameter where the waves have the largest influence on the bed.

7.3.2 Clay content

As stated in the former paragraph different layers contain different clay content. There are layers with 100% clay but also layers with only 10% clay. It is possible in Delft3D to define a layer with for example 50% clay and 50% sand. Now there are two possibilities in the model:

1. Assume that the bed composition is uniform

The erosion rate is proportionally to the availability of the sediment fraction in the top-most layer of the bed. The sand will than act non-cohesive and the clay will act as a 100% clay layer. So if the sand erodes more easily than the clay after a while the sand is eroded away and a layer which consist for 100% out of clay. This will give an underestimation of the erosion rate especially with low clay content.

2. The considered cohesive sediment fraction forms a layer that covers the other sediment fractions.

The erosion rate of the cohesive sediment will not be reduced. The erosion rate will be doubled when two cohesive fractions are implemented and the erosion rate is than overestimated.

In reality however the sand and clay is mixed and also the sand particles are subject to cohesive forces. Therefore it is better to define a layer which consists for 10% out of clay and for 90% out of sand as a full cohesive layer, but with different parameters for a layer with different contents. According to [Van Ledden, 2003] it is expected that erosion rate M decreases logarithmically with increasing clay content. The critical shear stress τ_e increases with increasing clay content.

7.4 Calibration parameter settings

Before computing the layered system which is present in the area of interest the parameters for cohesive sediment need to be calibrated. For different values of the erosion parameter M and the critical shear stress τ_e computations were made. For this calibration a single layer with clay is applied. First the computations were made without waves and thereafter the waves were added.

7.4.1 Without waves

The different values of τ_e and M which are computed for calibration are listed in table 7.1. In the last column the erosion rates are given. These rates are computed in the centre of the scour hole for the different parameter settings.

Table 7.1 , erosion rates without waves

M [kg/m^2/s]	τ_e[N/m^2]	Erosion rate [m/year]
1,00E-04	0,5	1,6
1,00E-04	1	0,8
1,00E-04	1,5	0,4
1,00E-06	0,5	0,04
1,00E-06	1	0,01
1,00E-06	1,5	0,002

The development and the extent of the scour hole are similar to the computations done with non-cohesive sediment. The development of the depth of the scour hole depends highly on the chosen parameter settings for M and τ_e. As can be seen in the table the erosion rates and therefore the depth of the scour hole can take every value for the range which was found for M and τ_e in the previous paragraph.

7.4.2 Waves included

In the case with non-cohesive sediment the erosion rates were higher when waves were added. For the present case with cohesive sediment though this is not true. In figure 7.1 the cumulative erosion is shown for the case with waves. The used parameters for cohesive sediment were 1.0 N/m^2 for the critical shear stress and 10^{-4} kg/m^2/s for the erosion parameter. On the right side in figure 7.1 the same parameters are used but without waves. As can be seen in these figures there is erosion in the case without waves and an irregular pattern in the case with waves. On some locations the sediment accreted and on some locations the sediment eroded. Because the pattern of the erosion in the simulation with waves some parameter settings have been adapted. In figure 7.2

a better erosion pattern is achieved with a lower fall velocity and a lower critical shear stress. The erosion is than considerably and the erosion rate is larger than expected for the old clay. Applying a higher critical shear stress gives erosion patterns as in figure 7.1 (left).

As posed in the previous paragraph the critical shear stress for deposition has to be set on 10^{-6} because of the difference in parameters for old clay and fresh clay. Supposing this reduced critical shear stress locally will of course result in erosion in the defined area. Supposing this critical shear stress in the whole model area will give considerably erosion in the whole area. It does not make sense to decrease this parameter in the actual case where uniform clay is applied.

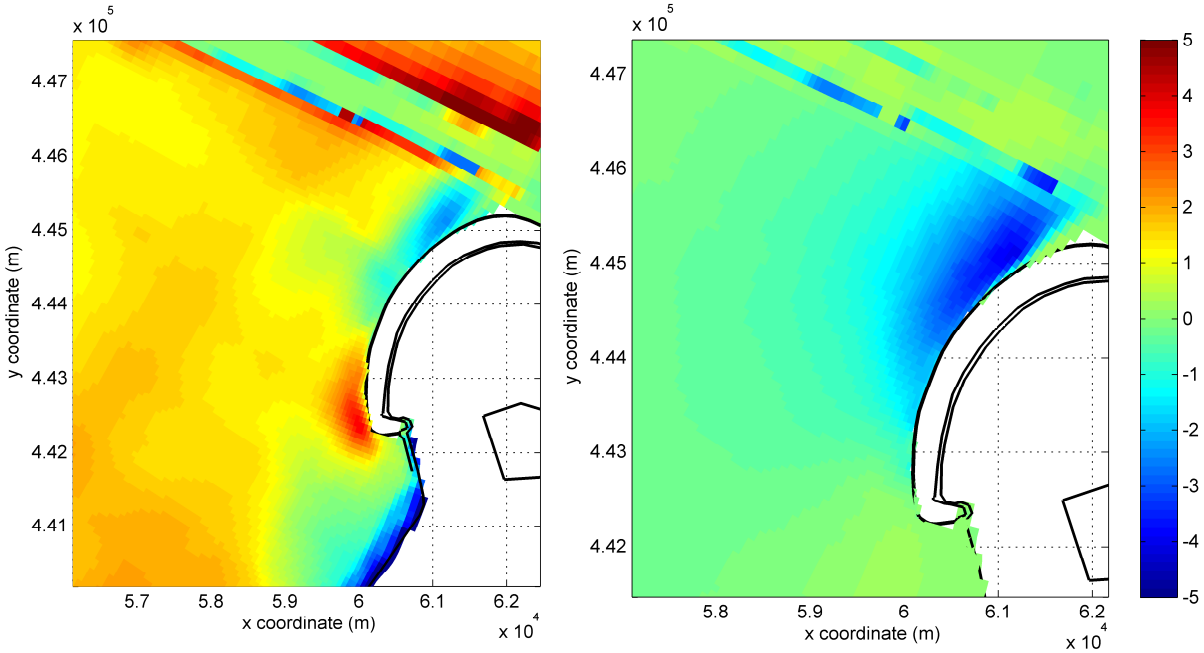

Figure 7.1 Cumulative erosion after 5 years, τ_e=1.0, M=10^{-4}, waves included (left), no waves (right)

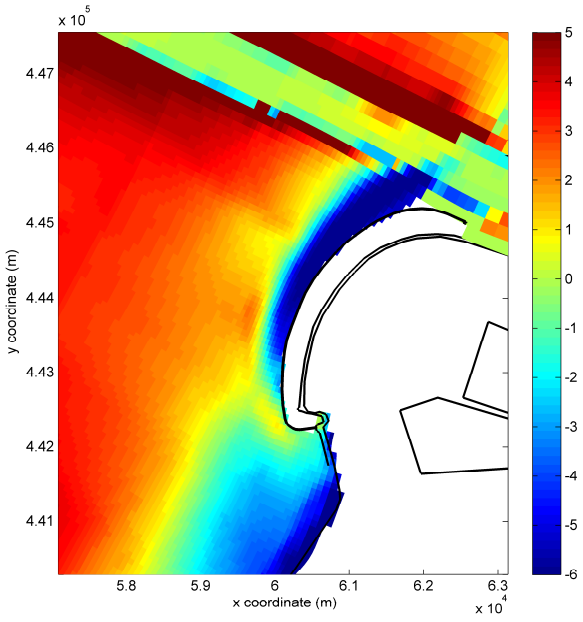

Figure 7.2 Cumulative erosion: τ_e=0.25, M=10^{-4} and fall velocity w_s=0.1 instead of 0.25 m/s

7.5 Computations with schematized model

In this paragraph the model schematization as proposed in paragraph 7.3 with the calibrated parameter settings will be used in the computer model. The aim is to reconstruct the same development of the scour hole in the model as can be seen in reality.

In the surrounding area there is no clay exposed. In the former paragraph model simulations have been made where the whole area was covered with cohesive material. In figure 7.1 can be seen that if waves are added that on some places accretion occurs where the scour hole is expected. Though if the cohesive material is only exposed locally this can be different. There will be less cohesive sediment available which can accrete. On the other hand when the hard to erode clay is exposed there will only be little erosion during relatively high current velocities but during small current velocities (slack water) the accretion will be large because also the non-cohesive material can accrete in the area were clay is exposed.

In the Delft3D model reference concentration, erosion rates and sediment transport rates will be reduced proportional to the availability of sediment fraction in the top most layer.

7.5.1 Schematization 1

The first schematization which has been modelled is as follows: A layered system consisting out of 5 layers. The top layer is a thin layer which is actual the transport layer. The layer below consists for 100% of non-cohesive material and has a thickness of 1 meter. The remaining layers consist out of cohesive material. All the layers have a uniform thickness. Several simulations have been made for a period of 3 years. In this schematization first the layer with non-cohesive material is eroded away relatively easily. After this the transport layer is only replenished by cohesive material from the initially deeper cohesive layers.

In figure 7.3 the resulting bed levels after three years are shown for different parameter settings concerning the cohesive material. For comparison also the result for uniform sediment is added. In this figure very clearly the border can be seen were the clay layer has been reached. This will be treated later in this paragraph.

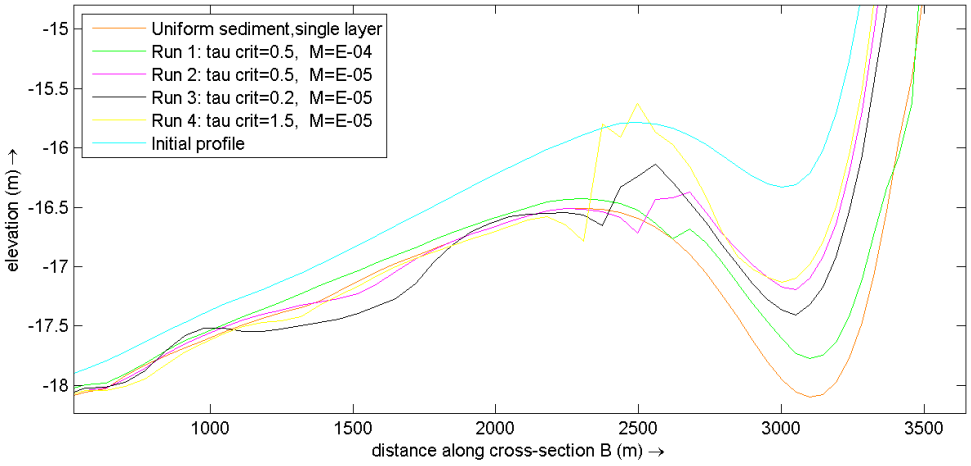

Figure 7.3 Bed levels cross section B for different clay parameters in a multiple layer model

Comparison of *run 1* and *run 2* shows a larger erosion depth for *run 1* (smaller erosion parameter M). In the part of the cross section where the erosion has not reached the cohesive layer shows more erosion for *run 2*: the lack of erodable sediment result in more erosion outside the area where clay is exposed (clear water scour). *Run 2, 3* and *4* have the same erosion parameter M but different values for the critical shear stress τ_e. The difference in erosion depth is only marginal. Major reason for this is that most of the erosion is due to the cohesive sediment layer. The erosion outside the area where cohesive material is exposed shows more erosion for a higher critical shear stress. Noticeable is the erosion on the border where clay is exposed. For increasing values of the critical shear stress especially the erosion on and around this border decreases. For *run 4* there is accretion on this place.

In figure 7.4 cross section B is shown for *run 3* after 3 years. In this figure the containing fraction of cohesive material for each layer is displayed. On the left side (between 500 and 1500m along cross section B) the transport layer and the layer below consist completely out of non-cohesive sediment. The dark red layer below (100% cohesive material) is not reached yet in this part of cross section B. On the right side in the figure the layer with non-cohesive material is completely eroded away and the layer with cohesive material has been reached. Erosion of the transport layer is replenished by cohesive material only. The transport layer consists therefore partly out of cohesive and partly out of non-cohesive material. On the transition were cohesive material is exposed the bed level is there discontinues. On the side of the transition where no cohesive material is exposed the erosion continues while on the other side there is accretion. This is explained with the fact that for non-cohesive sediment there is erosion on this position but for cohesive material there is accretion on this place as observed in the previous paragraph. The influence of clay is even with a small content directly noticeable in the scour hole.
There is more accretion for an increasing critical shear stress as displayed in figure 7.3 (in point of fact equal accretion but less erosion).

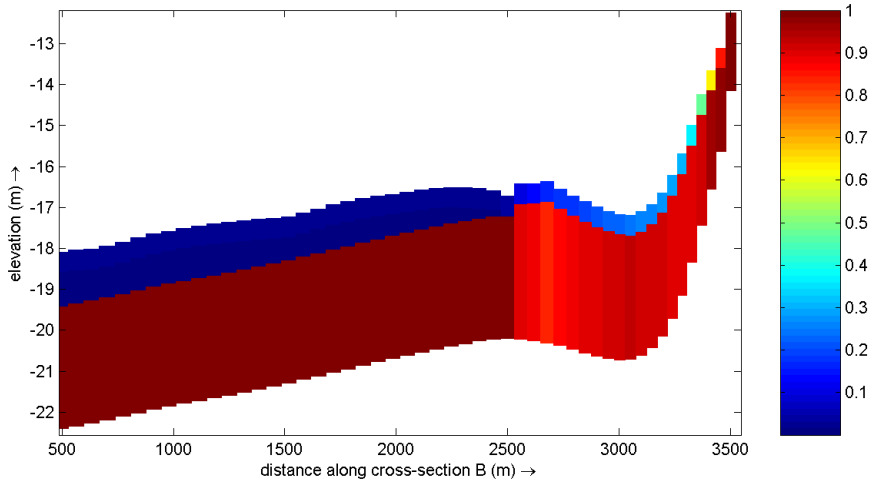

Figure 7.4 Fraction cohesive material along cross section B

The cumulative erosion after 3 years for run 3 is shown in figure 7.5. The transition between cohesive and non-cohesive sediment can be seen clearly. It must be noted that a large part of the erosion only slightly exceeds the 1.0 meter threshold. This means that the erosion of clay is small. The erosion after 5 years (figure 7.5, figure on the right) is only marginally larger than the erosion after 3 years. Except directly adjacent to the Zuiderdam where noticeable erosion is observed.

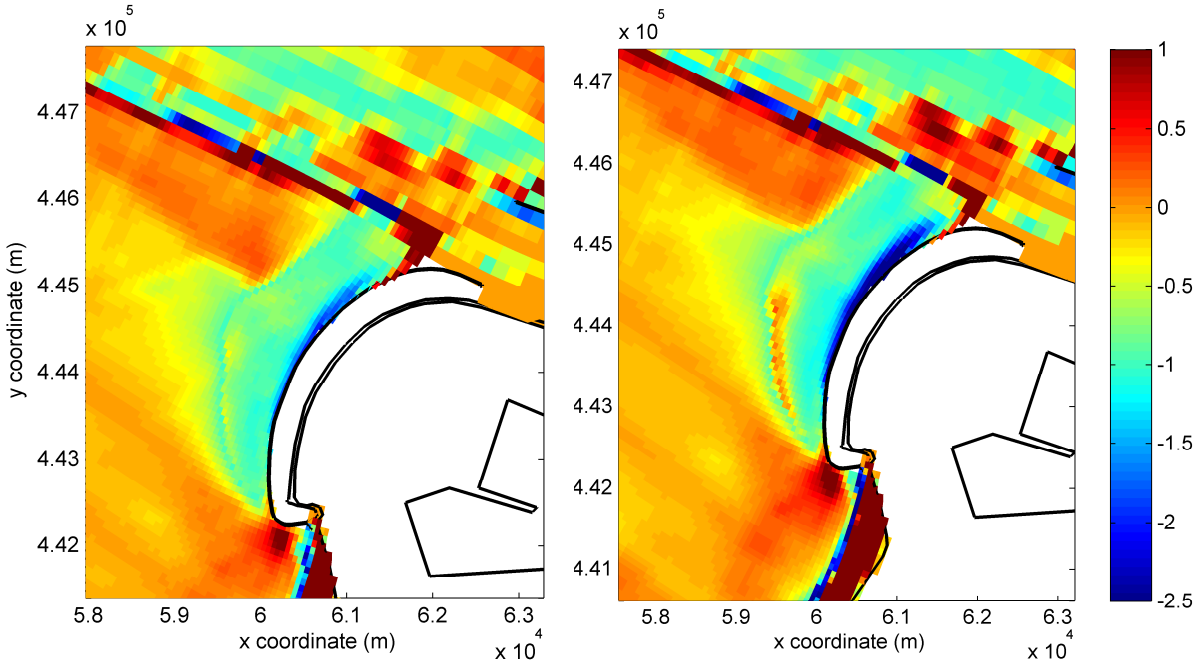

Figure 7.5 Cumulative erosion run 2: tau_crit=0.5 and $M=10^{-5}$: 3 years (left) and 5 years (right)

In figure 7.6 the cumulative dredged volume is shown for run 2. In the first years the dredged volume is equal to the dredged volume in the simulation with uniform sediment. After a few years the cohesive material is getting of importance which results in a lower dredge effort.

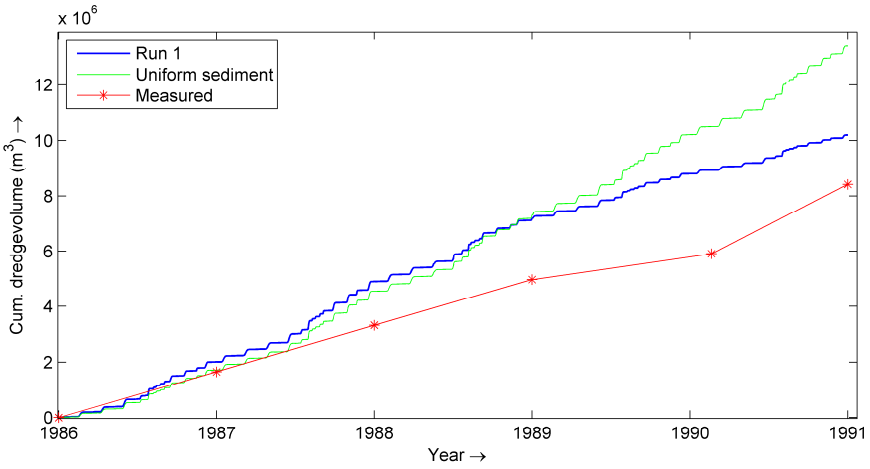

Figure 7.6 Cumulative dredged volume for run 2

7.5.2 Schematization 2

In the above used schematization the clay layer lies parallel to the surface. At the location of the scour hole this means that in the centre of the scour hole the layer is positioned deeper. In reality of coarse this is not true. In reality the clay layer exists only locally and the clay layer lies almost horizontal and most likely it is positioned slightly deeper when located more seaward. In this way the clay layer is exposed first and most in the centre of the scour hole.
Another schematization has been made. Again the top most layer consist out of non cohesive material. The layer below also consists of non-cohesive material but the thickness of this layer varies spatially. There is a smaller thickness closer to the Zuiderdam and a large thickness in the southern part of the area of interest. All the layers below consist out of cohesive material.

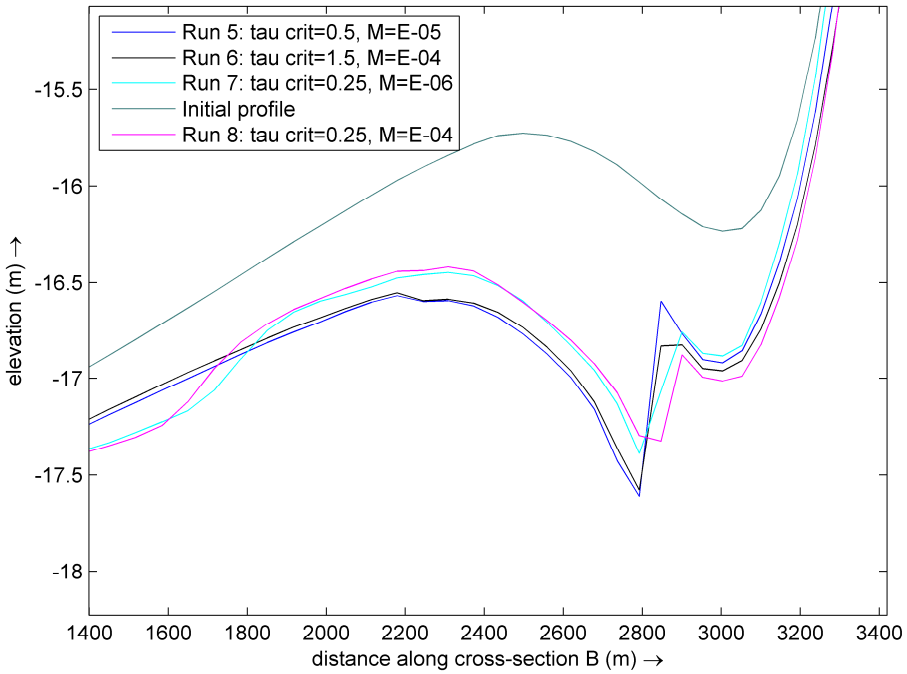

Figure 7.7 Bed levels cross section B for different clay parameters for schematization 2

As shown in figure 7.7 here is also a discontinuity at the transition between cohesive and non-cohesive material. The magnitude of this discontinuity again depends on the erosion parameter and the critical shear stress. The true erosion, so not the erosion and accretion effects at the transition, is close for the regarded runs. But again here the erosion of the non-cohesive material plays a role.

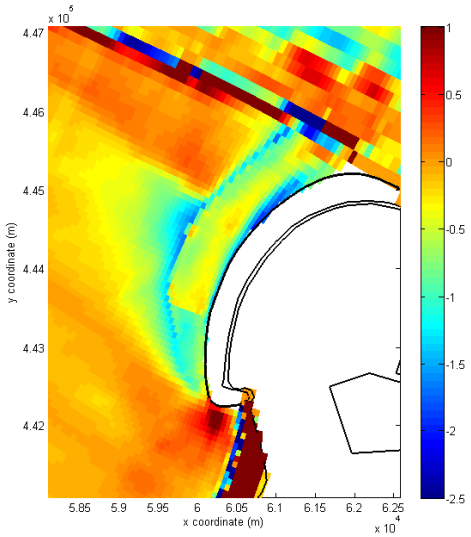

Figure 7.8 Cumulative erosion run 5: tau_crit=1.5 and M=10^{-5} : 3 years

The cumulative erosion figure (figure 7.8) shows the transition as well. Also a large extent of the scour hole can be seen. The erosion as shown here displays erosion between 0.3 and 0.6 meter on the locations where cohesive material is exposed. That is an erosion rate between 0.1 and 0.2 meters a year which is comparable with reality.

7.5.3 Schematization 3

All the former computations in this chapter have been performed with the 1986 bathymetry as initial bed level. In this subparagraph the simulations have been done with the 2000 bathymetry as initial bed level. In the former paragraph there was a cover of a non-cohesive layer. The cohesive layer below has a thickness of 3 meters. In this paragraph again the area will be covered with 0.5 meter of non-cohesive material and a transport layer of 0.5 meter. Under the cover of these two layers there will be one cohesive layer of 0.2 meter. In this way the influence of one thin layer will be investigated.

The parameters of the simulations are shown in table 7.2. Run 9 is used as the reference simulation. The other simulations only differ in one parameter with run 9. There is varied in the critical shear stress, the erosion parameter and the thickness of the clay layer.

Table 7.2 Parameter setting run 9-12

	Critical shear stress, τ_e [N/m^2]	**Erosion rate, M** [kg/m^2/s]	**Thickness claylayer** [m]
Run 9	0,5	1,00E-05	0,2
Run 10	0,25	1,00E-05	0,2
Run 11	0,5	1,00E-06	0,2
Run 12	0,5	1,00E-05	0,5
Run 13	2,5	1,00E-05	0,2

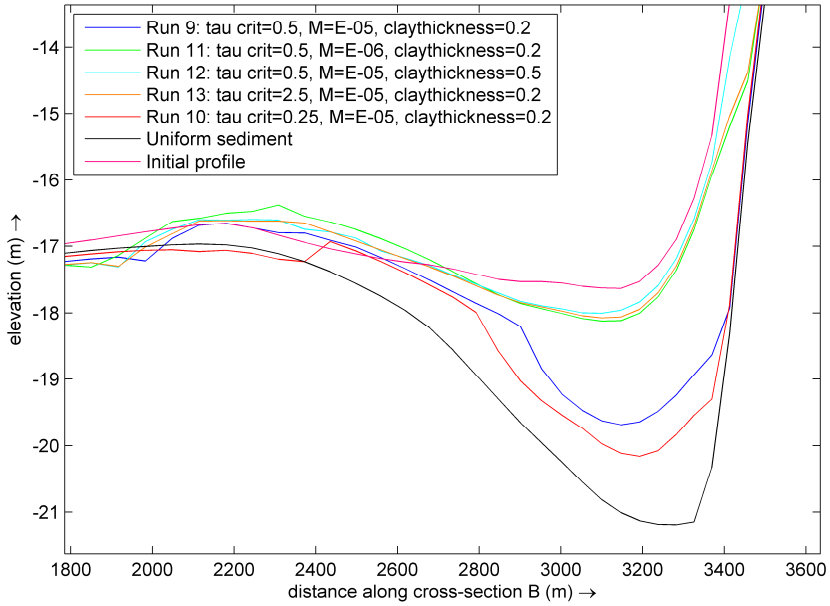

Figure 7.9 Bed levels cross section B for different clay parameters for schematization 3 after 5 years

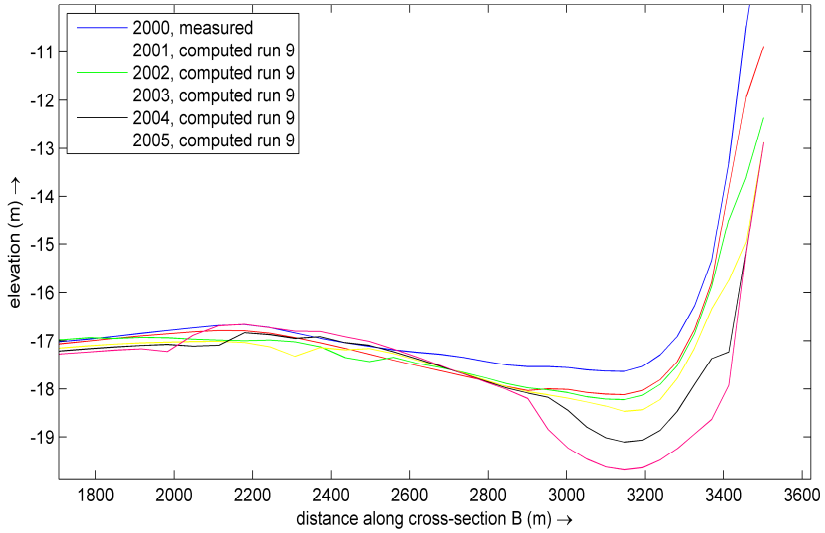

Figure 7.10 Development bed levels cross section B for run 9

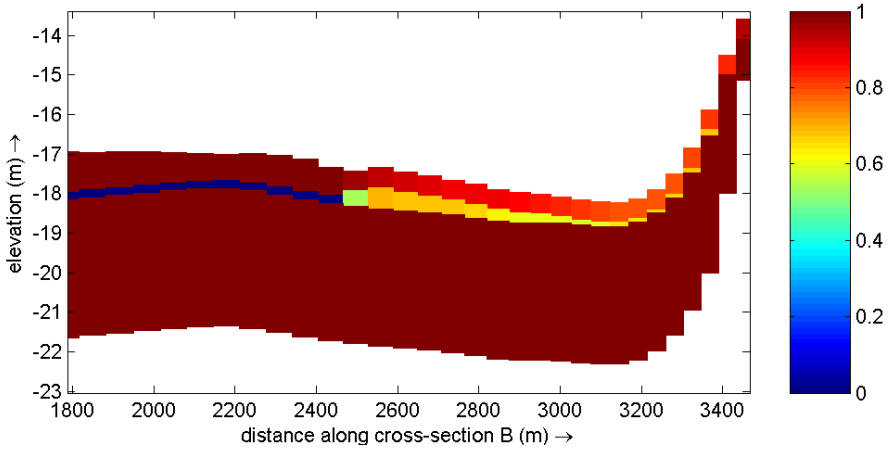

Figure 7.11 Fraction cohesive material along cross section B 2002 for run 9

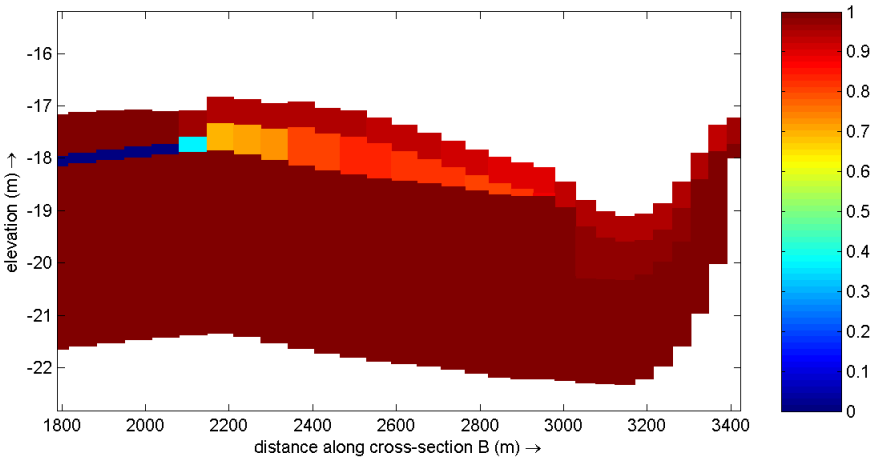

Figure 7.12 Fraction cohesive material along cross section B 2004 for run 9

In figure 7.9 the resulting bed levels for cross section B after 5 years are shown for the five simulations. Again the discontinuity on the transition between purely non-cohesive and cohesive sediment can be seen. But here it is less clearly as in the former paragraphs and is positioned more westward. In figure 7.12 this transition is more clearly for run 9. The discontinuity on the transition can be observed around 2150 meters along cross section B.

In figure 7.9 also the initial bed level is shown. Comparison with this initial bed level shows that there is a part with erosion and a part with accretion. Figure 7.13 shows the cumulative erosion for run 9 after 5 years of simulation. The transition between where cohesive sediment is exposed can be observed. Also the erosion and the accretion can be clearly seen. This shows that there is developing a scour hole but that the extent is substantially smaller: substantially smaller compared to the case with non-cohesive sediment but also with reality.

In run 10 and run 13 there is varied with the critical shear stress relatively to run 9. In run 11 a lower erosion parameter is applied relatively to run 9. In run 12 a thicker cohesive layer is applied relatively to run 9. In figure 7.9 can be seen that these variations all have the same effect: The variations affects the depth of the scour hole but has only minor influence on the extent of the scour hole.

Figure 7.10 shows the erosion rate for run 9. The first year relatively high erosion is observed. Then it takes two years to erode the clay layer which goes very slowly. In figure 7.11 the content of the non-cohesive fraction is shown for cross section B after two years. It is clear that there is relatively high clay content in the scour hole. When the cohesive layer is eroded away the erosion rate increases again. Figure 7.12 shows that there is hardly any clay content left after 4 years. In figure 7.10 can be seen that the erosion rate than already has increased. In this figure a transition between erosion and accretion can be observed around 2800 meters along cross section B. Left from this transition there is accretion during the years, right from this transition there is erosion.

In figure 7.14 the erosion rate is shown for run 12 along cross section B. After reaching the clay layer within one year the erosion in the scour hole seems to stop. The same happens for run 11 and run 13.

The extent of the simulated scour hole is not like reality. Nevertheless an erosion rate can be determined for the simulations. Because the erosion stops for the runs 11, 12 and 13 the erosion rates reduces zero.

The erosion rate for the runs 9 and 10 are respectively 0.4 and 0.5 meters a year. These erosion rates are averages over 5 years and therefore a mix of erosion for cohesive and non-cohesive sediment. The erosion rate for run 9 between 2001 and 2003, the period in which the clay layer erodes, is 0.05 meter/ year.

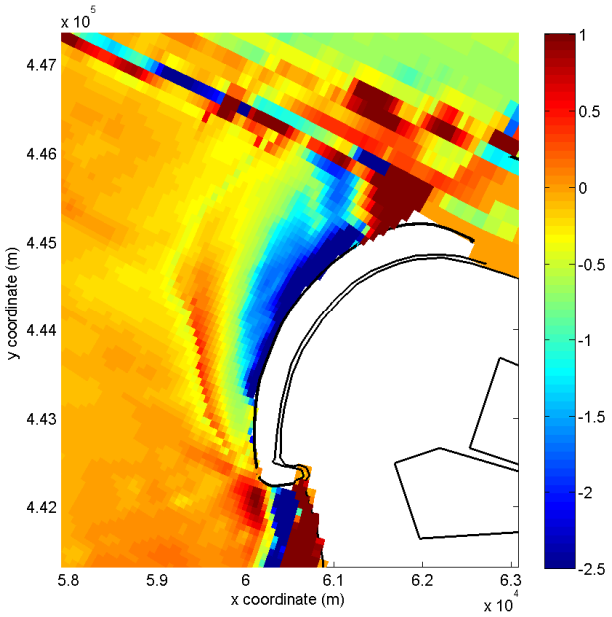

Figure 7.13 Cumulative erosion run 9 after 5 years

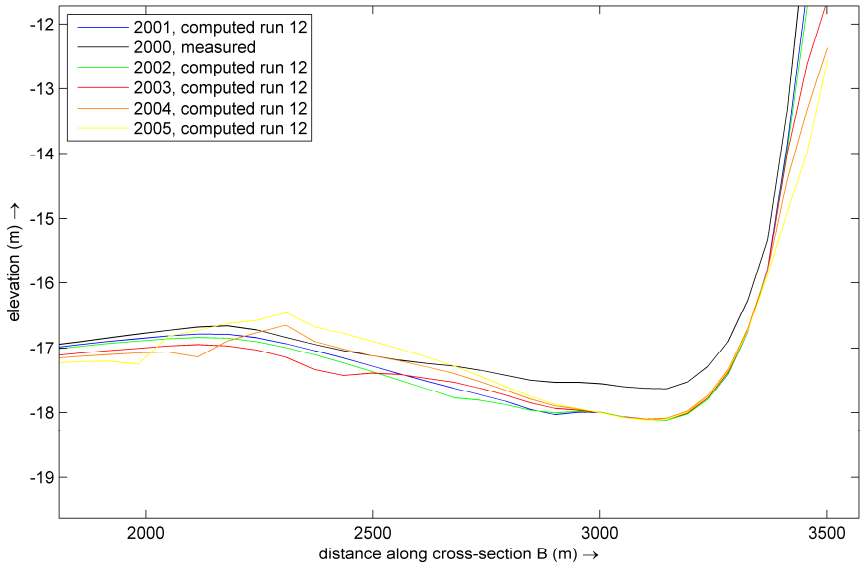

Figure 7.14 Development bed levels cross section B for run 12

In figure 7.15 and table 7.3 the cumulative dredged volume out of the Maas trench is depicted. In table 7.3 also the volume eroded out of the scour hole (as defined with the polygon in figure 4.8) is given. As can be seen in the figure is the accretion for run 9 less than for the case with uniform sediment but still overestimated when compared to the measurements. The difference between the accretion between the uniform sediment case and run 9 can be almost completely explained with the difference in eroded volume: There eroded 3.23 * 10^6 m^3 more sediment out of the scour hole and there accreted 4.30 * 10^6 m^3 more in the Maas trench.

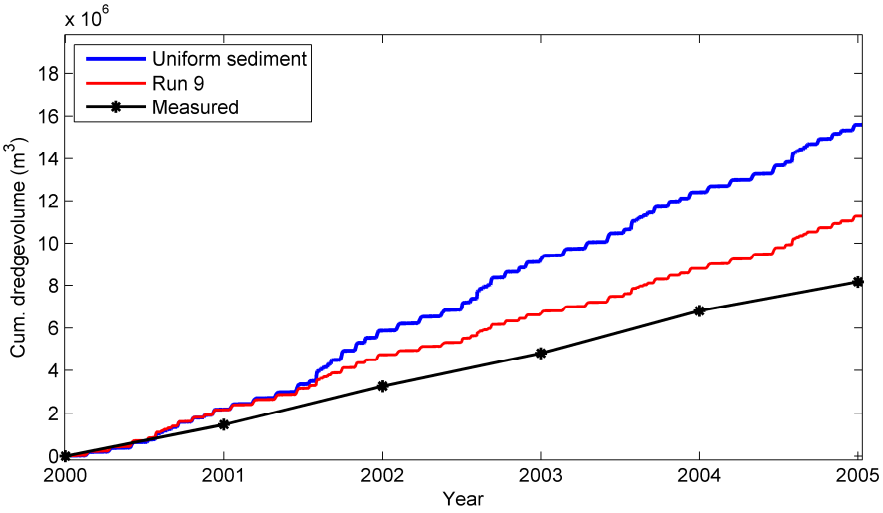

Figure 7.15 Cumulative dredge volume for run 9

Table 7.3 Eroded volume out of the scour hole and the cumulative dredge volume for run 9

	Eroded volume [m^3]	Accreted volume [m^3]
Run 9	5,19E+06	1,13E+07
Measured	3,17E+06	8,20E+06
Uniform sediment	8,42E+06	1,56E+07

7.6 Conclusions cohesive material

Because of the occurrence of cohesive material a lower erosion rate is expected compared with non-cohesive material. Therefore the occurrence of cohesive material can explain the overestimation of the scour hole in the model where exclusively non-cohesive material was applied.

In the formulation for erosion of cohesive material two parameters depend on the condition of the soil. These two parameters, the erosion rate M and the critical shear stress τ_e have a large range. These values mainly depend on the clay condition. Old overconsolidated clay is harder to erode than fresh deposited clay. The appropriate values for these two parameters have to be determined by calibration or field survey.

Different erosion rates were found during the development of the scour hole between 1986 and 2006. In the case without waves these different erosion rates can be simulated by tuning the above mentioned parameters.

In the case where waves are included in the simulation the erosion pattern appears to be different. On some places there is also accretion in the scour hole.

Several simulations have been done with a multiple layered model. The whole area is covered with non-cohesive material. Below this layer lies a cohesive layer. After a short simulation time this layer is exposed at the location of the scour hole. Locally exposed cohesive material displays a different erosion pattern.

Three schematizations have been simulated. It was not possible to simulate a highly stratified bed as expected in reality. It was difficult to obtain useful results with only one cohesive layer. This is an obvious simplification compared to the highly stratified system. Because of this simplification it is not possible to determine appropriate values for the parameters for cohesive sediment.

The layered system can be best simulated with schematization 3: here only a thin (0.2 meter) cohesive layer is defined. Furthermore the below treated discontinuity in the erosion pattern is smallest and the erosion pattern is most comparable with reality.

A discontinuity in the erosion pattern is present at the transition from purely non-cohesive material to cohesive material. Erosion occurs at the non-cohesive side of the transition and accretion occurs at the cohesive side.

The rate of erosion which is observed in the scour hole in reality is simulated well when cohesive material is implemented in the model. The large discontinuity on the transition though is not as observed in reality. Also the extent of the scour hole as simulated in the schematized model is not equal to reality. Especially the extent in west-east direction considerably differs with reality: In reality the scour hole extends about 1200 metres measured from the Zuiderdam in westward direction while for the simulations an extent is found of about 650 meters. The erosion in the model is also closer to the construction.

The initial bed levels in the simulations already showed a scour hole. This scour hole has the extent of 1200 metres. The extent of the scour hole in the simulations is smaller compared to this initial bed levels. Part of the bed level in the initial bed level already lies under the equilibrium level of the computations with cohesive sediment. Therefore there is accretion in this part.

The accretion in the trench of the Maas has better results than for uniform sediment: there is a smaller overestimation. But this improved result can almost completely be explained with the smaller eroded volume out of the scour hole.

To recap: The occurrence of cohesive clay in the area of interest can explain the found erosion in reality very well. However it is very difficult to simulate the highly stratified system and therefore it is difficult to find appropriate values for the erosion parameters. The erosion rate found in reality can be simulated well with cohesive sediment. The extent, especially in east-west direction is simulated considerably different compared to reality. The erosion is also located closer to the Zuiderdam. The extent and the position of the scour hole are not yet simulated satisfactory.

7.7 Non-cohesive fractions versus cohesive fractions

By implementing several non-cohesive fractions in the model the depth of the scour hole will be reduced as seen in chapter 6. The erosion rate in the model is still considerably higher than the erosion rate observed in reality. Furthermore this model does not explain the large differences in erosion rate observed between 1986 and 2006 in the scour hole.

The concept of cohesive material can explain the observed erosion in reality. By implementing cohesive material this observed erosion rate can also be simulated. The change in erosion rate as observed in reality is due to the highly stratified bottom. Each layer with its own erosion rate. However it is very difficult to simulate this highly stratified system and therefore it is difficult to find appropriate values of the erosion parameters. In contrast to the erosion rate is the extent of the scour hole not simulated satisfactory.

The following can be concluded:

The effect of cohesive material is dominant over the effect of armouring. Furthermore the cohesive sediment can be used to simulate the erosion as observed in reality. Implementation of several non-cohesive fractions still gives an overestimation of the scour hole and can therefore never be the sole reason of the overestimation of the model where uniform non-cohesive sediment is applied.

The cohesive sediment is dominant. Therefore a number of simulations will be done for the Maasvlakte 2 case.

The cohesive sediment is dominant but the armouring by non-cohesive sediment also influences the development of the scour hole. Also for the Maasvlakte 2 case the occurrence of cohesive material is indistinct. Therefore a simulation with graded sediment will be done for the Maasvlakte 2 case.

Chapter 8 MV2: Hydrodynamic processes

In this chapter the hydrodynamic processes around the Maasvlakte 2 will be investigated. First the flow will be investigated (8.1) and second the influence of the waves will be investigated (8.2). The results will be compared to the Maasvlakte 1 case.

8.1 Flow around the Maasvlakte 2

In figure 8.1 the flow pattern around the Maasvlakte 2 is shown for respectively the flood and the ebb situation. As in the Maasvlakte 1 case the tide driven current contracts around the bulge in the sea. The bulge is larger for the Maasvlakte 2 case and therefore also the contraction is larger. The resulting maximum depth averaged flow velocities are 1.1 m/s and 1.3 m/s for respectively ebb and flood flow. The maximum depth averaged velocities where 0.85 and 1.1 m/s for the Maasvlakte 1 case. This is an obvious increase.

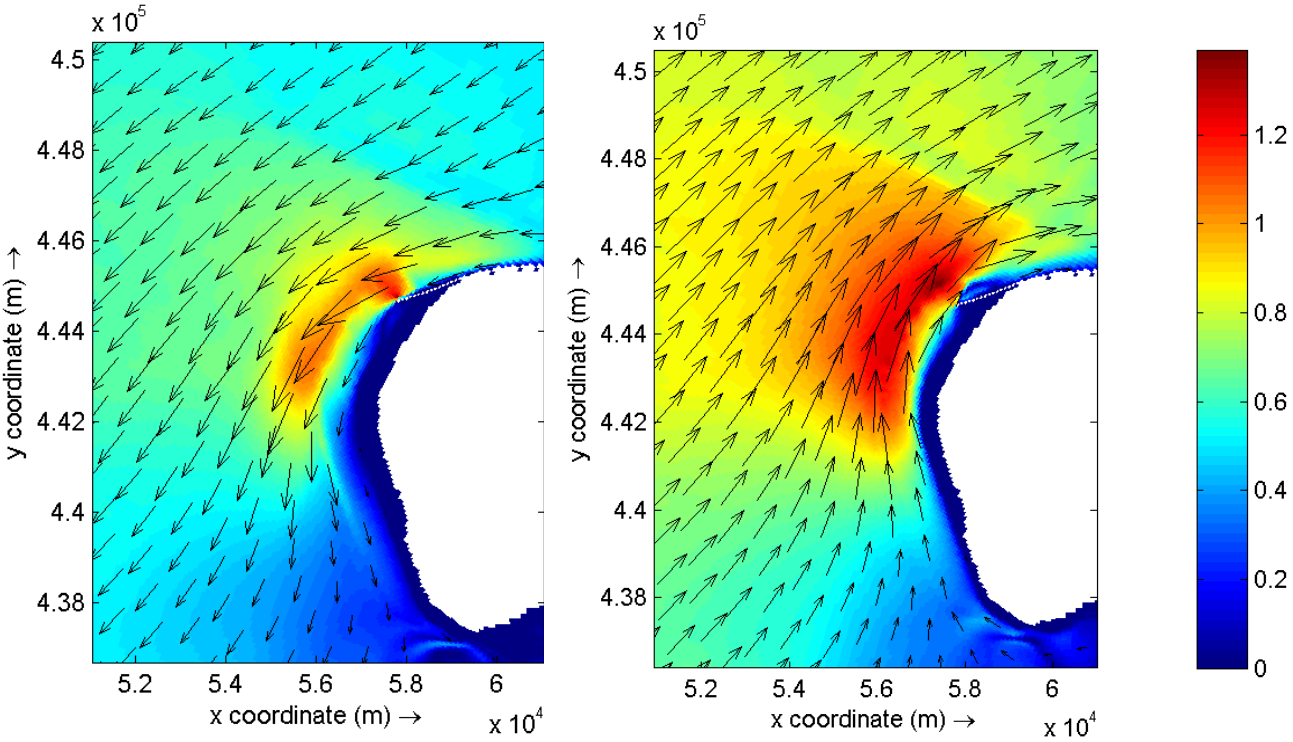

Figure 8.1 Flow pattern around Maasvlakte 2: ebb (left) and flood (right)

8.2 Waves

In chapter 5 the effect of the waves is investigated by means of an investigation of the bed shear stresses. In this chapter that will be done for the Maasvlakte 2 situation.

For the waves a wave driven current is observed in the surf zone. There is no influence on the current at the place of the expected scour hole.

In figure 8.3 the maximum bed shear stress τ_{cw} for combined waves and current are shown for cross section B and D. The location of cross section B and D are shown in figure 8.2. Figure 8.4 shows the according bed levels for cross section B and D. The shown bed shear stresses are the stresses during maximum flood current. As can be seen in this figure the shear stresses are lowest at the seaside and increase in the direction of the coast. In the area of the soft defence of the Maasvlakte 2 the bed level increases fast and therefore a high increase of the maximum bed shear stress is observed. Because of the lower flow velocity there is a lower bed shear stress observed in the surf zone for the simulation without waves (W00). Clearly an increase is observed of the maximum bed shear stresses when waves are added. Compared to the Maasvlakte 1 case the bed shear stress without waves shows a slightly increase. The maximum bed shear stress shows a high increase because of the higher waves. The waves are higher further offshore and because of the larger current velocities the wave enhancing effect of opposing current is larger. This is well shown in figure 8.5. In this figure the flow velocity, the wave height and the maximum bed shear stress are shown. The alternating flow results in a varying wave height and therefore a varying bed shear stress (the imposed wave height at the boundaries is constant).

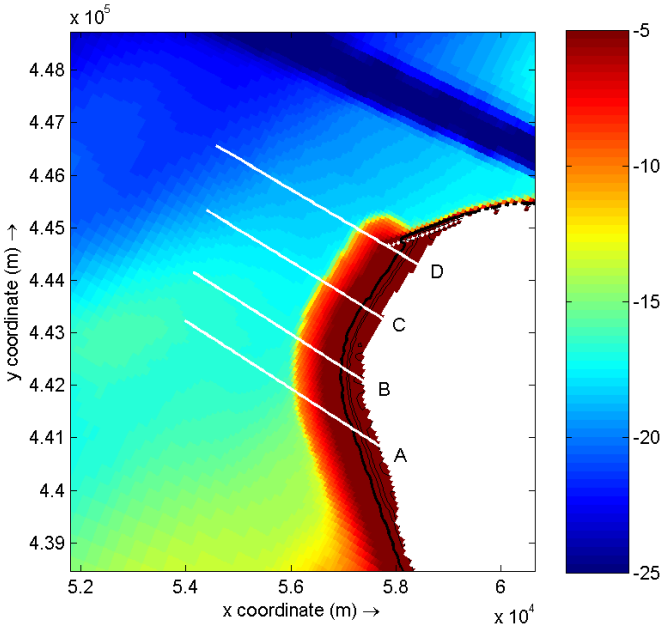

Figure 8.2 Initial bed level 2000 and location cross sections

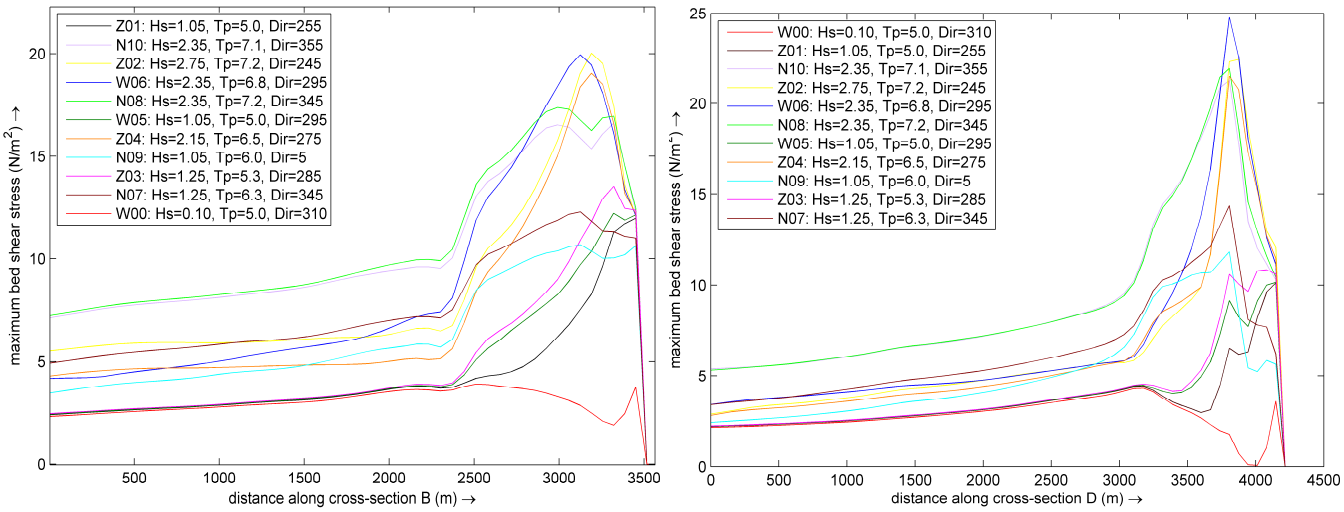

Figure 8.3 Maximum bed shear stress for cross section B and D

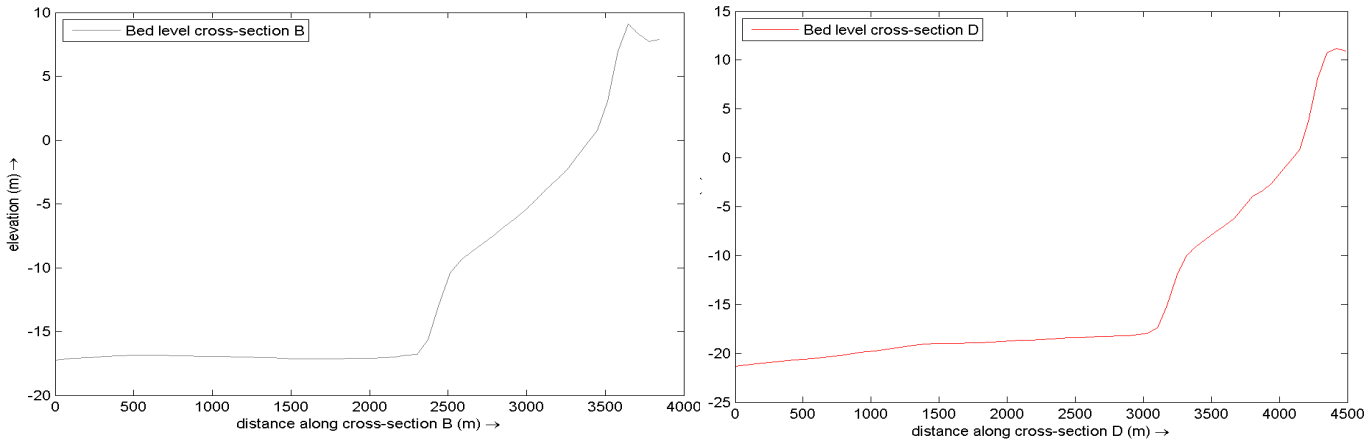

Figure 8.4 Cross section B and D

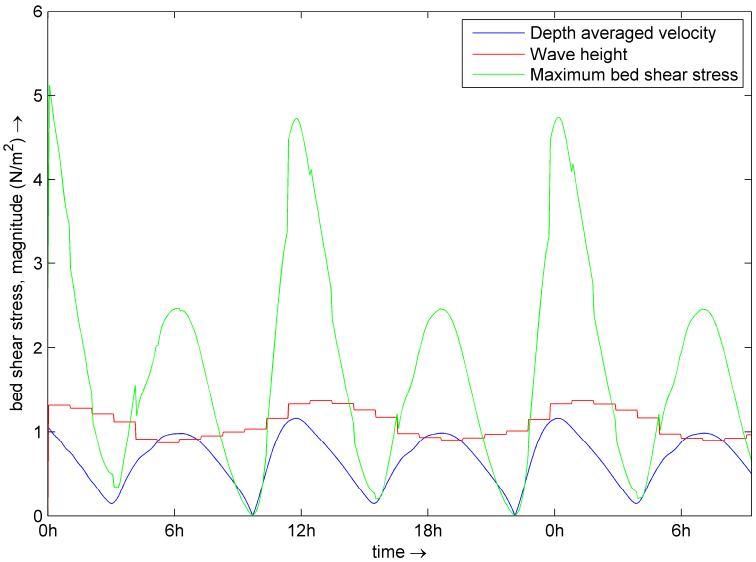

Figure 8.5 Centre cross section B: Wave height, depth averaged velocity and max. bed shear stress: Wave N09: Hs=1.05 m., Tp=6.0 s., Dir=5 ^{0}N

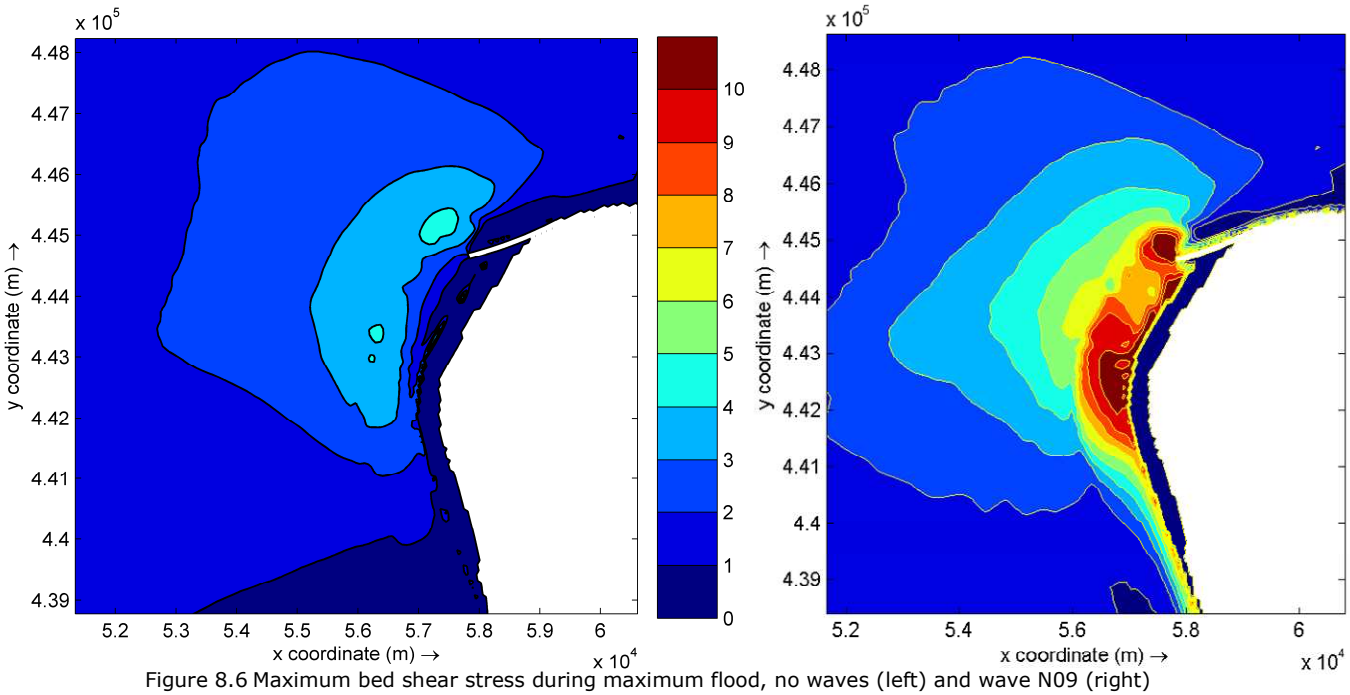

Figure 8.6 Maximum bed shear stress during maximum flood, no waves (left) and wave N09 (right)

In figure 8.6 the distribution of the maximum bed shear stress is shown for the case without waves (left) and with waves (right, wave N09: Hs=1.05m, Tp=6.0s, Dir=5^0N). In both figures the enhanced maximum bed shear stress in front of the Maasvlakte 2 can be seen. The figure shows that the maximum bed shear stresses are enhanced in the case were waves are included. At the soft defence of the Maasvlakte 2 the shear stresses increase because of the smaller water depth.

Chapter 9 MV2: Armouring non-cohesive fractions

In chapter 6 the Maasvlakte 1 is simulated with graded sediment. Comparison with simulations with uniform sediment showed an obvious decrease of the erosion. This decrease was due to two reasons: Armouring by coarse material and also the smallest particle results in a smaller scour hole.

The armouring in and around the scour hole was clearly observed in the model: an increase was found of the amount of the larger particles and a decrease of the amount of smaller particles.

The reduction of the erosion was 25% for the best fit of the sieve curves. Comparison with the other graded runs showed 8-39% reduction of this erosion reduction which is an indicator of the bandwidth.

In this chapter will be investigated if the two mechanisms which results in a smaller scour hole will occur in the Maasvlakte 2 situation. Also the erosion reduction can be compared with the Maasvlakte 1 case. The simulations do not aim to give an accurate prediction of the scour hole.

In paragraph 9.1 the simulations for this chapter are mentioned. In paragraph 9.2 the results of the simulations are shown and analysed. Paragraph 9.3 investigates the occurrence of the armouring effect. This chapter shall be ended with conclusions (9.4).

9.1 Simulations

In this chapter two simulations have been done. The first simulation is done with uniform sediment as in chapter 5 for the Maasvlakte 1 case. Uniform sediment with a D50 of 200 µm and a single layer is applied. In the original study [Roelvink and Aarninkhof, 2005] a uniform D50 of 285 µm was applied for the soft defence of the Maasvlakte 2 and a uniform D50 of 160 µm for the remaining model area. The D50 at the location of the expected scour is larger in this study than in the former studies. Therefore a smaller scour hole is expected. On the other hand in [Roelvink and Aarninkhof, 2005] a nourishment mode has been used. A nourishment mode (which will keep the initial profile for the soft defence by nourishing after each computation step) will result in a smaller scour hole.

The second simulation will be done with graded sediment and a multiple layered model as in chapter 6 for the Maasvlakte 1 case. The data analysis in chapter 3 showed that there was hardly spatial difference in the analysed sieve curves. Therefore the same representative sieve curve as used for the Maasvlakte 1 situation can be used for the Maasvlakte 2. In chapter 6 a schematization of the representative sieve curve has been made which can be used in the model. The same schematization (figure 6.5) is used for the simulation in this chapter: 5 layers with the same composition: This composition of each layer consists of 5 fractions, each fraction with its own D50. The D50's where: 0.100mm, 0.140mm, 0.230mm, 0.350mm and 0.500mm and the initial amount of each fraction in each layer was respectively 20%, 30%, 30%, 10% and 10%.

9.2 Results

9.2.1 Mutual comparison

In figure 9.1 the cumulative erosion for the two simulations is shown. For both simulations a large scour hole is shown. An area at the north side of the scour hole shows an area with accretion.

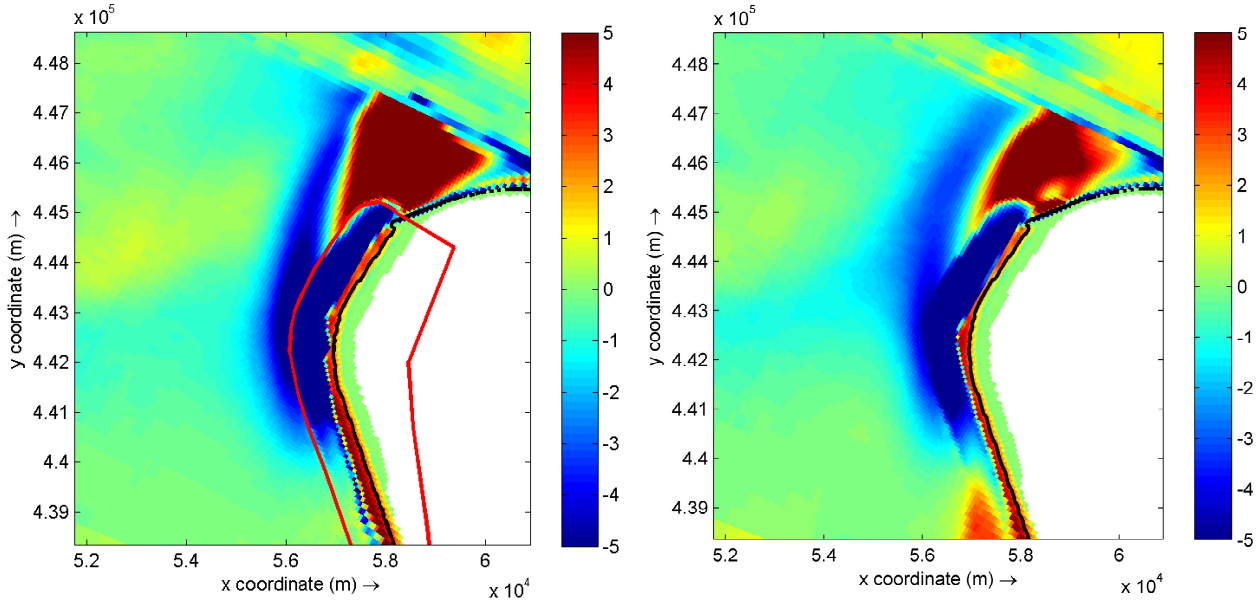

Figure 9.1 Cumulative erosion for uniform sediment (left) and graded sediment (right)

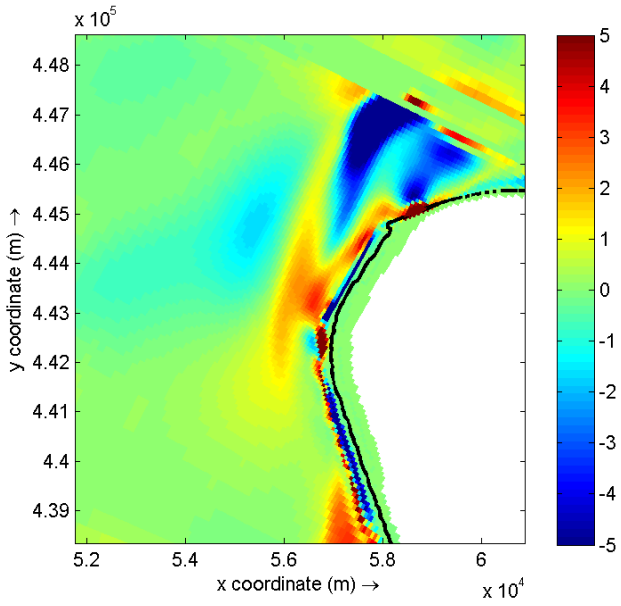

Figure 9.2 Cumulative erosion uniform sediment subtracted from graded sediment

Figure 9.2 shows a comparison of the erosion for the two simulations: The cumulative erosion for the uniform sediment simulation is subtracted from the graded sediment simulation. These figures (figure 9.1 and 9.2) show the difference in erosion very well:

- Deeper erosion for the centre of the scour hole for the uniform sediment simulation.
- A slightly larger extent of the scour hole for the graded sediment simulation.
- More accretion northerly from the scour hole for the uniform sediment simulation.

The polygon in figure 9.1 (left) shows the area which is part of the soft defence of the Maasvlakte 2. In reality this area shall be nourished regularly. In former models [Roelvink and Aarninkhof, 2005] the area in this polygon is kept in the initial profile. In this model there is rather large erosion in this area. This shows that the lack of a nourishment mode is a considerably shortcoming of this model.

Figure 9.3 till 9.6 shows the bed levels for cross section A-D as defined in figure 8.2. For each cross section the deepest point is found for the simulations with uniform sediment. As can be seen a larger extent is found for the graded sediment. Around the water level accretion occurs for both simulations.

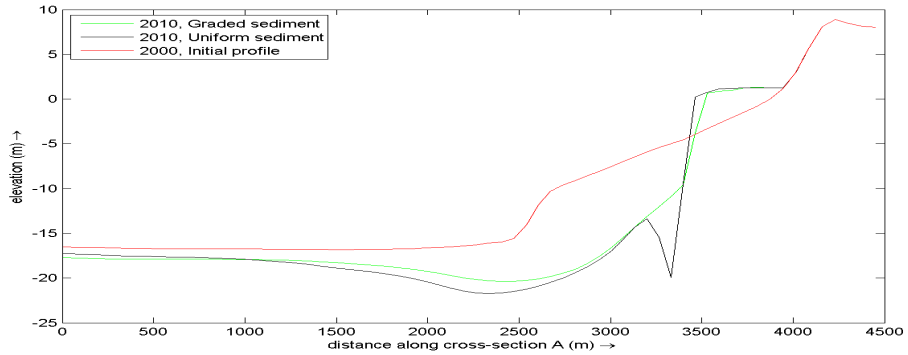

Figure 9.3 Bed levels along cross section A

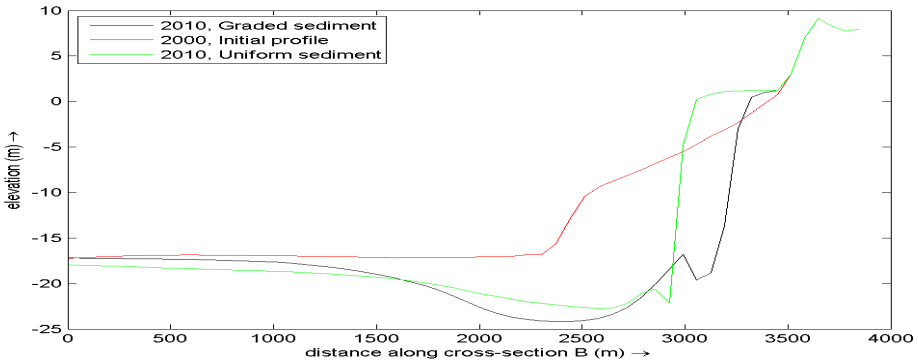

Figure 9.4 Bed levels along cross section B

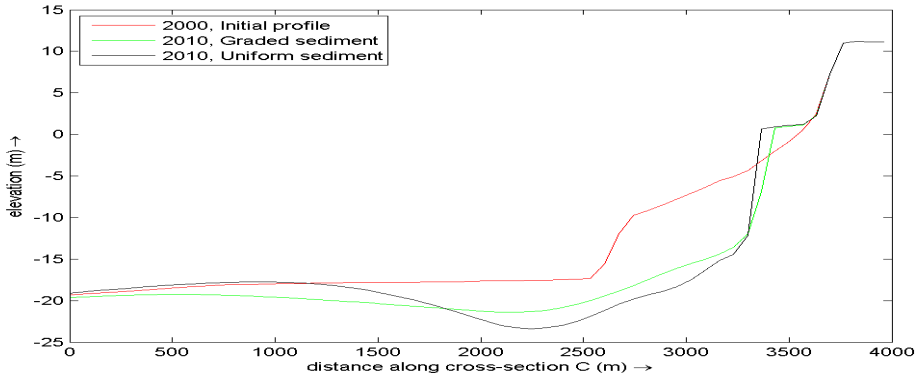

Figure 9.5 Bed levels along cross section C

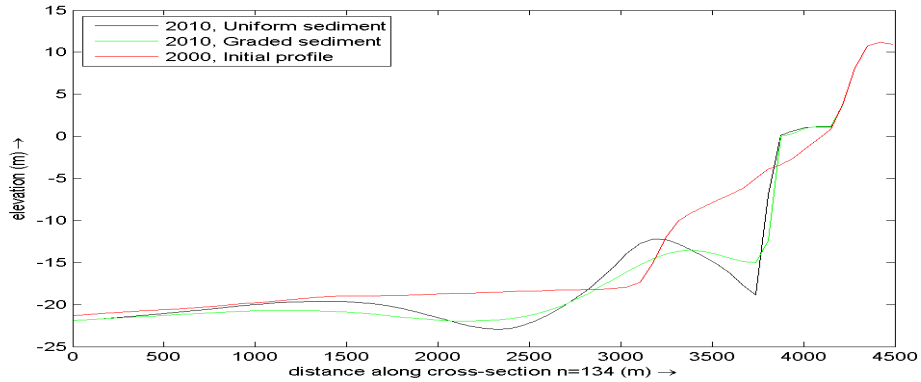

Figure 9.6 Bed levels along cross section D

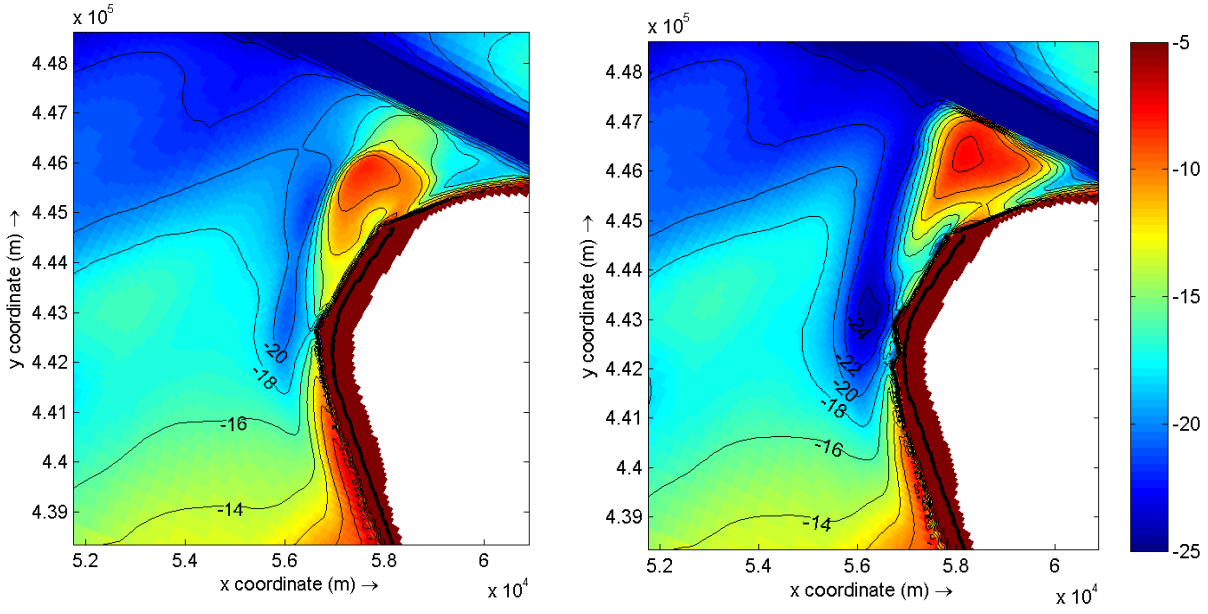

Figure 9.7 Bed level uniform sediment: 5 years (left) and 10 years (right)

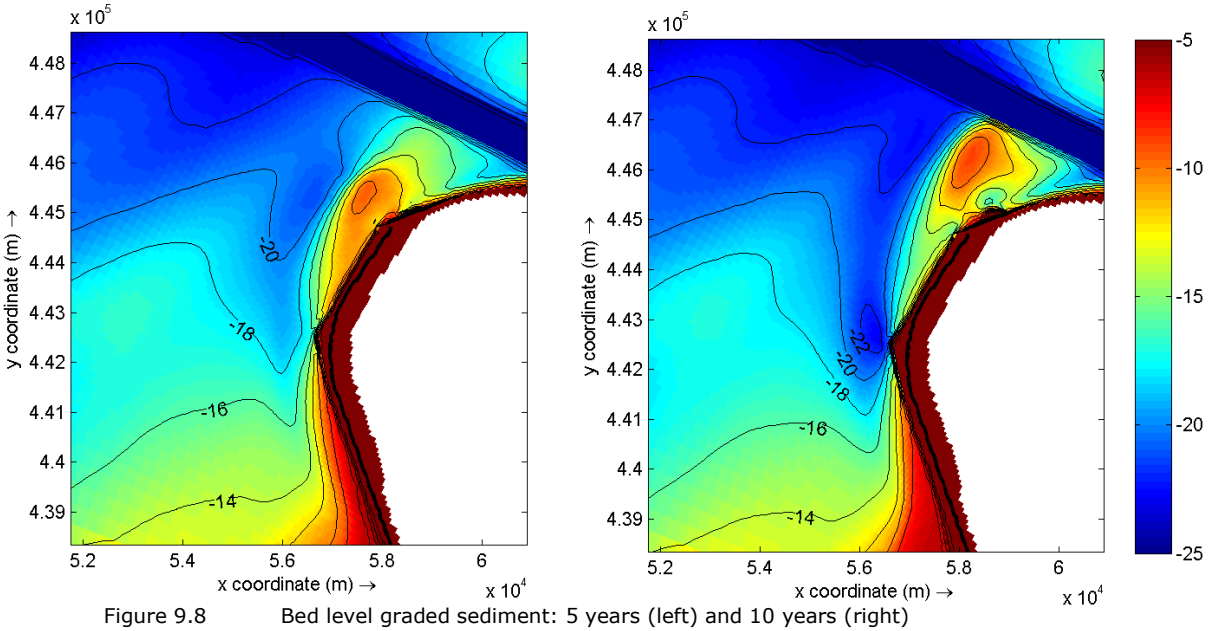

Figure 9.8 Bed level graded sediment: 5 years (left) and 10 years (right)

Figure 9.7 and 9.8 show the bed levels for both simulations after 5 and 10 year. The uniform simulation reaches a depth of 25 meter while the graded simulation reaches 22.5 meters after 10 years. The extent of the 20 meter polygon is quite similar after 10 years for both simulations.

9.2.2 Comparison with MV1

The Maasvlakte 1 case showed a more straight forward scour hole. Like in reality a kidney shaped scour hole developed. In the Maasvlakte 2 case shows besides considerably erosion also considerably deposition. An important difference between Maasvlakte 1 and 2 must be noted: The Maasvlakte 1 is constructed in the seventies. The hindcast simulations in this study cover the period 1986-

2006. The simulations start with the bathymetry of 1986 which already displays a scour hole (figure 3.14). So the simulations start in the middle of the development of a scour hole while the simulations in this chapter start at the beginning of the development.

In the Maasvlakte 1 case the extent of the scour hole was comparable when the cases with graded sediment were compared to the case with uniform sediment. The extent in the simulations in this chapter are slightly less comparable. The Maasvlakte 1 case showed a slower development of the maximum depth for the graded sediment simulations. The found reduction was 25 % and varies between 8 and 39% for the other simulations with graded sediment.

The reduction in erosion rate in this chapter is found of nearly 30 % for the deepest point. This is in agreement with the Maasvlakte 1 case.

9.3 Armouring

In figure 9.9 till figure 9.11 the distribution of the different fractions in the transport layer along cross sections A and C (as defined in figure 8.2) after 10 years is shown. The dotted orange lines indicate the initial sediment distribution for each fraction. This initial distribution is: Fraction 1: 20%, fraction 2: 30%, fraction 3: 30%, fraction 4: 10%, fraction 5: 10%.

The finer sediments are eroded and give a lower content in the cross section. The coarser sediments give a higher content. The proportion fine/ coarse sediments becomes lower and therefore the D50 in the transport layer increases as can be seen in figure 9.12 for the same cross sections. The D50 distribution of the whole area of interest is shown in figure 9.13. In the whole area an increase of the D50 occurs. Especially on the locations with the deepest erosion the increase occurs. Also in the accretion area northerly of the scour hole an increase of the D50 has been found.

Investigation of the fraction distributions in figure 9.9 till figure 9.11 shows strong reductions for fraction 1,2 and 3 and enhancement for the fractions 4 and 5. The highest content reduction is found for fraction 2 which is up to 70%. Fraction 1 has a smaller reduction, up to 50%. Again the extent of the reduction for fraction 1 is larger.

The simulated fraction distribution is comparable to the Maasvlakte 1 situation although the influence of the smallest fraction is smaller. A large increase of fraction 1 near the coastline which was found in the Maasvlakte 1 case has not been found in this chapter.

The D50 in the Maasvlakte 1 case has a peak value of 0.23 mm while in the present situation a peak value is reached of more than 0.25 mm after 5 years. It must be noted that the armouring effect depends on the amount of eroded material. In chapter 6 there was 3.7 meter erosion for the deepest point (figure 7.15) after 5 years. In this chapter there was 5.5 meter erosion for the deepest point. From this point of view a larger D50 was already expected for the Maasvlakte 2 situation.

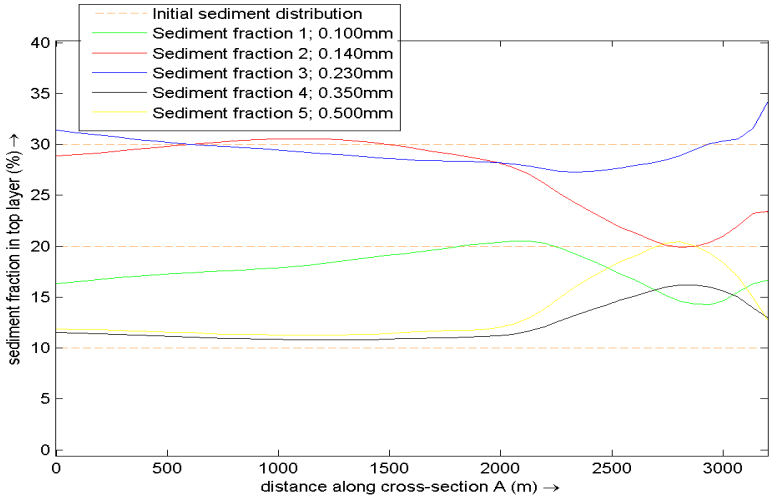

Figure 9.9 Sediment fraction distribution along cross section A (left) after 10 years

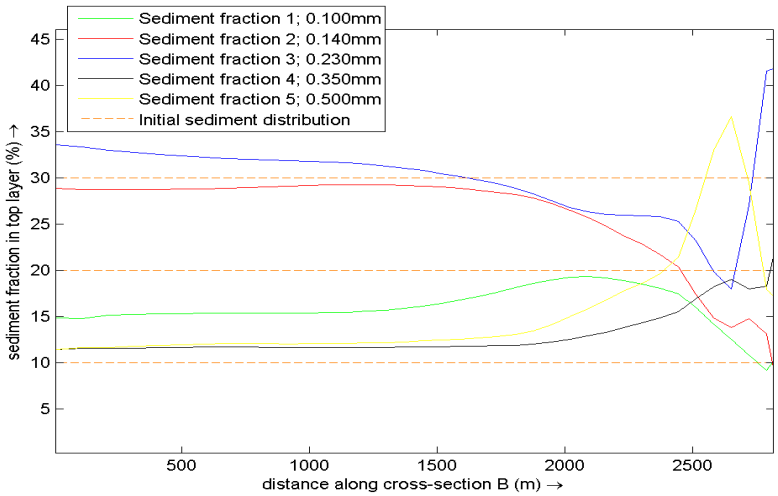

Figure 9.10 Sediment fraction distribution along cross section B after 10 years

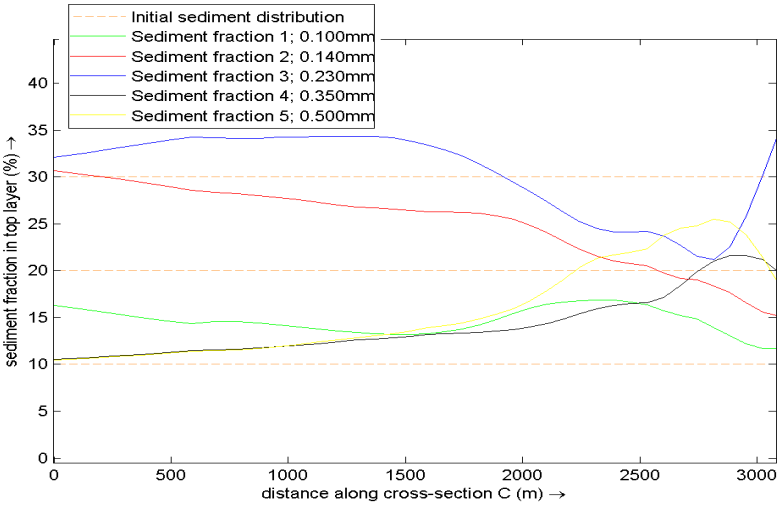

Figure 9.11 Sediment fraction distribution along cross section C after 10 years

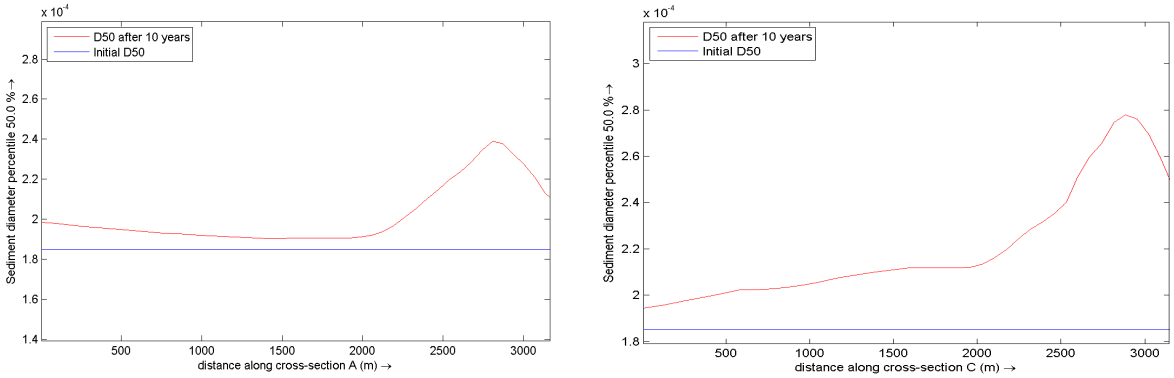

Figure 9.12 D50 distribution along cross section A (left) and C (right)

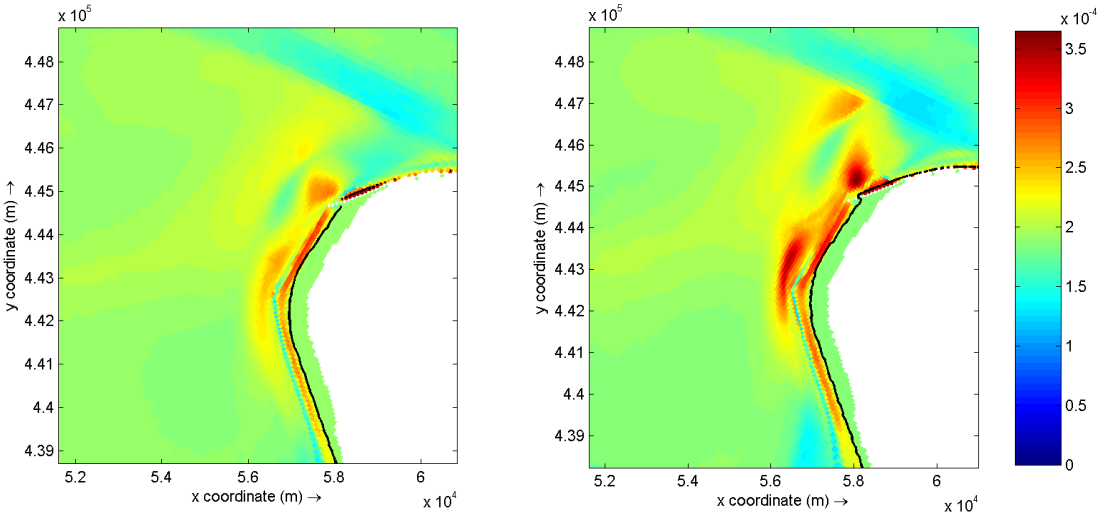

Figure 9.13 D50 distribution around scour hole after 5 years (left) and 10 years (right)

9.4 Conclusions

The aim of this chapter was to investigate whether the two mechanisms which resulted in less scour around the Maasvlakte 1 also count for the Maasvlakte 2 case. Also is investigated if the reduction is similar.

It can be concluded that both mechanisms count for the Maasvlakte 2 situation.

The finest sediment has a lower content reduction in the transport layer than the second finest sediment. This is similar to the Maasvlakte 1 situation and indicates lower erosion because of the finest sediment.

The coarsening of the transport layer because fine material erodes faster than the coarse material (armouring) is also shown in the Maasvlakte 2 situation. Because there is more erosion in the Maasvlakte 2 situation the armouring effect develops faster. Therefore also a higher D50 is found in this situation.

For the Maasvlakte 1 situation comparison was made between the simulation with uniform and the simulation with graded sediment. The conclusions were that the extent of the pattern was similar and for the erosion a reduction of 25% was found. This reduction varies between 8 and 39% for the other simulations with graded sediment.

In this chapter the extent of the scour hole shows a larger extent for the graded sediment simulation: This is a small disagreement with the Maasvlakte 1 situation. The reduction in erosion rate in this chapter is found of nearly 30 % for the deepest point. This is in agreement with the Maasvlakte 1 case.

Chapter 10 MV2: Cohesive sediment

In chapter 7 the Maasvlakte 1 case with cohesive sediment is treated. It was concluded that erosion rates found in reality can be simulated when cohesive material is implemented in the model. The extent and the position though differ from reality when cohesive material is implemented in the model. Although the validation results were not satisfactory in the Maasvlakte 1 case the Maasvlakte 2 case will also be simulated with cohesive sediment. The simulations do not intent to give an accurate prediction of the scour hole but to give an indication what the occurrence of cohesive sediment can do with the scour around the Maasvlakte 2.

The limitations of the simulations in this chapter are mentioned in paragraph 10.1. In paragraph 10.2 the results are shown of a simulation where one layer with purely cohesive material is implemented. In paragraph 10.3 and 10.4 the simulations and the results of the simulations are shown and analysed. The conclusions (10.5) summarize the main findings of this chapter.

10.1 Limitations

In chapter 3 the soil composition of the bed around the Maasvlakte 2 has been investigated: From four soil samples close to the expected scour hole in front of the Maasvlakte 2 it can be expected that a cohesive layer starts between 19 and 22 meters below NAP. The possible thickness of this cohesive layer has a high range (1.24 to 3.61 meter) but it is also possible that there is no cohesive layer in the most seaward area of the expected scour hole. The cohesive layer as mentioned here is a schematization for a highly stratified system and does not represent one single layer.

The formula of Partheniades [Winterwerp and Van Kesteren, 2004] is implemented in the Delft3D model environment for erosion of cohesive sediment. For this formula the critical shear stress for erosion τ_e and the erosion parameter M are of importance. Both parameters have a large range and are usually determined by calibration. In Chapter 7 these parameters were already investigated. In literature values and formula are found (appendix D). The found parameters in this way still show a large range. With the range for the parameters every wanted erosion rate can be reached as shown in chapter 7. The Maasvlakte 1 case should serve as a calibration case for the mentioned parameters. Because of the expected highly stratified system it is not possible to determine appropriate values for the erosion parameters.

The hindcast of the Maasvlakte 1 (chapter 7) with cohesive sediment showed disagreements with the reality. The erosion rate was simulated correct but the pattern was of the scour was different and showed sedimentation on locations where erosion is observed in reality (and also in the simulation with non-cohesive material).

In summary: the results of the simulation of the Maasvlakte 2 with cohesive sediment are not accurate because of the following:

- A high range for the possible vertical position of cohesive layers
- A high range for the possible thickness of the cohesive layers
- A high range for the parameters used in the model (critical shear stress for erosion τ_e and the erosion parameter M)
- The hindcast did not show satisfactory results for the extent of the scour around Maasvlakte 1.

Therefore the simulations in this chapter do not intent to give accurate predictions of the scour hole but only show what the influence of cohesive material can be.

10.2 Simulation with clay only

Before the simulations with locally exposed cohesive material a simulation has been done with purely cohesive material. The cumulative erosion is shown in figure 10.1. Large erosion is observed at the soft defence as can be seen in the red polygon. This erosion is not of importance: This erosion will be nourished in reality (See chapter 9 for more discussion about this nourishment) and this erosion does not result in a scour hole since the eroded material is located above the surrounding bed level.

Comparison with case where uniform sediment is simulated (D50=200µm, figure 10.1, right) shows a wider erosion for the simulation with cohesive material. Note that the legends in figure 10.1 are not the same. This shows that the erosion is much smaller. The non-cohesive simulation shows a large accretion northerly of the scour. In the cohesive simulations this accretion is not observed.

The difference in erosion pattern is also observed in the Maasvlakte 1 case. In the Maasvlakte 1 case though there was erosion on unexpected locations. There is no erosion in this situation because the critical shear stress for erosion is set very low.

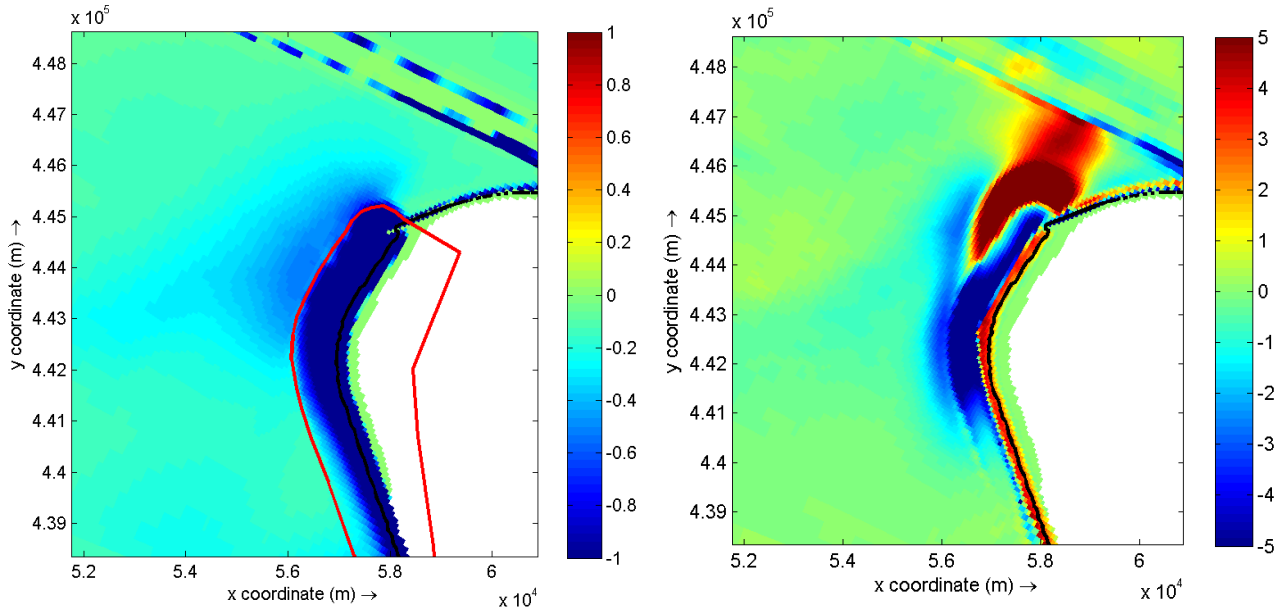

Figure 10.1 Cumulative erosion after 5 years for purely cohesive material: τ=1.0 Pa. and M=10^{-5} m/Pa/s (left) and non-cohesive uniform sediment (right). (note the difference in legend)

10.3 Simulations

In chapter 7 a number of simulations have been done. First several simulations have been done with a small non-cohesive cover. The underlying cohesive layer will be exposed in the scour hole after a short time due to erosion. The simulations with a thick cohesive layer (schematization 1 and 2) showed a large area with sedimentation and a large discontinuity on the transition between purely non-cohesive material and partly cohesive material.

The same happens for the Maasvlakte 2 situation. This can be clearly seen in figure 10.2 where the cumulative erosion is shown for a simulation where a thick cohesive layer is applied. Within the white circle a sedimentation area is observed. This area was clearly an erosion area in the non-cohesive simulations and also shows discontinuities at the boundaries (the yellow edge within the white circle). These discontinuities are on the transition between non-cohesive and partly cohesive material.

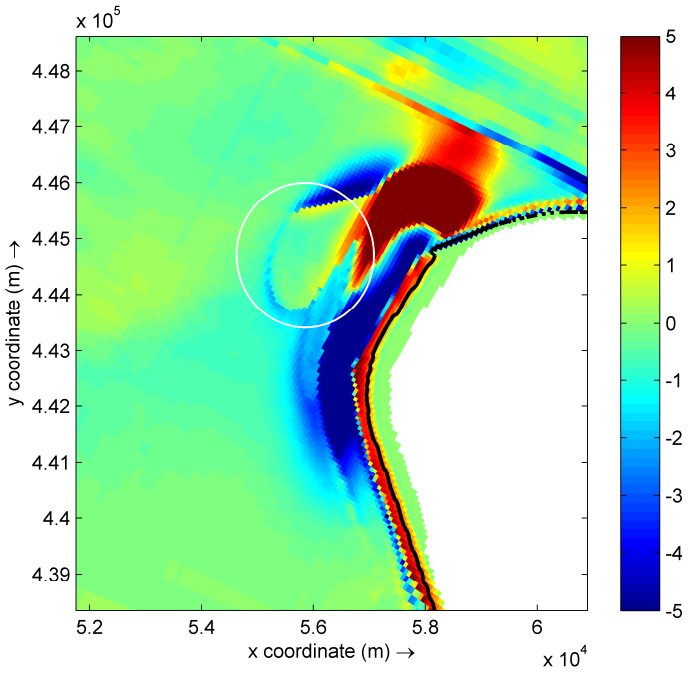

Figure 10.2 Cumulative erosion after 5 years: τ=0.5 Pa. and M=10^{-5} m/Pa/s

In chapter 7 better results were obtained with a thin cohesive layer: Practically no discontinuity at the transition and a better result for the pattern. Therefore also in this chapter only the effect of a very thin layer will be investigated. Several simulations will be done with varying critical shear stress for erosion τ, erosion parameter M and vertical position of the clay layer. The parameters for the simulations are shown in table 10.1.

Compared to the Maasvlakte 1 the cohesive layer is positioned at a lower vertical position. The vertical position in the Maasvlakte 1 case is unknown because it was already scoured away. In the present case, as seen in chapter 3, the cohesive layer starts between 19 and 22 meters below NAP. The bed level is around 17 meters below NAP. Therefore the simulations contain a non-cohesive cover of 2 meters. Therefore it takes a longer simulation period to reach the cohesive layer compared to the Maasvlakte 1 situation.

Table 10.1 Parameters in simulations

	Critical shear stess τ	Erosion parameter M	claythickness	non-cohesive cover
	[Pa]	[m/Pa/s]	[m]	[m]
Run 1	0,5	E-05	0,2	1
Run 2	0,25	E-05	0,2	2
Run 3	0,5	E-04	0,2	2
Run 4	0,5	E-06	0,2	2
Run 5	0,5	E-05	0,2	2

10.4 Results

In figure 10.4 to 10.7 the bed levels along cross section B and D as defined in figure 8.2 are shown for run 1-5. The reference simulation is run 5. In the other simulations only one parameter differs from this simulation.

In all the simulations can be seen that the effect is relatively small because the height of the non-cohesive cover is larger. In all runs first this non-cohesive layer has to erode. Nevertheless there is less erosion when a cohesive layer is applied. Very clearly the above mentioned discontinuities on the transition can be found in some of the simulations.

In cross section D the sedimentation which occurs northerly of the scour hole can be seen between 2500 and 3000 meters along cross section D.

Compared to the reference simulation the effects of the parameters can be investigated. In run 1 the non-cohesive cover is smaller and therefore the cohesive layer positioned higher. Because the erosion meets the cohesive layer earlier this result in less erosion. An increase of M (run 3 and run 4) results in a deeper scour hole. Run 4 (M=E-06 m/Pa/s) is the only run which shows an obvious larger extent of the scour which can be due to the lack of erodable sediment to meet the transport capacity. This lack of sediment is replenished in the area where sediment is available. Lowering of the critical shear stress for erosion (run 2) gives a slightly deeper scour hole.

The extent of the scour is similar for the different parameters (except run 4). The erosion rate is affected by variation of the parameters. This is consistent with the Maasvlakte 1 case. Figure 10.3 shows the cumulative erosion for run 3 and run 5: Clearly the similar erosion patterns and the difference of erosion depth can be seen (the area within the red polygon is not considered).

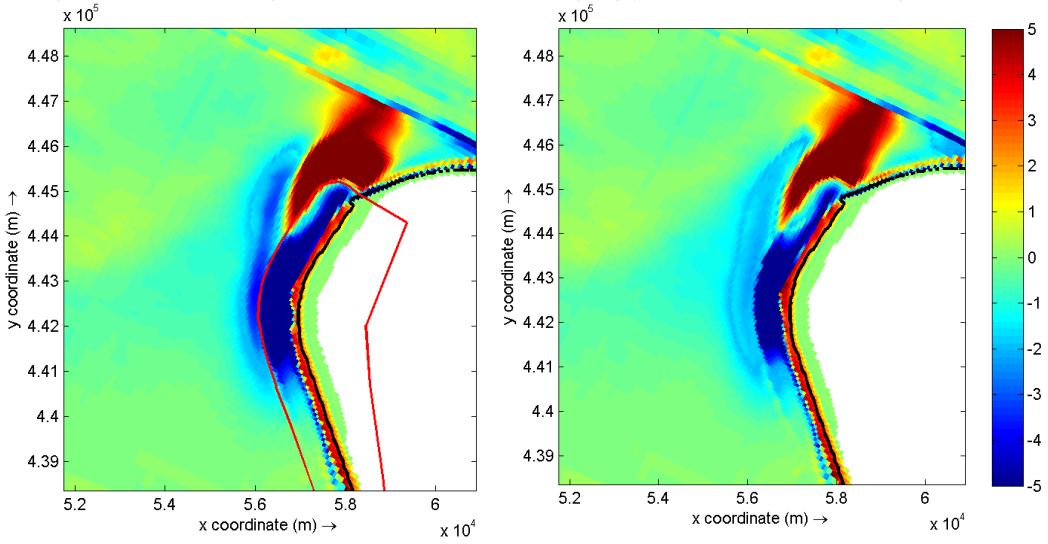

Figure 10.3 Cumulative erosion after 5 years for run 3 (left) and run 5 (right)

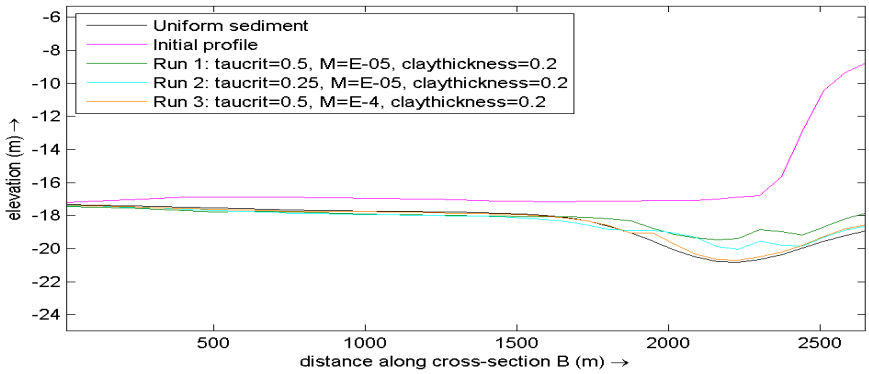

Figure 10.4 Bed levels cross section B for run 1-3 after 5 years

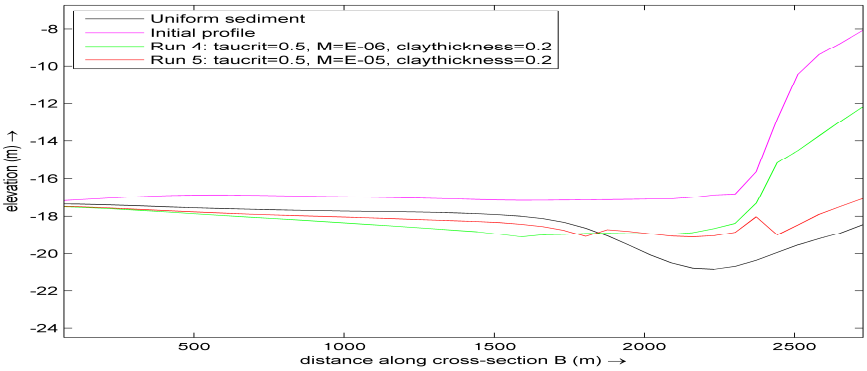

Figure 10.5 Bed levels cross section B for run 4-6 after 5 years

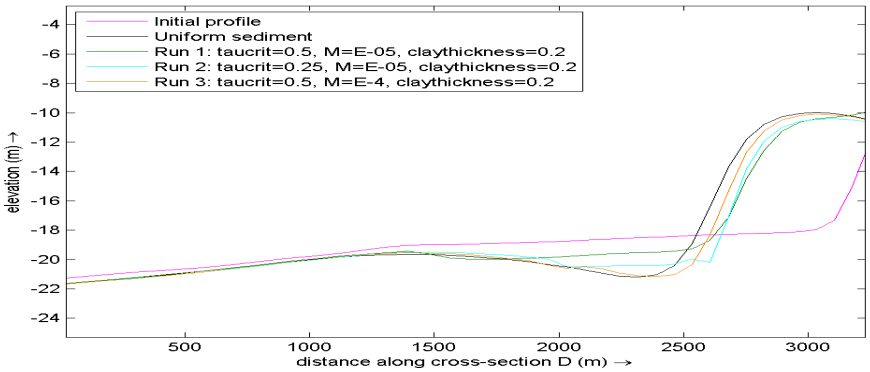

Figure 10.6 Bed levels cross section D for run 1-3 after 5 years

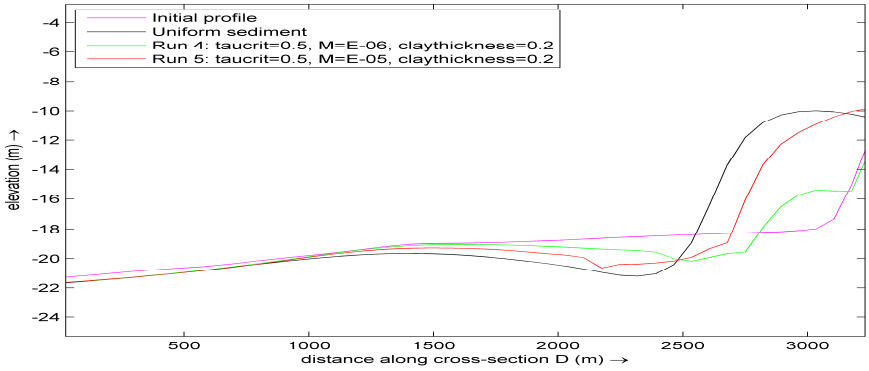

Figure 10.7 Bed levels cross section D for run 4-6 after 5 years

In figure 10.8 the development of the bed level of run 1 is shown. In figure 10.9 the amount of non-cohesive material is displayed after 5 years. As can be seen in the latter figure the cohesive layer is nearly completely eroded away at the right side of the figure. Erosion through the cohesive layer is very slow as can be seen in the difference between the computed bed level in 2002 and 2003 (figure 10.8).

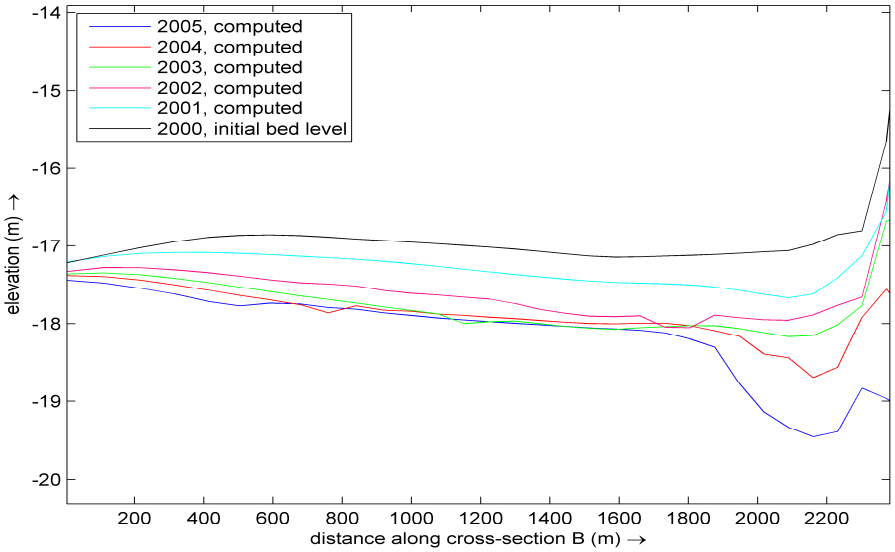

Figure 10.8 Development bed levels cross section B for run 1

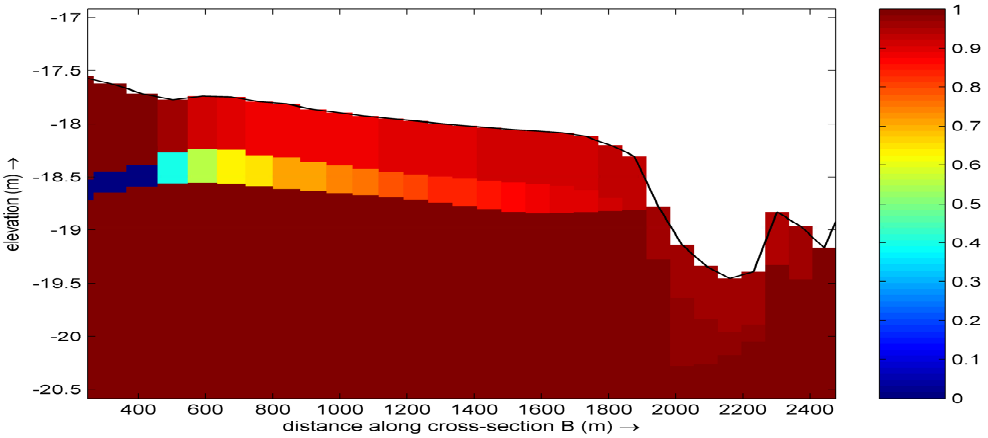

Figure 10.9 Fraction of non-cohesive material along cross section B for run 1 after 5 years

10.5 Conclusions

From paragraph 10.1 can be concluded that certain shortcomings in the simulations performed in this chapter lead to inaccurate results:

- A high range for the possible vertical position of cohesive layers
- A high range for the possible thickness of the cohesive layers
- A high range for the parameters used in the model (critical shear stress for erosion τ_e and the erosion parameter M)
- The hindcast did not show satisfactory results for the extent of the scour around Maasvlakte 1.

Therefore the simulations in this chapter do not intent to give accurate predictions of the scour hole but show only of what influence cohesive material can be.

Several simulations have been done with varying critical shear stress for erosion τ, erosion parameter M and vertical position of the clay layer. Because the lower vertical position of the cohesive layer it takes a longer time before the erosion reaches this layer. Variation of parameters had an effect on the erosion rate but hardly influence on the extent of the scour around the Maasvlakte 2. This is consistent with the findings for the Maasvlakte 1 situation.

The extent of the scour is comparable with the simulations where purely non-cohesive material was applied. This is not in accordance with the Maasvlakte 1 situation where the simulations with cohesive sediment showed a smaller extent of the scour hole. This can be due to the large non-cohesive cover which predominantly determines the extent of the scour. Longer simulations should show whether this is true or not.

The development of the scour hole in reality shall start with a relatively high erosion rate. This erosion rate is probably overestimated in the simulations and the results of the model should therefore be taken as the upper limit. As already concluded the vertical position and thickness of the cohesive layer is not certain and beside that the vertical position and thickness are not uniform in the area of interest. When the erosion reaches a cohesive layer the erosion rate will decrease. This new erosion rate depends on the erosion parameter M and the critical shear stress τ. There is not one cohesive layer but a stratified system what was schematized as one layer in the current study. The parameters differ for the different layers in the stratified system. When a layer within the stratified system is eroded, erosion of the next layer will commence. This can result in an increase or a decrease of the erosion rate on that point. The results of the simulations in chapter 7 and the present chapter show that every erosion rate can be accomplished with the range for the above mentioned parameters.

When the erosion reaches the cohesive layer this will also influence the extent and the pattern of the scour. As seen in chapter 7 this erosion extent is simulated inappropriate. The extent was far less compared to reality and the simulations with non-cohesive sediment. In the present chapter the extent was comparable for simulations with cohesive and non-cohesive sediment. Though if there was implemented a thicker cohesive layer an extra area with sedimentation appeared (figure 10.2). A relatively thicker cohesive layer is expected in reality. The model does not show appropriate results for a thicker layer. In reality a cohesive layer, independent of the thickness, will give a decrease of the erosion rate, but will not result in an extra sedimentation area (The model is there obviously wrong). In reality the cohesive layer will probably

result in a larger extent of the scour hole. The lower erosion will result in a lack of erodable sediment to meet the transport capacity. This lack of sediment is replenished in the area where sediment is available and will result in a larger erosion area unless the area where sediment is available the transport capacity already is fulfilled.

Chapter 11 Conclusions and recommendations

In this chapter conclusions will be drawn on the results of this master thesis project. The main findings are stated in relation to the study objectives. Furthermore the posed hypotheses will be evaluated and recommendations will be given.

In paragraph 11.1 the research objectives which will be evaluated are repeated. Paragraph 11.2 show the conclusions of the data analysis executed in this study. The study objectives are treated in paragraph 11.3 till 11.5. Recommendations for further study are posed in paragraph 11.6.

11.1 Problem definition and study objectives

The problem definition as posed in chapter 1 was threefold:

- The present hindcast of the scour hole in front of Maasvlakte 1 shows an unrealistic strong development of this scour hole compared with field observations. The difference may be explained by the occurrence of natural armouring processes by graded non-cohesive sediments and/or the resistance against erosion by layers with stiff cohesive sediments which were not included in the original hindcast computations.

- Sensitivity computations in Delft3D have shown that armouring effects by non-cohesive sediment reduce the extent and depth of the scour hole in front of the Maasvlakte 2. An accurate prediction is not given by these computations because the model is not calibrated and validated. Furthermore the effect of both wave-induced and flow-induced sediment transport and also a sand nourishment mode are not incorporated in this model. These aspects should be incorporated in the model to give accurate predictions.

- The extent and the depth of the scour hole in front of the Maasvlakte 2 is not yet predicted with a model where cohesive layers are incorporated.

The study objectives following from the problem definition was also threefold:

- Two new hindcasts of the scour hole in front of Maasvlakte 1: The first hindcast with a model where the effect of armouring by non-cohesive sediment is schematized by implementing several sand fractions and a number of bottom layers. The second hindcast with a model where also cohesive sediment is implemented. Both models calibrated and validated against 20 years of field observations. The hindcasts should result in

parameters for the Maasvlakte 2 model and should show which mechanism is dominant.
- Determining the development of the location and the extent of the scour hole in front of the Maasvlakte 2 using a model where the effects of armouring by non-cohesive sediment, wave- and flow-induced sediment transport and also a sand nourishment mode are incorporated. This model has to be calibrated and validated against known properties of the system following from the Maasvlakte 1 model. This is possible because of the great resemblance between the Maasvlakte 1 and 2.
- Determining the development of the location and the extent of the scour hole in front of the Maasvlakte 2 using a model where cohesive sediment layers are implemented. This model has also to be calibrated and validated against known properties of the system following from the Maasvlakte 1 model.

Two new hindcasts and two new forecasts have been made. In one hind and forecast a number of non-cohesive fractions and several layers are implemented to simulate the armouring effect. In the other hind and forecast a cohesive layer is implemented.

The two concepts results in a less deep erosion hole when simulated with Delft3D compared to simulations with uniform (non-graded) non-cohesive material. The effect of cohesive material is dominant over the effect of armouring by non-cohesive fractions. The implementation of cohesive layers can simulate every erosion rate observed in reality.

Implementation of a number of non-cohesive fractions gives a smaller erosion hole for two reasons: Armouring by coarser material but also relatively fine material gives a less deep scour hole. The simulations show a smaller scour hole when compared to the simulations where uniform (non-graded) sediment is applied. The erosion however is still overestimated when compared to reality: The effect of armouring as simulated in this study can never simulate the erosion rates as found in reality.

The simulation results were validated against several criteria. Especially the extent of the scour hole in case of cohesive sediment showed inaccurate results. Both models lacked a nourishment mode. Nourishments have a major influence on the scour hole. Because the hindcasts were not yet satisfactory and because the lack of a nourishment mode the predictions for the Maasvlakte 2 did not tend to give accurate predictions. The for the Maasvlakte 1 investigated bed composition did show similar effects for the Maasvlakte 2 situation.

The development of the scour hole strongly depends on the bed composition while this composition is vaguely known because of inhomogeneity of the bed. Therefore the predictions of the Maasvlakte 2 are expected to be less accurate.

The study objectives will be further elaborated in the paragraphs 11.3 till 11.5.

11.2 Data analysis

Bathymetric data

From the analysis of the bathymetric data the following is concluded:

- In contrast to what was suggested in former studies the scour hole did not reach equilibrium yet. The scour hole still develops.

- The erosion rate in the scour hole fluctuates. Three periods can be distinguished

  1986-1989: high erosion in the whole area which is comparable with the computations done with non-cohesive material (chapter 4)

  1989-2000: Low erosion with more spatial variance

  2000-2006: higher erosion rate with a low spatial variance

Sieve curves

Analysis of the sieve curves showed a very wide range of the particle size distribution. The representative particle size distribution is obtained by averaging the curves. There was no clear difference between the upper samples and the samples below. For two reasons this does not directly imply there is no armouring: 1) An armour layer can be smaller than the range where the sediment samples are taken in; 2) The armouring does not have to occur all the time, but only during certain flow.

Analysis soil composition and cohesive layers for the MV1-case

For the hindcast of MV1 it is difficult to determine what kind of sediment is scoured away in the period 1986-2006. There are four indicators which suggest that part of the erode material was cohesive material:

- Strong alternating erosion rate suggest difference in bed material
- An irregular bed level is observed which suggest a spatial variation of the bed material
- Clay is exposed at two locations close to the centre of the scour hole
- Geotechnical analysis suggests clay on higher positions in the area of interest

Analysis soil composition and cohesive layers for the MV2-case

From four soil samples close to the expected scour hole in front of the Maasvlakte 2 there can be expected that a cohesive layer starts between 19 and 22 meters below NAP. The thickness of this cohesive layer has a high range (1.24 to 3.61 meter) but it is also possible that there is no cohesive layer in the most seaward area of the expected scour hole.

11.3 Objective 1: Two new hindcasts of MV1

In chapter 6 and 7 two hindcasts have been made: The first hindcast is by a model where the effect of armouring is schematized by implementing several non-cohesive fractions (graded sediment) and a number of bed layers. The second hindcast is done by a model where a cohesive layer is implemented. In general the following can be said about the two hindcasts:

Calibration period

Both hindcasts should be calibrated and validated against 20 years of field data. The simulation time appears to be too large to cover 20 years. Several grids has been investigated which could reduce the computation time. Investigated grids did not give the intended computation time or did not give appropriate accuracy. Other simulation time depending parameters like the morphological factor and the computational time step have been optimized to minimize the computation time without losing accuracy. (to give an indication: simulation of 1 morphological year for the graded sediment has a computation time of 24 hours on a computer with a clock speed of 3 GHz)

Nourishment mode

It is not possible yet to incorporate a nourishment mode in the model when multiple fractions and layers are applied: this is a clear shortcoming of the model because the yearly nourishment has a considerably influence on the scour hole.

11.3.1 Hindcast 1: Armouring by non-cohesive fractions

The first hindcast concerns the armouring by non-cohesive fractions: Finer sediment will erode and the coarser material will stay behind forming an armour layer on the surface of the seabed. All performed runs show clearly a decrease of the erosion compared with the uniform sediment run. The displayed erosion pattern is similar to the erosion pattern in reality.

Two reasons for the decrease of the erosion:

1. Armouring: the transport layer coarsens because the relatively fine material erodes faster. This relatively courser layer causes a decrease of the erosion
2. The finest sediments (100 µm) cause a decrease of the maximum erosion depth as shown in paragraph 6.1.

Uniform sediment of 200 µm already showed an overestimation of the accretion of the Maas trench. All the simulations with graded sediment show an even larger accretion. Though the eroded volume eroded out of the scour hole is smaller compared to the case with uniform sediment. The larger accretion is due to the small fractions which cause a relatively high accretion in the Maas trench. When the five simulations with graded sediment are mutually compared a larger accretion is found when a larger volume is eroded out of the scour hole. The complete increase of accretion can not be clarified by the larger eroded volume out of the scour hole.

Armouring
The armouring effect is observed well. In and around the scour hole an increase of the content of the larger sediment fractions is found and a decrease for the smaller sediment fractions (except for the smallest particles, 100 µm). The armouring effect depends on the ratio D90/D10. A high value for this rate gives more armouring.

Quantification
One of the simulations has been done with the best fit resulting from the data analysis. This best fit showed 25% reduction of the erosion depth in the scour hole. The other simulations gave 8 -39% reduction depending on the average D50 and the ratio D90/D10.

11.3.2 Hindcast 2; cohesive material

In the formulation for erosion of cohesive material used in the Delft3D model two parameters depend on the condition of the soil. These two parameters, the erosion rate M and the critical shear stress τ_e have a large range. These values mainly depend on the clay condition. The appropriate values for these two parameters have to be determined by calibration or field observations.

In the simulations the erosion pattern appears to be different when compared to reality. On some places there is also accretion in the scour hole. The layered system as observed in reality can be best simulated with a thin (0.2 meter) cohesive layer. Thicker layers resulted in unwanted sedimentation areas. Furthermore, a discontinuity in the erosion pattern is found at the transition from purely non-cohesive material to cohesive material. Erosion occurs at the non-cohesive side of the transition and accretion occurs at the cohesive side.

The in reality observed rate of erosion is simulated well when cohesive material is implemented in the model. The large discontinuity on the transition though is not as observed in reality. Also the extent of the scour hole as simulated in the schematized model is not similar to reality. Especially the extent in west-east direction considerably differs from reality: In reality the scour hole extents about 1200 metres measured from the Zuiderdam in westward direction while in the simulations an extent is found of about 650 meters. The erosion is also closer to the construction. The initial bed levels in the simulations already showed a scour hole. This scour hole has the extent of 1200 metres. The extent of the scour hole in the simulations is smaller compared to this initial bed level. Part of the bed level in the initial bed level already lies under the equilibrium level of the computations with cohesive sediment. Therefore there is accretion in this part.

The accretion in the trench of the Maas has better results compared to uniform sediment: there is a smaller overestimation. But this improved result can almost completely be explained by the smaller eroded volume out of the scour hole.

It is difficult to simulate the highly stratified system and therefore it is difficult to find appropriate values for the erosion parameters. The erosion rate found in reality can be simulated well with cohesive sediment. The extent, especially in east-west direction is simulated considerably different compared to reality. The erosion is also located closer to the Zuiderdam. The extent and the position of the scour hole are not yet simulated satisfactory.

11.3.3 Non-cohesive fractions versus cohesive fractions

By implementing several non-cohesive fractions in the model the depth of the scour hole will be reduced as seen in chapter 6. The erosion rate in the model is still considerably higher than the erosion rate observed in reality. Furthermore this model does not explain the large differences in erosion rate observed between 1986 and 2006 in the scour hole.

By implementing cohesive material the erosion rate observed in reality can be simulated. The change in erosion rate is due to the highly stratified bottom. Each layer with its own erosion rate. However it is very difficult to simulate this highly stratified system and therefore it is difficult to find appropriate values of the erosion parameters. In contrast to the erosion rate is the extent of the scour hole not simulated satisfactory.

The following is concluded:

The effect of cohesive material is dominant over the effect of armouring. Furthermore the cohesive sediment can be used to simulate the erosion rates observed in reality. Implementation of several non-cohesive fractions still gives an overestimation of the scour hole and can therefore never be the sole reason of the overestimation of the model where uniform non-cohesive sediment is applied.

11.4 Study objective 2: MV2; armouring by non-cohesive sediment

As stated before an obvious shortcoming of the model used in this study is the lack of a nourishment mode. This does not meet part of the second study objective.

For the Maasvlakte 1 situation two reasons were found for a reduction of the scour depth. Both mechanisms count for the Maasvlakte 2 situation.

1. The finest sediment has a lower content reduction in the transport layer than the second finest sediment. This is similar to the Maasvlakte 1 situation and indicates lower erosion because of the finest sediment.
2. The coarsening of the transport layer because fine material erodes faster than the coarse material (armouring) is also shown in the Maasvlakte 2 situation. Because there is more erosion in the Maasvlakte 2 situation the armouring effect develops faster. Therefore also a higher D50 is found in this situation.

For the Maasvlakte 1 situation comparison was made between the simulation with uniform and the simulation with graded sediment. The conclusions were that the extent of the pattern was similar and for the erosion a reduction of 25% was found. This reduction varies between 8 and 39% for the other simulations with graded sediment.

In this chapter the extent of the scour hole shows a larger extent for the graded sediment simulation: This is a small disagreement with the Maasvlakte 1 situation. The reduction in erosion rate in this chapter is found of nearly 30 % for the deepest point. This is in agreement with the Maasvlakte 1 case.

11.5 Study objective 3: MV2: cohesive layers

It can be concluded there are certain shortcomings in the simulations regarding this objective which result in inaccurate results:

- A high range for the possible vertical position of cohesive layers
- A high range for the possible thickness of the cohesive layers
- A high range for the parameters used in the model (critical shear stress for erosion τ_e and the erosion parameter M)
- The hindcast did not show satisfactory results for the extent of the scour around Maasvlakte 1.

Therefore the simulations regarding this objective did not intent to give accurate predictions of the scour hole but do show of what influence of cohesive material can be.

Because of the lower vertical position of the cohesive layer it takes a longer time before the erosion reaches this layer. Variation of parameters (critical shear stress for erosion τ, erosion parameter M and vertical position of the clay layer) had an effect on the erosion rate but hardly influence on the extent of the scour around the Maasvlakte 2 which is consistent with the Maasvlakte 1 simulations. The extent of the scour is comparable with the simulations where purely non-cohesive material was applied. This is not in accordance with the Maasvlakte 1 situation where the simulations with cohesive sediment showed a smaller extent of the scour hole. This can be due to the large non-cohesive cover which predominantly determines the extent of the scour.

The development of the scour hole in reality shall start with a high erosion rate. This erosion rate is probably overestimated in the simulations and the results of the model should therefore be taken as the upper limit. As already concluded the vertical position and thickness of the cohesive layer is not certain and beside that the vertical position and thickness are not uniform in the area of interest. When the erosion reaches a cohesive layer the erosion rate will decrease. This new erosion rate depends on the erosion parameter M and the critical shear stress τ. There is not one cohesive layer but a stratified system which was schematized as one layer in the current study. The parameters differ for the different layers in the stratified system. When a layer within the stratified system is eroded away, erosion of the next layer will commence. This can result in an increase or a decrease of the erosion rate on that point. The simulations in this report show that the erosion rate which can be accomplished with the range for the concerning parameters has a high range. This rate can be larger than the erosion rate as simulated with non-cohesive material but can also be so small that there is practically no erosion.

11.6 Recommendations

The scour hole in front of the Maasvlakte 1 has been studied before. All the hindcasts showed an unrealistic strong development of the scour hole compared with field observations. Therefore there is expected that the scour hole in front of the Maasvlakte 2 is overestimated as well. An aim of the present study was to give a better understanding of why the scour hole was overestimated. Two concepts have been investigated. Both concepts turned out to give a smaller erosion hole when simulated with Delft3D. But the hindcast simulations were not yet satisfactory and therefore the predictions for the Maasvlakte 2 will not be very accurate. An accurate prediction is desirable. More study is needed to give this more accurate prediction. The following recommendations are for future research such that better hindcasts and therefore more accurate predictions can be made.

- The computation time was very large in the present study. Using the 'parallel online approach' [Roelvink, 2006] will decrease this computation time but demands a number of computers. A circular grid was investigated in this study (Appendix A). The computation time was considerably smaller for this grid but it showed irregularities in the flow and the water level. There seems to be a trick to avoid this. By avoiding this the circular grid can be used which results in a considerably smaller computation time.
- To give accurate predictions of the scour hole a nourishment mode should be incorporated. As discussed in this study the nourished volume is rather large. Only nourishment data of the period 1990-2000 was available. For the remaining years the nourished volumes on the Slufter beach should be gathered as well.
- The Maasvlakte 1 was constructed in 1970; the Slufter was added in 1986. In this study only the situation including the Slufter has been used. Bathymetric data of the situation between 1970 and 1986 do exist but were lost at RIKZ. This data would give an extra calibration/ validation case.
- In the present study the influence of individual waves is not investigated. Some waves have a positive and some a negative effect on the scour hole. Also the sequence of the waves is important. Further investigation on this subject shall bring more insight in the development of a scour hole.
- The following parameters concerning cohesive material are not well known yet: The erosion parameter M, the critical shear stress for erosion τ, the thickness and the vertical position of cohesive layers at the expected location of the scour hole in front of MV2. Box cores on location should give more accurate values for these parameters. These parameters can be used for the Maasvlakte 2 situation. Furthermore the values of the erosion parameter M and the critical shear stress τ can be used to improve the hindcast of MV1.
- The simulations for cohesive material with the Partheniades formulations that are implemented in Delft3D did not show satisfactory results. Other formulations or even other computer models should be investigated.
- Very fine sediment results in a scour hole with a smaller depth and a larger extent. Reasons for this are a smaller gradient in the sediment transport but also slope effects can be the reason. In this study only relatively fine sediment with a diameter of 0.100mm was investigated. It should be investigated if an even smaller particle will result in an even less deep scour hole.

- Deposited material in the Maas trench should be kept up for each fraction separately.
- In the present study the effect of armouring is simulated by implementing more than one fraction. There is no hiding and exposure correction which means that finer particles cannot hide behind coarser sediments and coarser sediments are not extra exposed to the flow. The effects of hiding and exposure should be further investigated.

References

BOER,S., ROELVINK, J.A., VELLINGA, T.(2006) Large-scale scour of the seafloor and the influence of bed material gradation Maasvlakte 2. Int. Conf. on Scour and Erosion, ICSE, 2006, 2006.

ELIAS, E., ROELVINK, J.A., AARNINKHOF, S., (2006) Ontwikkeling Ontgrondingskuil bij Maasvlakte 2, *Z4114.00*, WL|Delft Hydraulics

Van Ledden, M., 2003, Sand-mud segregation in estuaries and tidal basins, Doctoral thesis, Delft University of Technology.

Lesser, G.R., Roelvink, J.A., Van Kester, J.A.T.M., Stelling, G.S., (2004) Development and validation of a threedimensional model, Coastal engineering 51, pp. 883915

Project Mainportontwikkeling Rotterdam (PMR), PKB- plus deel 4: definitieve tekst, 2003, Rotterdam, the Netherlands

ROELVINK, J.A., (1998), Kleinschalig morfologisch onderzoek MV2. Fase 1: Validatie Morfologische modellering Haringvlietmonding. *Z2428.00*, WL|Delft Hydraulics

ROELVINK, J.A., AARNINKHOF, S.G.J. (2005) Onderbouwend onderzoek MER Maasvlakte2. Onderdeel Morfologie, *Z3959*. WL|Delft Hydraulics

ROELVINK J.A., (2006) Coastal morphodynamic evolution techniques. Coastal Eng 53:277–287

SOULSBY, R.L., L. HAMM, G. KLOPMAN, D. MYRHAUG, R.R. SIMONS AND G.P. THOMAS, 1993. 'Wave-current interaction within and outside the bottom boundary layer', Coastal engineering, 21 (1993) 41-69,Elsevier science Publishers B.V., Amsterdam.

STEIJN, R.C ET AL., 2000. Morfologisch onderzoek Maasvlakte 2. Onderhoud zachte zeewering, grootschalige ontgronding en aanzanding Maasgeul. Alkyon, Delft Hydraulics.

STORMS J.E.A., WELTJE G.J., VAN DIJKE J.J., GEEL C.R. AND KROONENBERG S.B.(2002) Process-response modeling of wave dominated coastal systems: simulating evolution and stratigraphy on geological timescales. J. Sedimentary Research, 72: 226-239

GRAAFF VAN DE, J. (2006) Coastal morphology and coastal protection, Lecture notes CT5309 , Faculty of Civil Engineering and Geosciences, TU Delft, The Netherlands.

VAN HETEREN, S., VAN DER SPEK, A.J.F. AND DE GROOT, T.A.M. (2003) Architecture of a preserved holocene tidal complex offshore the rhine-muese river mouth, the Netherlands. Proceedings Coastal Sediments ’03, 5th Int. Symposium on Coastal Engineering and Science of Coastal Sediment Processes; May 18-23, 2003, Clearwater Beach, FL, USA (CD-ROM; ISBN 981 238 422 7 (CD)), 12 p.

VAN RIJN, L.C. (1993) Principles of Sediment Transport in Rivers, Estuaries and Coastal Seas. Aqua Publications, Amsterdam.

VAN RIJN, L.C. (1998) Principles of Coastal Morphology. Aqua Publications, Amsterdam

VAN RIJN, L.C., BOER, S.,(2005) Invloed van zandkorreldiameter op het zandtransport in de kustzone ter plaatse van Maasvlakte 2. Z4035. WL|Delft Hydraulics

WHITEHOUSE R., SOULSBY, R., ROBERTS, W., MITCHENER H.,(2000) Dynamics of Estuarine Muds, Thomas Telford, London, UK (2000).

WINTERWERP, J.C., VAN KESTEREN, W.G.M.,(2004) Introduction to the Physics of Cohesive Sediment in the Marine Environment, Elsevier, Amsterdam, The Netherlands (2004).

WL | DELFT HYDRAULICS. 2006 (NOVEMBER). DELFT3DFLOW, User manual. Version 3.13, Delft, The Netherlands.

YE, Q. (2006) Modelling of Cohesive Sediment Transportation, Deposition and Resuspension in the Haringvliet Mouth. Master thesis, Unesco IHE, Delft

Appendices

Appendix A Computational grids

A.1 Introduction

A computational grid has to cover the area for the computations. In former studies on the Maasvlakte a rather fine grid has been used. This grid is shown in figure A.1. It extents from the Brouwersdam in the south till Noordwijk in the North. The highest resolution is in the mouth of the Haringvliet and in front of the Maasvlakte 1 and 2. Initially this grid will not be used in the current study because it has a very high resolution, which will result in large computation times. Because the focus of this study is narrower than in the former studies grids with a smaller total number of grid-cells will be investigated. This grid has to constrain the computation time and still has to be sufficient for the purpose of the model. To ensure a good grid quality the grid can be checked on a number of properties: Smoothness, resolution, orthogonality and the ratio M-size/N-size.

Smoothness: Ratio between adjacent grid cell lengths (<1.2)
Resolution: The resolution has to be high enough to represent the cross section, currents and waves well enough. A resolution of 50 meters is enough to represent wave-driven currents and the cross-section of the scour-hole.
Orthogonality: Cell centred cosine value (0.02-0.04 in area of interest)
Ratio M-size/N-size: Must be in the range [1,2] unless the flow is predominantly along one of the grid lines.
Furthermore the extent of the grid has to be such large that the boundary conditions will not influence the area of interest.

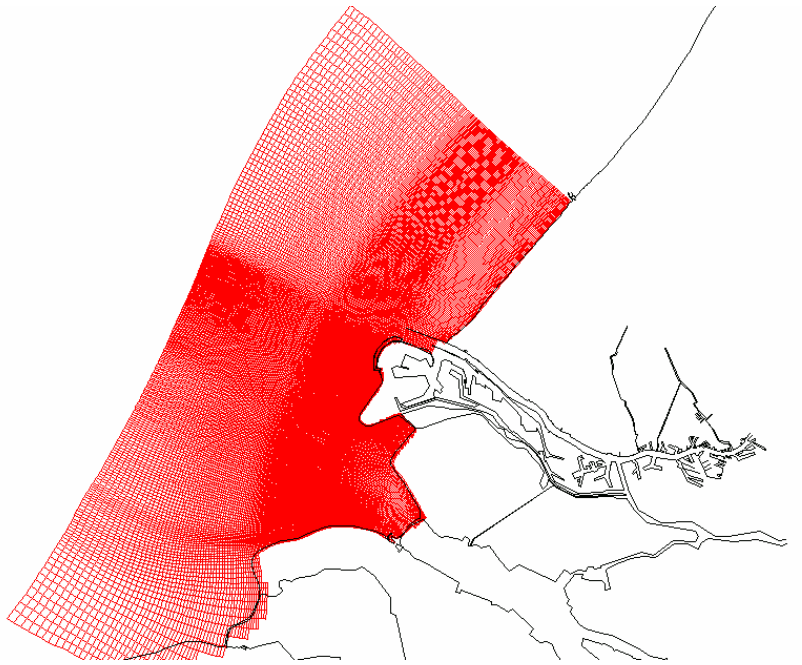

Figure A.1 Computational grid used in former studies

A.2 Grid 1, domain decomposition

In figure A.1, the original model, the grid is very fine in the Haringvlietmonding and in front of the Maasvlakte. The grid becomes coarser in the direction of the boundaries of the grid, but it still has to meet the requirements and therefore

two strips of finer cells can be seen. As a consequence this grid counts a rather large number of grid cells.

The extent of the model has to be large enough to prevent influences of the boundary conditions. For this purpose a rather coarse grid will be sufficient. In the area of interest a rather fine grid is necessary.

A way to obtain a fine grid in the area of interest and a coarse grid outside is by making use of domain decomposition. Domain decomposition is a technique in which a grid is subdivided into several non-overlapping smaller grids. It is possible to refine one of the domains. Therefore it is possible in this case to have a very fine grid around the Maasvlakte and a coarser grid outside.

To determine which part of the area has to be covered by a fine grid and which part by a coarser grid the influence of the Maasvlakte 2 on the water level and the current is investigated. In figure A.2 the depth-averaged velocity during flood is depicted. This is computed with the model that was used in the former studies. In this figure clearly the influence of the Maasvlakte 2 on the flow velocity is visible. The black line in front of the Maasvlakte 2 has been taken as the border between the coarse and the fine grid. In the area where the scour hole develops a third sub-domain will be created which has again a higher resolution.

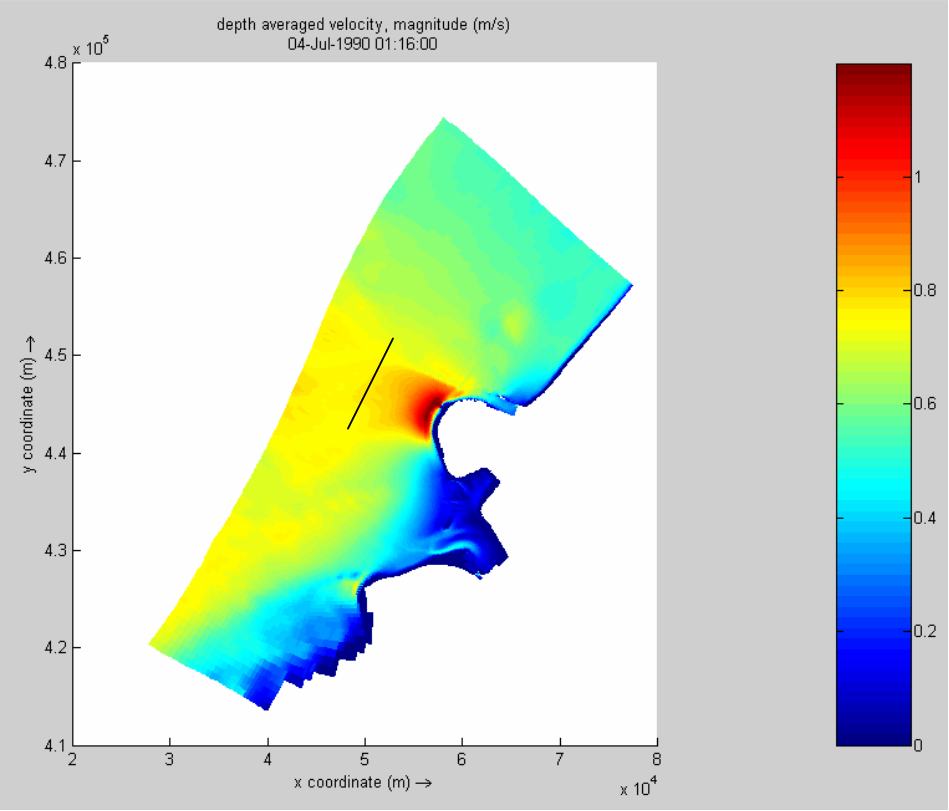

Figure A.2 Depth averaged velocity in front of MV2

Starting point is a grid created by [Ye, 2006]. Domain composition is applied two times and the result is three grids with a raising resolution into the direction of the area of interest. This is shown in figure A.3.

On the boundaries between the sub-domains (DD-boundaries) the water levels, current velocities and transports are passed on. Due to the domain decomposition the number of grid cells for the three grids together is 15277

(table A.1). This is far less than the original grid and therefore the computation time is far less as well.

Analysis of the water level, depth averaged velocity and cumulative erosion/sedimentation gives information about the quality of the model. The water level is as expected and comparable with the original model. The depth-averaged velocities though give irregularities on the boundaries between the sub-domains. The irregularities extend as long ridges in the finer domains. This is no problem if these irregularities do not reach the area of interest. The cumulative erosion/ sedimentation after 2 morphological years is shown in figure A.4. It can be seen that the irregularities reaches the area of interest and even the location of the scour hole. This is not acceptable if an accurate estimation of the scour hole has to be made. This grid is not suitable for this master thesis.

If the fine grid would be enlarged so that the boundaries of the fine grid will be farther away from the area of interest but this will also increase the number of grid cells. When domain decomposition is applied extra calculation time is demanded because of the interaction between the sub-domains. The growth of the number of grid cells and extra needed computation time will give a larger computation time compared with the original grid. Therefore another grid will be investigated.

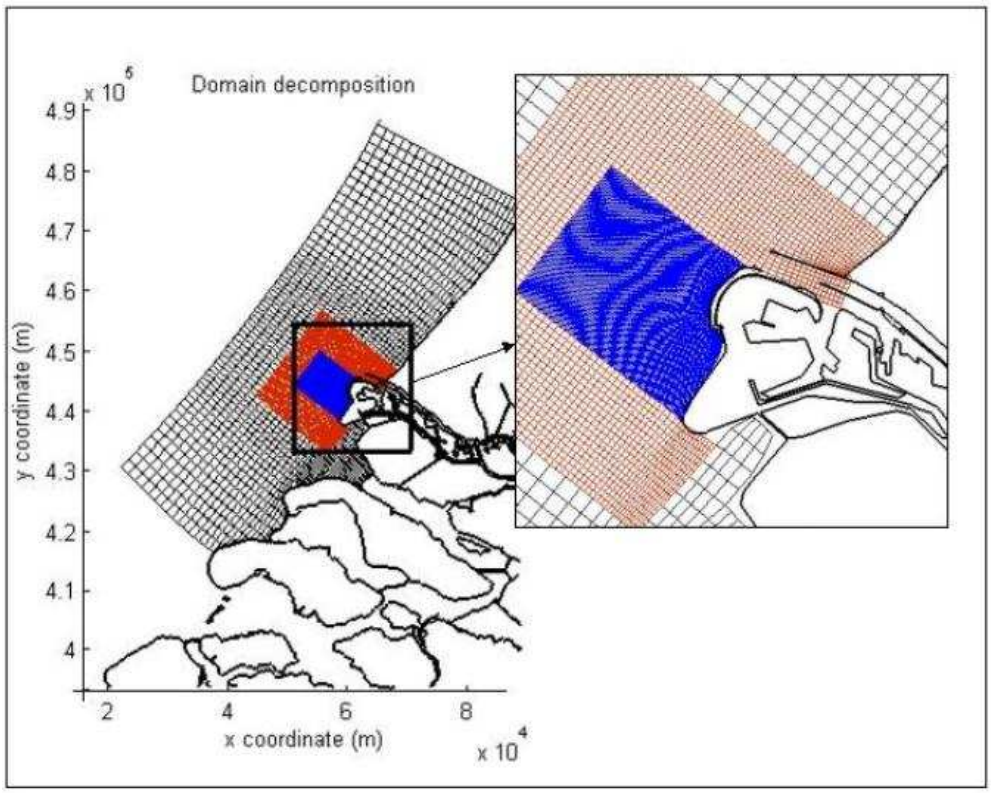

Figure A.3 Domain decomposition grids

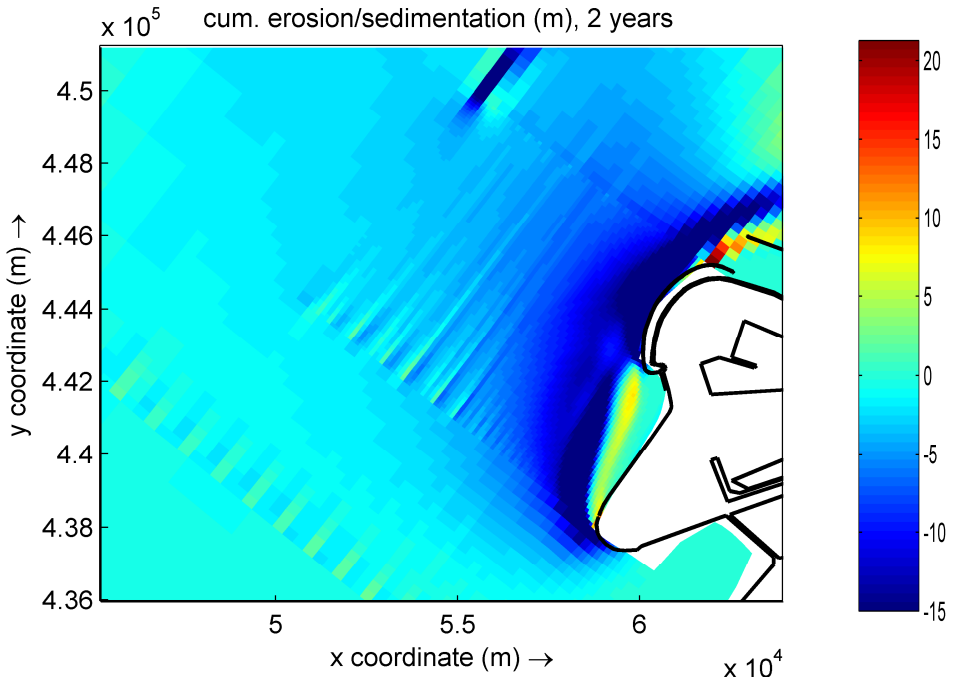

Figure A.4 Cumulative sedimentation/ erosion

A.3 Grid 2, a circular grid

For purpose of a grid with lesser grid cells a circular grid is proposed. When using a circular grid the focus of the grid is primarily on the Maasvlakte and not anymore on the 'Haringvlietmonding' as in the original Maasvlaktegrid. In front of the Maasvlakte an equal resolution is obtained, but in the 'Haringvlietmonding' a coarser resolution is created. In a rectangular grid always a cross shape is visible when a high resolution is created in one place (see figure A.1). This is not necessary in a circular grid. The circular grid is shown in figure A.5. As can be seen in table A.1 this model also has a lower number of grid cells.

Analysis of the flow and water level shows however irregularities. As can be seen in figure A.6 irregularities in the shape of a semicircle and in line with the grid-cells in m-direction appear. It seems that the flow wants to go predominantly along a gridline and because the flow in this case is not at all along the gridlines the irregularities occur. Also these irregularities are not acceptable and therefore another option is investigated to come to a smaller computation time.

Table A.1 Number of grid cells

		Number of gridcells
Flow	Original grid	50652
	DD-grids	1237+2232+11808=15277
	Circular grid	17607
	Optimal grid	23000
	final grid	32629
Wave	final grid	8016+4186=12202

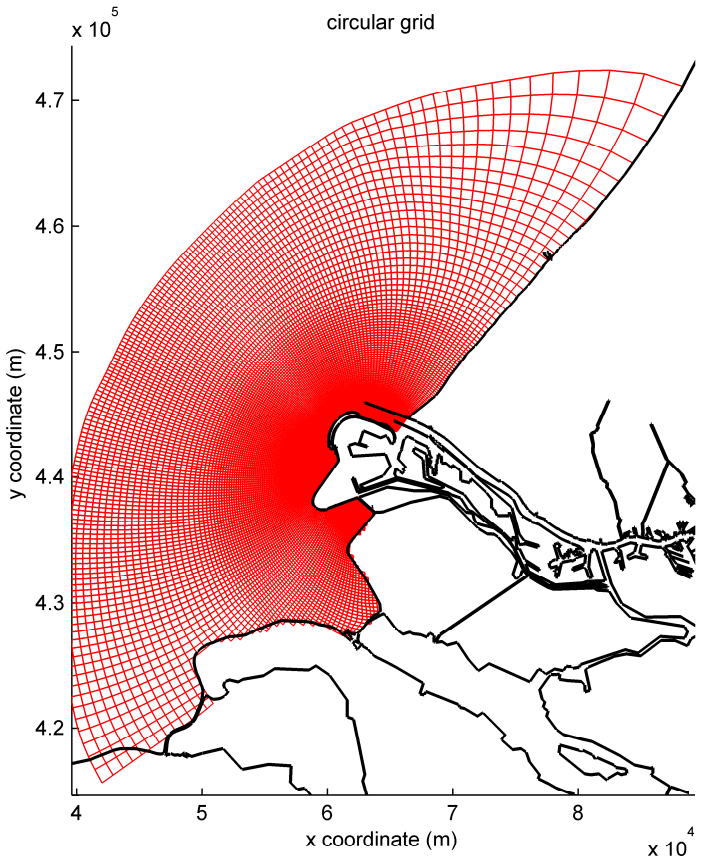

Figure A.5 Circular grid

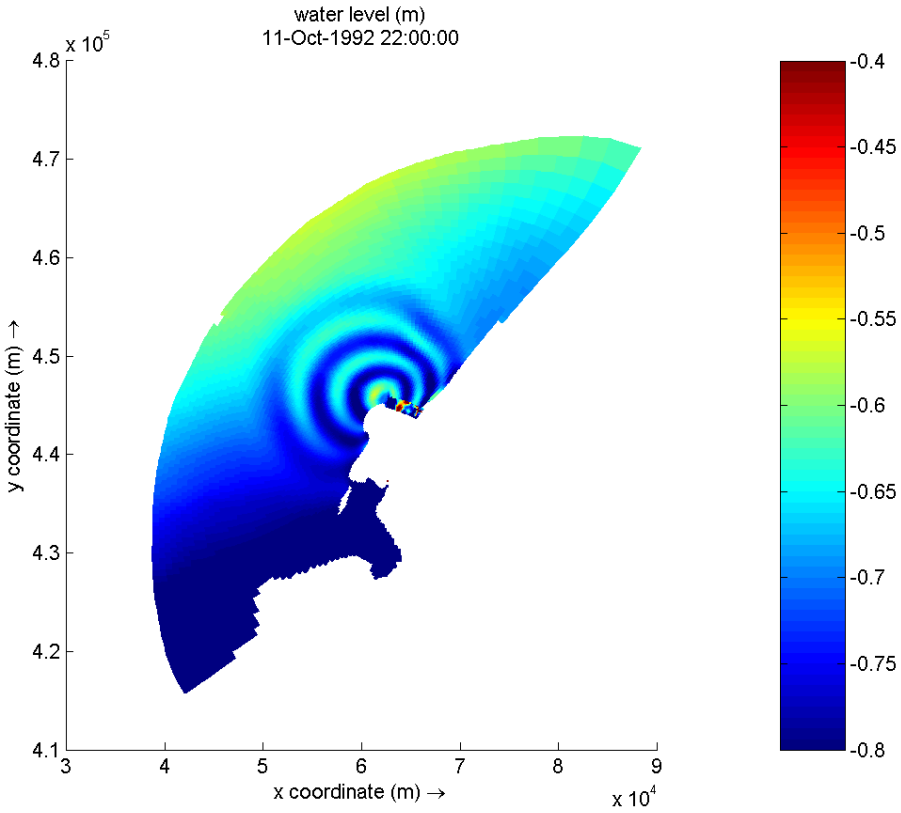

Figure A.6 Water level, circular grid

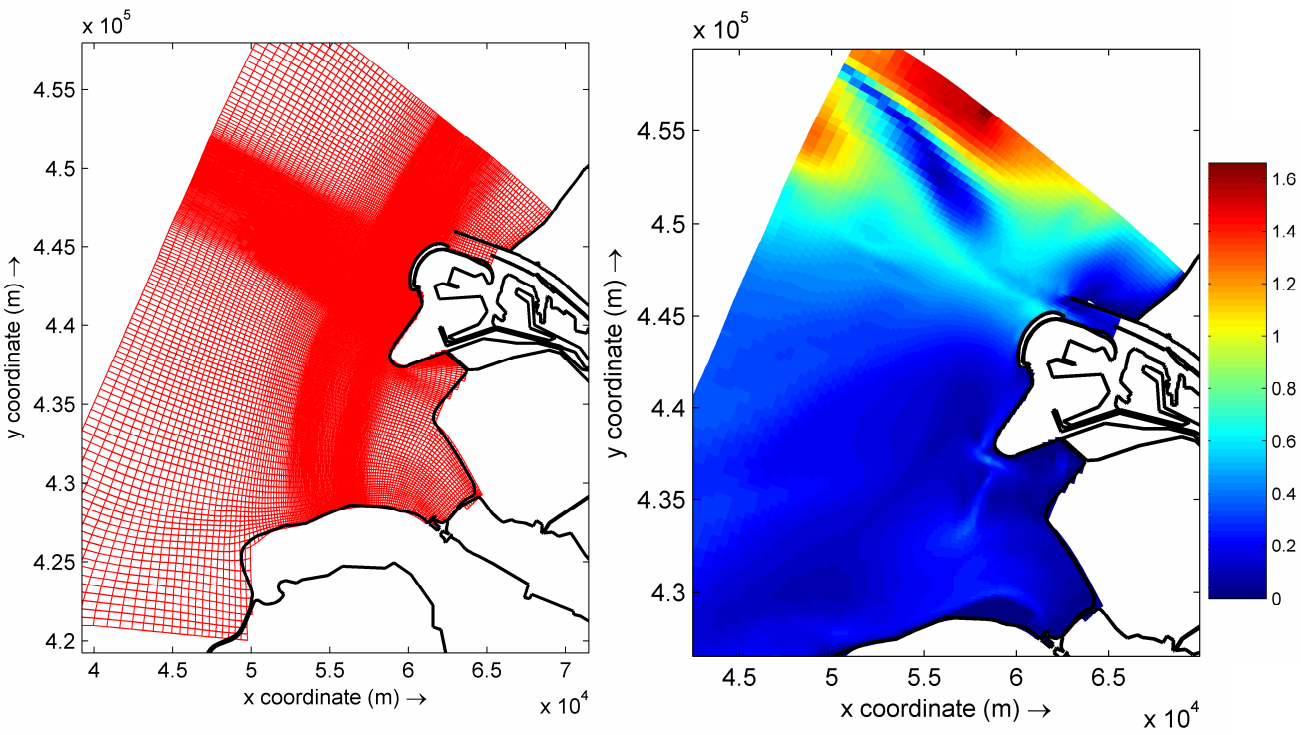

Figure A.7 Optimal grid (left) and depth averaged velocity optimal grid (right)

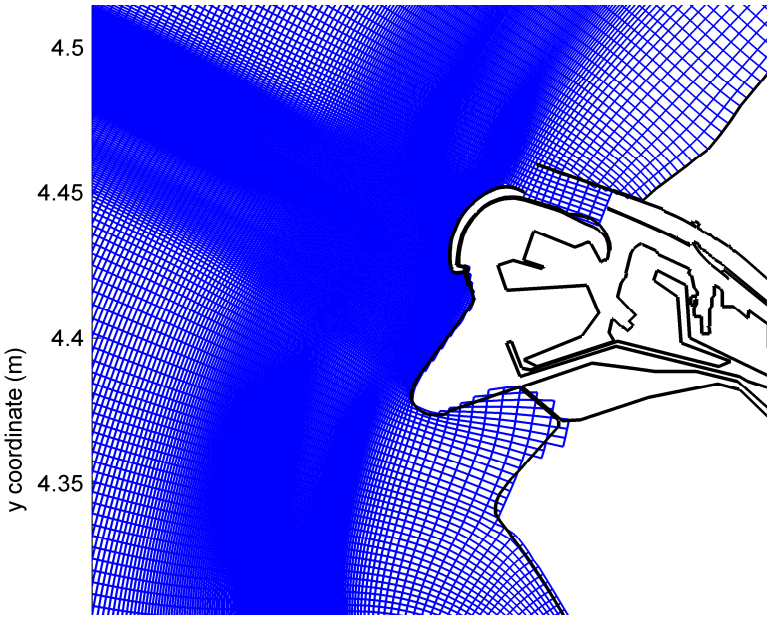

Figure A.8 Final grid, detail

A.4 Grid 3, Optimization of the original grid

The original grid can be optimized in two ways. The first way is to derefine the grid on the places that are not interesting in this study. The second way is to reduce the area that is covered by the grid. A combination of these two ways resulted in a grid with 23,000 grid cells. However a lot of discrepancies can be seen in the depth averaged velocity (Figure A.7). Because of the decreasing resolution in the direction of the boundaries the profit of number of grid-cells is

limited when the covered area is reduced. Therefore a grid is created as shown in figure A.8 (detail) which is only derefined outside the areas of interest. The covered area is equal to the covered area in the original grid. The output for this grid is satisfactory. The computation time though is still rather large. An advantage is that the same water level boundary conditions can be used as in the former studies.

Appendix B Geological setting

The Rhine-Meuse river mouth, which comprehends the area of interest, is dominated by the estuary of the Rhine and the Muese. Canal construction and continues dredging have turned this highly dynamic river mouth into a stabilized form.

At the end of the Pleistocene, the Rhine-Meuse system has formed a thick layer of primarily coarse, gravely sand. Rising Holocene sea level caused a decrease in river gradient, a reduction in discharge velocity and increasingly frequent flooding. Clay and peat dominate the floodplain here, sand was deposited in point bars and levees. During the Boreal, an early stage of the Holocene, the sea level was about 25 meters lower than today. Tidal flats and tidal channels dominated the outer part of the river mouth. Outside the area of marine influence, a meandering river system dominated. During the middle Holocene discharge obstruction due to barrier development forced the river to change sediment patterns. River sand supply was stored in abandoned channels resulting in a labyrinth of small sand-ribbons encased in peat and flood-basin clays. In the end of the Middle Holocene the system was abandoned by the Rhine channel and only dominated by the smaller Meuse.

Van Heteren et al, 2003 combined high-resolution seismic data with core data and identified eight seismic facies. These eight facies are shown in a cross-section perpendicular at the Slufter beach (figure B.1). The layer PL is seen as the mentioned above Pleistocene sediment. This layer is covered by an up to 5 meter thick layer of fine graded sediments (PH). This Preboreal and Boreal deposits are laid down in the area during different phases of meandering fluvial activity. Peat formed as well here due to drowning of the area as a result of the sea-level-rise. At the easternmost part of the area thick fluvial clays locally cover this peat. PL and PH are locally dissected by estuarine fills (CF) of tidal channels as can be seen in the figure. The layer CL-1 covers the layers CF and PH. This layer represents a complex estuarine system, composed of highly mobile and tidal channels and tidal flats probably formed in the middle Holocene. This layer consists of sand-clay alternations or silty sand with clay and peat. When the sea-level rose further during the Holocene flood plains were gradually submerged. A wide estuary developed, characterized by a multitide of broad, generally shallow subtidal channels. The broad subtidal channels were highly mobile, migrating laterally across considerable distances and cross-cutting deposits of older channels. The layer TR-1, consisting of homogeneous fine-medium sand with whole shells or shell fragments, was interpreted as a subtidal flat or shore face sediments, formed on the seaward side of estuaries. The other layers CL-2, BH and TR-2 are younger layers and are indicated as not important for the scour hole because of their position. In the case of the scour hole the CL-1 layer is of importance because of the clay content. The stratification of this layer is consistent with the stratification found in the sand samples taken at the location in and around the scour hole. Furthermore the alternative for the CL-1 layer is the PH layer which consists of fluvial deposits. From the samples also pictures are available. In the pictures little organisms in the concerning layer can be seen. This organisms indicates salt water, because in salt water live significantly more organisms than in fresh water. (Oral consultation, Van der Spek).

Therefore it is clear that the layered system is the complex estuarine system named Cl-1.

In figure B.2 a cross section parallel to the coast is shown. Very clearly the spatial derivation in the shore parallel direction can be seen.

The inter tidal system is influenced on one hand by the river and on the other hand by the marine system. The system is composed of highly mobile tidal channels and tidal flats. On the places with high velocity only erosion occurs, places with lower velocities sand will accrete. The lower the velocity the finer the material which will deposit. So the clay will deposit on places with the lowest velocity. In the complex estuarine system the clay will deposit on these places were the marine influence and the fluvial influence is limited. Due to the sea level rise the marine influence is moving eastward and therefore the place where the clay deposits is moving eastward as well. There is a gradient in the seabed. The stratified system of CL-1 lies parallel to this original seabed. Therefore the clay layers lie relatively to the sea level higher when positioned more eastward.

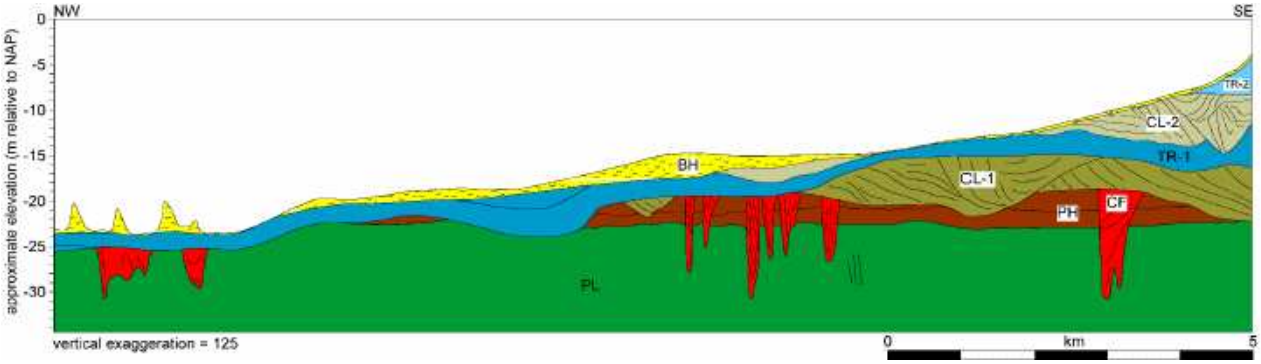

Figure B.1 Shore perpendicular cross section with seismic facies [Van Heteren et al., 2003]

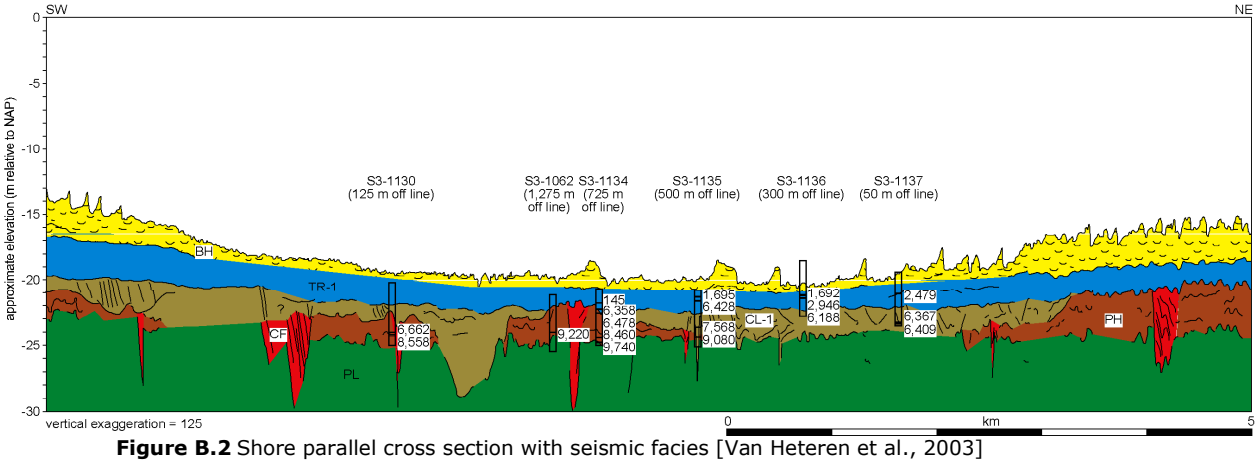

Figure B.2 Shore parallel cross section with seismic facies [Van Heteren et al., 2003]

Appendix C **Soil sample and sample report**

BL24. - 1 (geroerd monster)

Diepte (m tov MV) Monsternr. Bodembeschrijving volgens NEN 5104

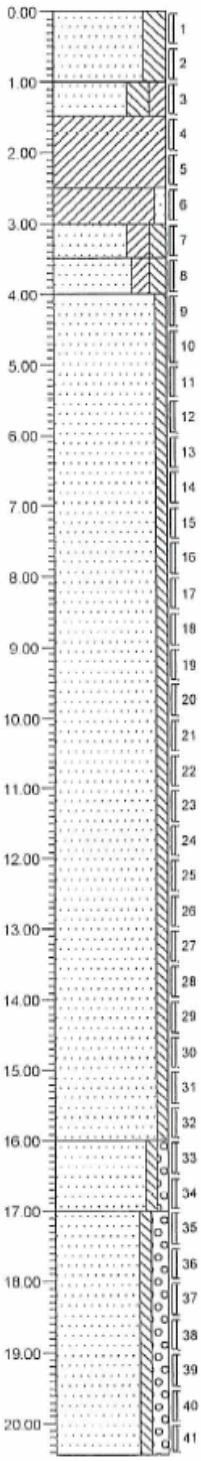

0.00 waterbodem

Zand, uiterst fijn, sterk siltig, grijs, kleilaagjes, schelpresten

1.00

Zand, uiterst fijn, sterk siltig, matig kleiïg, grijs, kleilaagjes, schelpresten

1.50

Klei, grijs, matig vast, schelpresten

2.50

Klei, zwak zandig, donkergrijs, matig vast

3.00

Zand, matig fijn, sterk kleiïg, matig siltig, grijs

3.50

Zand, matig fijn, matig kleiïg, matig siltig, grijs, kleilaagjes

4.00

Zand, matig grof, zwak siltig, grijs, schelpresten

16.00

Zand, matig grof, zwak siltig, zwak grindig, grijs, fijn grind

17.00

Zand, matig grof, zwak siltig, matig grindig, grijs, matig fijn grind

20.43

Uitvoering: 25-03-2006 X: 60007 Y: 445350 BODEM (m tov NAP): -17.85 GWS (cm tov MV): GHG (cm tov MV): GLG (cm tov MV): Bk PB (m tov NAP):

ONDERZOEKSRAPPORT			
Project	vervolg grondonderzoek t.b.v. aanleg Maasvlakte 2		
Opdrachtgever	Projectorganisatie Maasvlakte 2	Opdrachtnummer	2106-0053-000
Contact persoon	Ir. D.C. Roukema	Datum rapport	23-05-2006
Monstername	door Fugro ing.bur. B.V.	Datum ontvangst	vanaf 24-04-2006

ONDERZOEK KLEIMONSTERS		
Monster	Omschrijving	Diepte in m-NAP
1	Boring BL24-4	19.35-19.75
2	Boring BL24-5	19.85-20.25
3	Boring BL24-6	20.35-20.75
4	Boring BL24-8	48.85-48.95
5	Boring BL24-9	49.65-49.90

RESULTATEN								
Parameter/Verrichting		Monster					Eenheid	Methode van onderzoek
		1	2	3	4	5		
Watergehalte (A)							%(m/m)	proef 161.1 Std RAW 2000/NEN5112
Gehalte > 63µm	Q						%(m/m)	proef 2 Std RAW 2000
Gehalte < 16µm	Q						%(m/m)	proef 125 Std RAW 2000
Gehalte < 2µm	Q						%(m/m)	proef 125 Std RAW 2000
Gehalte organische stof	Q						%(m/m)	proef 124 Std RAW 2000
Gehalte $CaCO_3$	Q						%(m/m)	proef 124 Std RAW 2000
Geleidingsvermogen	Q						µS/cm	proef 122 Std RAW 2000
Vloeigrens (W_l)	Q	53	82	120	35	42	%(m/m)	proef 15 Std RAW 2000
Uitrolgrens (W_p)	Q	32	37	61	24	24	%(m/m)	proef 15 Std RAW 2000
Plasticiteits-index (I_p)	Q	21	45	59	12	18	–	proef 15 Std RAW 2000
A-lijn		24	45	73	11	16	–	berekend als 0,73*(W_l-20)
Zoutgehalte bodemvocht							NaCl g/l	1)
Wmax		38	48	75	27	28	%(m/m)	berekend als W_p + 0,25 I_p
Consistentie-index (I_c)							–	berekend als (W_l-A)/(W_l-W_p)
Vloeibaarheidsindex (I_l)							–	berekend als 1-I_c

OPMERKINGEN
De met "Q" gemerkte verrichtingen zijn erkend door RvA.
1) Uitgevoerd door Alcontrol Laboratories B.V. te Hoogvliet

Appendix D Critical shear stress τ_e and erosion parameter M

The critical shear stress for erosion τ is generally assumed to be a constant material parameter but normally it varies with depth and time because of consolidation and physicochemical effects. Typical values given in literature are 0.1 Pa < τ_e < 5 Pa. In 1996 Mitchener et al.,[Whitehouse et al., 2000] developed a relationship for mixed, consolidated and blended high-density beds. The relationship is of the form:

$\tau_e = A(\rho_B - 1000)^B$

Where ρ_B is the bulk density or wet density of the bed, and A and B are dimensional coefficients fitted to the data with A=0.015 and B=0.73. The laboratory tests which resulted in the above relationship were validated against in-situ measurements and the in situ critical shear erosion was considerably smaller compared with the laboratory tests.

In the samples a wet density in the clay layers is found between 1500 and 1900 kg/m^3. This empirical relationship results in a critical shear stress between 1.4 and 2.15 N/m^2. But these stresses are expected to be overestimated. An increase in (dry) bed density generally increases the number of bonds between the particles (flocs), hence increase the critical shear stress. In the samples rather high bulk bed densities are found. Therefore also a rather high critical shear stress is calculated.

In 1959 Smerdon and Beasley [Winterwerp and Van Kesteren, 2004] related the critical shear stress for erosion τ_e to the plasticity index.

$\tau_e = 0.163 PI^{0.84}$ (PI in %)

Also this was found from laboratory tests.

In three samples also the plasticity index is determined for cohesive material. In these samples the plasticity index ranges from 15% to 60%. The critical shear stress becomes 1.58 to 5. This τ_e can be regarded as the 'true' critical shear stress for erosion.

As stated in paragraph 7.1 there are four modes of erosion. Actually two modes are applicable in the treated situation, namely floc erosion and surface erosion. Floc erosion is the process in which flocs are disrupted individually from the bed. This erosion occurs when the mean bed shear stress is of the same order of magnitude or a little larger than the apparent threshold for erosion. This apparent threshold for erosion is considerably smaller than the 'true' critical shear stress namely in the range of 0.2 < τ_e < 0.8. This apparent threshold is smaller because the onset of the floc movement is governed by the peaks in the bed shear stress.

Surface erosion occurs when the induced stresses are considerably larger than the true critical shear erosion. Eroded flocs have to be replaced by water because of continuity. The bed becomes (locally) over-consolidated and the strength of the bed decreases. The weakened bed will erode easily. Here the 'true' critical shear stress can be used.

For the surface erosion also the parameter M can be determined. This can be done with the following formula [Winterwerp and Van Kesteren 2004]:

$$M = \frac{c_v \phi_{s,0} \rho_{dry}}{10 D_{50} c_u}$$

Where:

C_v = vertical consolidation coefficient

$\Phi_{s,0}$ = volume concentration = $1/(W_0\ \rho_s/\rho_w)$

W_0 = water content

c_u = undrained shear strength

ρ_s = density of primary sediment particles

ρ_w = density of water

ρ_{dry} = dry bed density

D_{50} = medium floc size

In the samples which are taken in 2006 (l24, l25, l30 and l32) values are given for these parameters. The results are shown in table D.1. This results in a range for M of $1*10^{-4}$ to $1*10^{-6}$kg/m^2/s.

Table D.1 Calculation of erosion parameter M

Cv [m^2/s]	ρ [kg/m^3]	Cu [kPa]	D50 [mm]	Φ [m^3/kg]	M [m/Pa/s]
1.1E-06 - 1.2E-07	360 - 1400	11 - 50	0,04 - 0,07	0,25 - 0,56	1E-04 - 1E-06

Winterwerp et al., has also done some experiments in an erosion flume. The measured results were comparable with the computed with the formula above. The measured parameters are given in table D.2.

Table D.2 Measured critical shear stress and erosion parameter [Winterwerp 2004]

	τ_e [Pa]	M [m/Pa/s]
Lake Ketel	1,2	2,30E-07
Lake Ketel	0,76	1,43E-06
Ijmuiden	1,28	2,26E-06
Ijmuiden	1,01	6,61E-06
Kembs	2,44	1,60E-06

For the mode floc erosion no formula is given, only a range: $5*10^{-4}$ to $1*10^{-5}$ m/Pa/s. These values are actually larger than the values for the surface erosion where a smaller M is expected for this erosion mode.

Whitehouse, who does not make distinction in the 4 erosion modes as mentioned before, gives a summary of parameter values for mud from English estuaries determined in laboratory tests. This is shown in table D.3.

Table D.3 Parameters found in English estuaries [Whitehouse, 2000]

Mud type	M [m/Pa/s]	τ_e [Pa]	τ_e [Pa] at ρ = 50 kg/m3	τ_e [Pa] at ρ = 900 kg/m3
Cardiff Taff/Ely	-	$2{,}2E\text{-}04*\rho^{1.5}$	0,08	1,44
Cardiff Rhymney	-	$4{,}2E\text{-}03*\rho^{0.9}$	0,14	2,52
Fawley	-	$5{,}0E\text{-}04*\rho^{1.4}$	0,13	2,34
Grangemouth	5E-04 - 14E-04	$4{,}5E\text{-}03*\rho^{0.9}$	0,15	2,7
Harwich	7E-4	$3{,}5E\text{-}04*\rho^{1.4}$	0,09	1,62
Hong Kong	6E-04 - 15E-04	$1{,}3E\text{-}03*\rho^{1.2}$	0,14	2,52
Ipswich	9E-04 - 30E-04	$2{,}8E\text{-}04*\rho^{1.5}$	0,12	2,16
Kelang	2E-04 - 9E-04	$5{,}0E\text{-}04*\rho^{1.4}$	0,12	2,16
Kingsnorth	7E-4	$5{,}0E\text{-}03*\rho^{0.9}$	0,17	3,06
Medway	7E-4	$7{,}0E\text{-}04*\rho^{1.3}$	0,11	1,98
Mersey Eastham	5E-4	$1{,}3E\text{-}02*\rho^{0.7}$	0,2	3,6
Mersey Runcorn	-	-	-	-
Poole	7E-04 - 14E-04	$3{,}0E\text{-}04*\rho^{1.5}$	0,11	1,98
Tees seal sands	2E-04 - 14E-04	$2{,}5E\text{-}03*\rho^{1.0}$	0,13	2,34
Tees dredged	5E-04 - 18E-04	$1{,}4E\text{-}04*\rho^{1.7}$	0,11	1,98

The critical shear stress depends directly on the dry density of the material. In Whitehouse et al., the formula is given for each estuary and the value when the dry density is 50 kg/m^3. This results in relatively low values. In the case of Maasvlakte there is found a very high density. In the last column the values are given for the critical shear stress calculated with the formula with a value for the dry density representative for the Maasvlakte 1 case. Again relatively high values are found for the critical shear stress.

τ_e versus M

In literature a large range can be found for the parameters τ_e and M. General formulae are available or a distinction can be made in four erosion modes. For the general case the former paragraph values for τ_e are found in the range 1.5 – 5 Pa. Only with the formula of Mitchener a lower value is expected because of the overestimation of the formulae compared with the measured data. The measurements performed by Whitehouse et al., confirm a value in that range when the founded values are extrapolated to the founded dry density.

When distinction is made in four modes, two different values for τ_e and M will be found for the governing two erosion modes. For floc erosion a relatively low τ_e and M. For surface erosion a relatively high τ_e and M.

The normative should be taken for the computations. Because for each value a rather high range is found it is difficult to determine which one is normative.

When computations are made to determine the equilibrium the relation between the critical shear stress and the apparent shear stress is important. When the rate of erosion is important the value for M is very important. For the extent of the erosion again the critical shear stress becomes important.

In the Maasvlakte 1 case the rate of erosion is very important for the hindcast of the scour hole. No equilibrium is reached yet and therefore the relation τ_e versus τ_{cw} becomes less important.

For the Maasvlakte 2 case the equilibrium state of the scour hole becomes more important and therefore also the relation τ_e versus τ_{cw}.

For two reasons the high value for the critical shear stress will be used for the Maasvlakte 1 case.

The erosion rate is the subject and therefore the parameter M is important and therefore the surface erosion is normative.

The high values for the critical shear stress are more comparable with the founded values in England and the Netherlands.

The actual values for the critical shear stress and the erosion parameter have to be established by calibration. The ranges which will be used are 1.0 – 2.5 Pa. for the critical shear stress and $1*10^{-4}$ to $1*10^{-6}$ m/Pa/s. for the erosion parameter.